MANUFACTURING AND TESTING OF CERAMIC BASED HYBRID COMPOSITES WITH VARIOUS FIBERS, MATRIX SYSTEMS, AND PROCESSING CONDITIONS

A THESIS SUBMITTED TO THE GRADUATE DIVISION OF THE UNIVERSITY OF HAWAIʻI AT MĀNOA IN PARTIAL FULFILLMENT OF THE REQUIREMENTS FOR THE DEGREE OF

MASTER OF SCIENCE

IN

MECHANICAL ENGINEERING

AUGUST 2018

By:

Brenden M. Minei

Thesis Committee:

Mehrdad N. Ghasemi Nejhad, Chairperson
Lloyd H. Hihara
Scott F. Miller

We certify that we have read this thesis and that, in our opinion, it is satisfactory in scope and quality as a thesis for the degree of Master of Science in Mechanical Engineering.

_____ THESIS COMMITEE

Mehrdad N. Ghasemi Nejhad, Chairperson

_____

Lloyd H. Hihara

_____

Scott F. Miller

ACKNOWLEDGEMENTS

The intellectual gains accumulated over the course of this project are many and varied, but the deepest belongs, as it has been throughout the past many years, to my advisor, Dr. Mehrdad N. Ghasemi Nejhad. He has been unfailingly generous with his time, constant support, day-to-day guidance and advice rendered throughout this research. He indeed has provided a motivating, enthusiastic and critical atmosphere during the many discussions we had. I do not think I could do better than to follow his example. I also acknowledge Drs. Lloyd H. Hihara and Scott F. Miller for serving on my thesis committee.

I wish to acknowledge the support of the Phantom Materials, and Trex Enterprises, particularly Dr. Bill Goodman, for funding this project. Sincere thanks to Kaveh Khosroshahi for dedicated support on prior research, making my work easier during the course of this research. Also, I would like to thank Starfire Systems, Inc. for their informative discussions on preceramic polymer technologies. Thanks, are also due to Tina Carvalho of Biology Department for discussions on usage of SEM, and Drs. Hope Ishii, John Bradley, and Kenta Ohtaki for their assistance with Optical Microscopy and SEM facilities at SOEST (School of Ocean and Earth Science and Technology) and for allowing to use their facility for the microscopic characterizations of the developed samples quality and fracture surfaces of the tested samples, and thanks to Reginald Tolentino for taking the microscopic pictures funded by the University of Hawaii at Manoa Materials Science Consortium for Research and Education (CoRE).

I would like to acknowledge the assistance of the support staff, particularly Joanne Yee and Greg Pang, in the Mechanical Engineering Department who have made my work easier and enjoyable. A special thanks to Robert Mcgehee, Gail Yamamoto, and Jamie Wong for the speedy procurement of required raw materials and equipment. Last but certainly not least, I am honored

by the support extended by my parents during these years. Many thanks go to my father, Robert Minei and my mother, Leilani Minei for their support for many years.

ABSTRACT

In this work, various types of Continuous Fiber Ceramic Composites (CFCCs) were manufactured using Polymer Infiltration and Pyrolysis (PIP) method for high mechanical performances. Two types of ceramic grade silicon carbide fibers, Nicalon™ and Hi-Nicalon™ Type S, as well as T300 carbon fiber were used as the reinforcements, and Polyramic® SPR-212, StarPCS™ SMP-10, and SMP-730 preceramic polymers were used as the matrix, in the study. Further, the effects of matrix sequence, referred to as "hybridization," and PIP processing at 1,000°C and 1,500°C on flexural mechanical performances of these newly developed CFCCs have been investigated and compared to their base CFCCs with their pristine matrices. Matrix hybridization method uses one type of preceramic polymer during the initial molding process and for the first iteration of PIP, then subsequent iterations of PIP use another type of preceramic polymer to infiltrate. All reinforcement fabrics, made of the three fiber systems mentioned above, were used for CFCCs at 1,000°C PIP, while only the HI-Nicalon™ Types S was used for CFCCs at 1,500°C PIP. Characterization analysis of the samples using optical microscopy as well as scanning electron microscopy were conducted. ASTM Standard four-point bending test at room temperature was conducted to evaluate the flexural mechanical performance of the developed ceramic composite samples. The mechanical performances were also compared across various fiber and matrix systems as well as PIP processing conditions of 1,000°C and 1,500°C. The different matrices displayed unique performance properties, while the matrix hybridization averaged two unique preceramic polymer properties closer together. A finite element method simulation technique was employed to verify the test results of the selected CFCCs that mechanically performed the best in their respective categories. The higher 1,500°C PIP CFCCs had higher stiffness compared to the 1,000°C CFCCs due to the ceramic changing

from amorphous to β-phase crystalline structure, while the lower 1,000°C CFCCs had higher strength, strain-to-failure, and toughness as compared with their 1,500°C PIP CFCC counterparts. Therefore, a manufacturing guideline is developed and suggested for the selection of the materials constituents and processing conditions depending on the desired mechanical properties for the developed CFCCs.

TABLE OF CONTENTS

LIST OF FIGURES

LIST OF TABLES

1. INTRODUCTION

Ceramic materials have various advantages over metallic materials and alloys for high temperature applications, especially in oxidizing environments. The applications in aerospace fields include rocket exhaust nozzles, heat shield and jet engine components [1]. Structural ceramics and composites have applications in areas including energy generation, environment, space, transportation and microelectronics [2]. Long-term mechanical reliability is a key issue in their final use for specific applications. Future use of advanced ceramics and various types of ceramic matrix composites in aerospace and astronautical applications include DoD applications in aircraft, missiles, munitions, and spacecraft, and civilian applications include aircraft, automotive transportation, and space vehicles [3]. This is due to ceramic's relative low density, high temperature strength, and corrosion and oxidation resistance capabilities in ceramic matrix composites [3]. Traditional monolithic ceramics meet most requirements for these applications; however, due to their brittleness and low toughness, they are not the ideal material of choice. Reinforcement of ceramic materials is a promising method for their increase toughness and fracture strength. Polymer matrix composites (PMCs) currently account for most of the composite materials used in gas turbines, despite their relative low temperature capabilities of typically less than 150°C [4]. Metal Matrix Composites (MMCs) are attractive for applications at intermediate temperatures while ceramic matrix composites (CMCs) offer greater possibilities for very high temperature applications where loads are modest [5]. CMCs combine reinforcing ceramic phases with a ceramic matrix to create materials with new and mostly superior properties. In CMCs, the primary goal of the ceramic reinforcement is to provide toughness to an otherwise brittle ceramic matrix. CMCs are being developed for applications that require

light-weight structural materials with oxidation and temperature resistance, including high strength and modulus [1, 2, 3]. Fillers can also be added to the ceramic matrix during processing to enhance characteristics such as electrical conductivity, thermal conductivity, thermal expansion, hardness, etc. The combination of these characteristics makes CMCs an attractive alternative to traditional industrial materials like high alloy steels and refractory metals. An important type of CMC that is currently being investigated is the Continuous Fiber-reinforced Ceramic Composite (CFCC). CMCs, particularly CFCCs, have received immense attention for use in high temperature structural materials [5, 6, 7, 8, 9]. CFCCs are significantly tougher and have higher fracture tolerance than their monolithic counterparts. These composites are attractive alternatives to monolithic ceramics and whisker-fiber CMCs [6], since CFCC fail with a tough, high strain mode, whereas conventional ceramics fail with a brittle mode [7]. It is the fiber reinforcement in the CFCC that prevent brittle failure, by providing various energy dissipation processes during crack propagation in the matrix as seen in Figure 1.1.

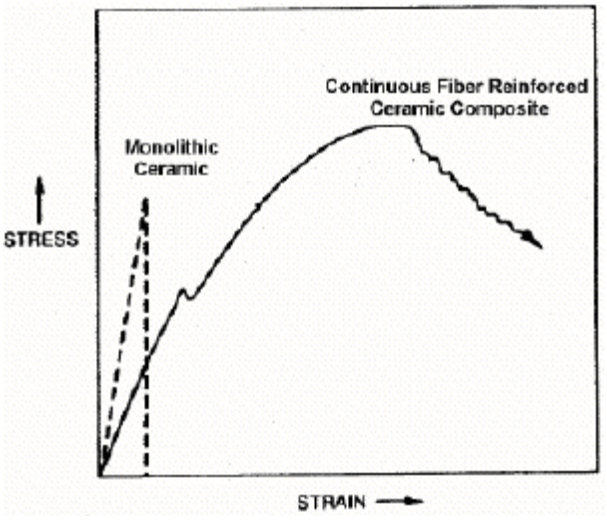

Figure 1.1: Failure modes for Monolithic Ceramic vs. CFCCs [7]

In both aerospace and automotive industry, there is an increasing demand for tougher, stronger, and lighter materials to replace metals and their alloys and structural materials. Future applications such as energy-efficient heat engines and high-subsonic or supersonic aircrafts and spacecrafts will utilize high-performance structural materials in selected elevated-temperature areas. The performance of CFCCs remains unchallenged by other materials in the temperature regime above 1200°C, as shown in Figure 1.2. The use of CFCC takes advantage of high strength and stiffness to weight ratios combined with the flexibility in tailoring the structure to meet loading conditions, resulting in greatly increased structural efficiency at very high temperatures. The performance properties in CFCCs coupled with multiple types of preceramic polymers and ceramic crystalline structures, provides a broad research area in processing and performance enhancements of CFCCs.

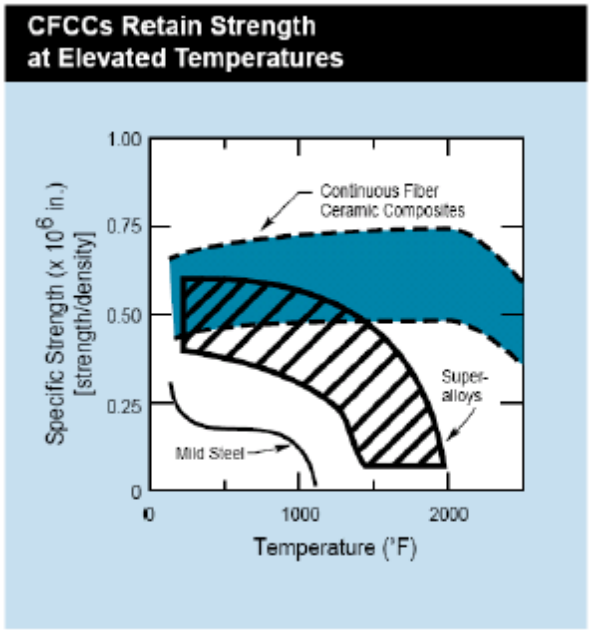

Figure 1.2: Advantages of using CFCC at elevated temperatures [9]

The preceramic polymer pyrolysis route to ceramic chemistry has attracted much attention, as it offers a promising and cost-effective way to manufacture CMCs/CFCCs with little to no final

machining [10, 11, 12, 13, 14, 15] and parts with greater compositional homogeneity [16, 17, 18]. Preceramic polymers are organo-metallic polymers which, after curing, are chemically transformed during their pyrolysis step to yield a contributing ceramic phase(s) in the final ceramic part. Other advantages of using the polymer pyrolysis technique include, the potential for high reproducibility of ceramic materials with respect to chemical properties and physical characteristics, lower processing temperatures and pressures, and improvement in the CMCs processing technique, including faster thermal cycles, lower rejects, and high reliability of parts. Traditional manufacturing techniques for CMCs, such as Chemical Vapor Deposition/Infiltration (CVD/CVI), powder processing, Sol-gel processing, etc., are time consuming and are in the order of two weeks [19, 20, 21]. Homogeneous parts with complex geometries cannot be manufactured by traditional methods due to the development of large density gradients within the CMCs leading to non-uniform parts [20, 21]. On the other hand, the disadvantage of the polymer pyrolysis technique is the inherent excessive matrix shrinkage [22, 23, 24, 25, 26] resulting in large residual stresses and micro-cracks. However, the percentage of the voids and micro cracks due to the pyrolysis can be reduced by successive reinfiltration/pyrolysis cycles. Other major disadvantage faced in processing CFCCs using Polymer Infiltration Pyrolysis (PIP) process is the amount of processing time it takes to attain the final good quality part. It was demonstrated that by adding different types of micron-sized inactive fillers, the amount of time required to manufacture CFCC samples can be considerably reduced [27]. However, samples manufactured by adding micron-sized inactive fillers, while reducing the processing time, considerably reduced the strength of the samples. This was attributed to premature closure of voids, and hence higher porosity and low final density of such samples [27]. Also, attempts have

been made to combine micron sized whiskers of chopped fibers with preceramic polymer, where whisker-fiber CMCs were developed [6].

1.1 Matrix Hybridization

Due to different characteristics of the preceramic polymers such as SMP-10 [28] & SPR-212 [29], we have undertaken a series of parametric manufacturing and testing of CFCCs with not only different matrices (i.e., SMP-10 and SPR-212) but also their hybridization. Of course, these matrices have different properties (see next section), adhesion characteristics to fibers, and final CFCCs performances even when used as single matrix. But, one of the goals of this study was to see the cost, processing, and performance relationship of the CFCCs made of the individual preceramic matrices as well as their hybrid to introduce, in this work, a system that is cost effective and performs well.

Two hybridizations of matrices were performed, they are SMP-10 hybrid and SPR-212 hybrid. SMP-10 hybrid uses SMP-10 only during initial wet-layup to mold the laminate, it is then infiltrated with SPR-212 for further PIP. SPR-212 hybrid is the opposite, it is molded with SPR-212 and further infiltrated with SMP-10.

1.2 Microstructure of Ceramic Matrix from Pre-Ceramic Polymers upon Pyrolysis

Silicon carbide (SiC) has a high specific stiffness and strength, with ideal applications in high stress and dynamic environments. It is only rivaled by beryllium metal but has 50% greater strength. SiC has a low coefficient of thermal expansion, allowing to maintain its dimensions in extreme hot or cold environments. It also has a very high thermal diffusivity that can carry heat

away quickly, preventing localized hot spots. The α-phase and β-phase structures of SiC are known for their high-temperature properties. SiC can be taken up to temperatures of 1700°C in pure oxygen with no drastic changes in mechanical properties, and at 1900°C and above, the β-phase ceramic begins transformation to α-phase [28].

StarPCS™ SMP-10 is a good baseline for comparison, as it produces the highest yield of SiC compared to Polyramic® SPR-212 which yields both SiC and SiOC. SMP-10 is liquid with a viscosity similar to water at room temperature [29]. As the temperature increases, the SMP-10 matrix becomes like "Gum-Rubber" at 250^{o}C (easily machinable). It will begin to harden like an epoxy at 400^{o}C (which is still easily machinable), then to a hard plastic at 650-700^{o}C (the hardness of this plastic phase increases between 700-850^{o}C), and finally to amorphous and crystalline silicon carbide at higher temperatures. Hardening occurs as the result of pyrolysis. During pyrolysis, the organic components of the polymer will outgas into the furnace atmosphere stream causing some cooling, leaving behind an inorganic ~35% porosity silicon carbide (***the char***), which will have relatively high emissivity (>80%) to provide radiative cooling in space while also being a relative insulator (due to the porosity) as compared to bulk SiC. Further Infiltration-Pyrolysis Iterations are needed to densify the part, and as the pyrolysis temperature increases the hardness of the material, and hence the stiffness of the final product increases. It becomes fully amorphous (glassy) between 850^{o}C and 1200^{o}C, and fully nano-crystallized β-phase between 1250-1700^{o}C (with Density of ~3.1 g/cc). The β-phase starts transferring to α-phase between 1900-2100^{o}C, and then it fully converts to α-phase nano-crystalline materials at 2400^{o}C. The ceramics formed are stable to 1800^{o}C in air and to 2200^{o}C in inert gases making them ideal for high temperature applications such as high porosity filters. The silicon carbide produced has a 1:1 silicon to carbon atomic ratio. Trace contaminating elements are typically at a

ppm level. It vaporizes at a temperature range of 2700-2800^{o}C. Therefore, the SMP-10 preceramic polymer to silicon carbide has a processing temperature dependent microstructure and material property. At lower pyrolysis temperatures, it yields β-SiC which can support operations all the way to 1700-1800^{o}C in an oxidizing atmosphere. Above a processing temperature of 1900^{o}C, α-phase SiC is obtained to support the upper temperature range of high-temperature applications (i.e., 2200^{o}C or more). It should be noted that the pyrolysis should be performed under an inert environment (e.g., argon gas), and as the pyrolysis temperature increases the hardness (and hence the stiffness for ceramics) increases, with a ceramic yield of 72% to 78%. The properties of StarPCS™ SMP-10 are given in Chapter 2.

Polyramic® SPR-212 is a liquid precursor to thermally stable silicon oxycarbide ceramics. SPR-212 is one of a family of polymers containing both Si-C and Si-O bond structures that cure to a thermoset at low temperatures. The cured polymer can then be fired to form a high temperature, oxidation resistant, glassy/ceramic material. The low viscosity liquid polymer can be used to produce coatings, molding compounds, and ceramic matrix composites. It is curable from RT to 180°C by use of suitable catalysts. Pyrolysis at 1°C/min to 850-1100°C in an inert environment (e.g., argon gas) produces black glassy/ceramic material with ceramic yields of 60% to 80%. The properties of Polyramic® SPR-212 are given in Chapter 2.

1.3 Continuous Fiber Ceramic Composites (CFCCs) by PIP

In the PIP process, the matrix polymer is first impregnated into the fiber architecture of choice, and then cured by conventional methods. Both the initial shaping and fabrication of the composite are carried out with low-temperature polymer processing and equipment. The composite is then pyrolyzed to temperatures equal or greater than 1000°C to convert the

preceramic polymer to a ceramic. Subsequent cycles of polymer infiltration and pyrolysis (PIP) steps are carried out to achieve the desired final density or open porosity.

1.4 Motivation

One of the important areas of concern is that even the best processed ceramic materials used in applications, pose many unsolved problems. Among them, relatively low toughness and strength, degradation of mechanical properties at high temperatures, and poor resistance to creep, fatigue, and thermal shock. Attempts to solve these problems may involve utilizing different preceramic polymers (and/or their hybridization), or reinforcement fabrics with varying mechanical characteristics. Another approach is to vary the PIP holding temperature to change ceramic crystalline microstructure, and hence changing their macro-properties. However, results using different reinforcements and matrices are rarely compared, arising difficulties for specific tailored mechanical characteristics. High temperature CFFCs studies above 1000°C have rarely been performed and oxidation or carbothermal decomposition during manufacturing processes with different materials are unknown. The main motivation of this work is to explore new techniques (such as hybridization) to improve the properties of the resulting ceramic-based composites employing the available pre-ceramic polymers. It also seeks to explore the effects of fiber properties and the processing temperatures on the properties of the resulting ceramic-based composites.

1.5 Goals of this Research Effort

The primary objectives of this research are to manufacture SiC/SiC, CFCCs using preceramic polymer infiltration and pyrolysis (PIP) route employing hybridization of preceramic polymers and various types of fiber materials. Other goals of this research are to investigate the influence of pyrolysis temperature on matrix hybridization and with differing reinforcement fabrics, and their effects on the mechanical performance of the resulting ceramic matrix composites. Mechanical performance of CFCCs were evaluated using four-point bending test (explained later in this thesis). SEM micrographs or optical microscopy were used to determine part qualities and performance of the manufactured specimens by studying the fracture surfaces.

1.6 Organization of Thesis

The first chapter contains a general introduction to CFCCs, matrix hybridization, microstructure of ceramic matrix based on the processing temperatures, and the motivation for the current study. The manufacturing methodology employed for the manufacturing of the CFCCs used in this study are discussed in Chapter 2. A detailed description of the manufacturing process involved, followed by a description of manufacturing route for different types of samples are presented in Chapter 3.

Quality assessment, and processing results for different CFCC samples are discussed in Chapter 4. Chapter 5 presents the four-point flexure test results for different sets of CFCC specimens, followed by comparison of mechanical property improvements/differences and fracture surfaces for CFCCs. Finally, conclusions are made in Chapter 6.

2 MANUFACTURING METHODOLOGY & MATERIAL SYSTEM

2.1 Introduction

The Polymer Infiltration & Pyrolysis (PIP) process used to fabricate CFCCs is widely recognized as a versatile method to fabricate large, complex-shaped structures. In comparison with other ceramic composite fabrication processes, the PIP process offers significantly greater flexibility. By utilizing low temperature forming and molding steps typically used in organic matrix composites, the PIP approach allows one to use existing polymer equipment and processing technology to form the parts.

2.2 Preceramic Polymer Technology

When the field of producing ceramics by preceramic polymer pyrolysis was emerging in the late 60's and early 70's, very few precursors were known. At that time, various carbon products were used. A review of the history of producing non-oxide ceramics from polymer pyrolysis is presented by Rice [15]. An investigative study was carried out to identify other precursors and structure-yield trends and determine the potentiality of producing ceramics via the preceramic polymer pyrolysis route.

The pyrolysis of organometallic polymers, or other precursors was found to be a novel method to manufacture ceramics. This extremely useful technique is widely applicable to include silicon carbide, silicon nitride, and boron nitride ceramics. Instead of using carbon polymers, silicon-based polymers are used to produce ceramics with high yield. The polymer-derived ceramics that can be produced by preceramic polymer pyrolysis include fibers, matrices, and coatings.

In preceramic polymer technology, a polymer is used as a starting material. Since a polymer is used as a precursor, conventional polymer manufacturing techniques and equipment can be utilized to fabricate ceramics and ceramic matrix composites. These methods include resin transfer molding, filament winding, pultrusion, wet lay-up using autoclave, etc. The part is shaped in the polymer condition using conventional manufacturing techniques, then cured and cross-linked to stabilize the shape of the part and finally is pyrolyzed to partially convert the polymer into a ceramic. During the pyrolysis, a portion of the polymer burns out and produces some combustion products that must be extracted from the furnace. This leaves the part with some porosity that must be overcome with subsequent reinfiltration and pyrolysis iterations through the cracks developed by residual stresses until the density convergence through a weight gain criterion is achieved. Pyrolysis is the necessary step of heating the part in order to convert the polymer matrix into a stable ceramic phase.

This is carried out in a high temperature furnace under a non-reactive gaseous, i.e., inert environment. Inert gases such as argon and nitrogen are used in preceramic polymer pyrolysis. Repeated infiltration steps are carried out to increase the density of the composite. With preceramic polymer fabrication, the number of infiltration steps used to fill the voids and pores caused by pyrolysis controls the density and porosity of the composite. The number of infiltration-pyrolysis steps range from 4 –13 depending on the fiber material and char yield of the polymer. Densities of preceramic polymers typically range from 1.1 to 1.2 g/cm3, with weight-based char yields ranging from 60% to over 90%.

The use of preceramic polymers overcomes many problems in processing conventional binders, including high part rejection rates and low part reliability. This technology has the advantage of fabricating and forming fiber-reinforced ceramic matrix composites that were difficult to make

via conventional binder techniques, and improvements in the CMC processing technique such as lower processing temperature.

Preceramic polymer technology in conjunction with wet lay-up opens the possibility of manufacturing complex-shaped CFCC's, which are tougher and stronger than their short fiber CMC counterparts.

2.3 Wet Lay-up Process

In the early days, the wet lay-up process was the dominant fabrication method for the manufacturing of composite parts. It is still widely used in the marine industry as well as for making prototype parts. This process is labor intensive, where liquid resin is applied to the mold and reinforcement and the process is continued until a desired thickness is obtained. It is a very flexible process that allows the user to optimize the part by placing different types of fabric and mat materials. Since the reinforcement is placed manually, it is called the hand lay-up process. This process requires little capital investment and expertise and is therefore easy to use [30].

There are four basic steps involved in a wet lay-up process of composites: wetting/impregnation, lay-up, consolidation, and solidification. All composites manufacturing processes involve more or less the same four steps, although they are accomplished in different ways. During the impregnation stage, the fibers and resins are mixed together to form a lamina. In this process, each fabric layer is wetted with resin using a squeezing roller for proper impregnation. The purpose of this step is to make sure that the resin flows entirely around all fibers. Viscosity, surface tension, and capillary action are the main parameters affecting the impregnation process. During the Lay-up stage, the desired composite thickness is built up by stacking various layers of wetted fibers on top of each other until the desires thickness is obtained. Performance of the composite structure relies heavily on fiber orientation and lay-up sequence.

Consolidation involves in creating intimate contact between each layer of prepreg or lamina. This step ensures that all entrapped air is removed from the in-between layers by resin flow during the processing. Consolidation is an important step to obtain good part quality. Poorly consolidated parts will have voids and dry spots. Proper consolidation is obtained when the applied pressure is equally shared by both the resin and fiber structure.

The final step is solidification, which may take less than a minute for thermoplastics or may take up to 120 minutes or more for thermosets. Vacuum and/or pressure is maintained during the period. The lower the solidification time, the higher the production rate achievable by the process. In thermoset composites, the rate of solidification depends on the resin formulation and cure kinetics. Heat is supplied during processing to expedite the cure rate of the resin and initiate linking in some cases.

On a commercial scale, this process is widely used for making boats, windmill blades, storage tanks, and swimming pools. Due to its process simplicity and little capital investment, this process is widely used for making prototype parts. Test coupons for performing various tests for the evaluation of reinforcements as well as resins are also made using this process [30].

2.4 Materials System

2.4.1 Preceramic Polymer

StarPCS™ SMP-10 [28] is a one-component liquid precursor to silicon carbide used to manufacture ceramic matrix composites, high-temperature silicon carbide coatings, and joined SiC materials. Monolithic ceramics are created from ceramic powders. It is capable of low temperature thermoset green cure where it produces a gel cure at 180°C to a hard cure at 400°C, depending on required hardness and machinability. SMP-10 produces an amorphous (glassy) SiC form at 850-1200°C, then transitions to nano-crystalline β-SiC form, and is completely

converted to β-SiC phase at 1700°C. This polymer produces near stoichiometric SiC of 1:1 silicon to carbon atomic ratio with high purity yields. Typical ceramic yields, an indication of mass conversion to ceramic material, as measured by thermal gravimetric analysis (TGA), is about 72-78% in argon. There are very few contaminants remaining after pyrolysis, typically measured in ppm. The ceramics formed are ideal for high temperature applications and is stable to 1800°C in open air and 2200°C in inert atmosphere. Table 2.1 gives the physical properties of SMP-10.

Table 2.1: Properties of StarPCS™ SMP-10 [28]

Density	0.998 g/cm^3
Appearance	Clear, Amber Liquid
Viscosity	40 to 100 cPs at 25°C
Compatible Solvents	Hexanes, Tetrahydrofuran, Toluene, Insoluble in water
Flash Point	89°C (192°F)
Moisture Absorption	<0.1% in 24 hours at room temperature
Surface Tension	30 dynes/cm^2
Odor	None
DOT / IATA Regulations	Non Hazardous
Storage	Vacuum container or inert environment; Refrigerated

Polyramic® SPR-212 [29] is a liquid precursor that pyrolyzes to a thermally stable silicon oxycarbide SiOC. SPR-212 cures to a thermoset at low temperatures and contains both Si-C and Si-O bond structures. It is a low viscosity liquid polymer for increased infiltration efficiency used to produce coatings, molding compounds, and CMCs, that can then be pyrolyzed to form high temperature, oxidation resistant, glassy ceramics. The low viscosity facilitates high solids loading with bulk fillers. This polymer can be cured at room temperature to 180°C with increased yields through the addition of a small amount of free radical initiators such as dicumyl peroxide or a platinum catalyst. Around 0.25-1.5 phr of dicumyl peroxide or 5-40 ppm of platinum is sufficient to initiate cure. Platinum catalyst [31] of 2% by weight was used in this work. Typical TGA ceramic yields are 60-80% depending on catalyst used. The ceramics

produced are thermally stable in open air till 1200°C and retains over 98% of original mass and appearance after 1hour at 1400°C or 500 hours at 1100°C with repeated thermal loading in open air. Table 2.2 gives the physical properties of SPR-212.

Table 2.2: Properties of Polyramic® SPR-212 [29]

Density	1.0 g/cm^3
Appearance	Clear, slightly milky
Viscosity	12 - 26 cPs
Compatible Solvents	Hexanes, Tetrahydrofuran, Toluene, Xylene
Flash Point	62°C
Moisture Absorption	< 0.1% in 24 hours at room temperature
Surface Tension	26 dynes/cm^2
Odor	Mild
Dot / IATA Regulations	Non Hazardous
Storage	Room Temperature*

StarPCS™ SMP-730 [32] is a polycarbosilane precursor that produces a thermally stable SiC. SMP-730 is unique in that it's solid at room temperature and is processable as a thermoplastic, with melt-processable temperatures up to 100°C. It can be recycled with repeatedly melting and solidification, making it one of the few ceramic precursors that can be used for prepreg manufacturing. This also accommodates simplified introduction of bulk fillers, that improve yields and decrease processing time. Upon heating to higher temperatures of 300°C, the polymer then cures to a thermoset solid that can be easily machined. The polymer pyrolyzes to form high temperature, oxidation resistant, amorphous SiC. Typical TGA ceramic yields are 65-67% neat or 85-87% with filler. Ceramics produced retain greater than 99.4% of mass after 48 hours of oxidation at 1000°C in open air. Table 2.3 gives the physical properties of SMP-730.

Table 2.3: Properties of StarPCS™ SMP-730 [32]

Density	1.0 g/cm^3
Appearance	Amber colored solid, clear / opaque
Viscosity	Solid at Room Temperature
Compatible Solvents	THF, Hexane, Toluene, Xylene
Flash Point	>93°C (>200°F)
Filler Type	Refractory; Starfire Proprietary Distribution (optional)
Filler Loading	0 - 15 vol%
Odor	Mild
Catalyst	None
DOT / IATA Regulations	Non Hazardous
Storage	Vacuum container or inert environment; Refrigerated

2.4.2 Fiber Selection

Nicalon™ [33] is a SiC type fiber and has a desirable combination of modulus, strength, density, and electrical properties with retention of these properties at elevated temperatures up to 1200°C. The fiber is homogeneously composed of small grain β-SiC crystallites and an amorphous mixture of silicon, carbon, and oxygen. It has a composition by weight of 31% carbon (C), 57% silicon (Si), and 12% oxygen (O). The architecture of the fiber used in this work is plain weave with 16 thread count/inch in both warp and weft directions. Table 2.4 gives the physical properties of Nicalon ™ SiC fibers

Table 2.4: Properties of Nicalon™ SiC fiber [33]

	Ceramic Grade	HVR Grade	LVR Grade
Tensile Strength, GPa	2.60	2.40	2.44
Tensile Modulus, GPa	188	174	180
Oxygen Content, wt%	10.5-13.5	10.0-15.0	
Density, g/cc	2.5-2.65	2.25-2.4	2.4-2.55
Tex g/km	200-220		
Fiber Denier	1800		
Sizing Amount, wt%	0.5-2.0		
Vol. Resistivity, Ω•cm	$1x10^3$-$1x10^4$	$1x10^6$-$1x10^7$	Report

Hi-Nicalon™ Type S [34] is similar to standard Nicalon™ SiC fibers but has a stoichiometric β-SiC crystallite and manufactured near-oxygen-free using decarbonization pyrolysis and electron-beam curing. It has higher modulus, creep resistance, thermal and oxidation resistance than it counterpart. It has an elevated thermal stability to 1800°C and has a composition by weight of 31% carbon (C), 68.8% silicon (Si), and 0.2% oxygen (O). This results in a large increase in stiffness, but slightly lower strength than standard Nicalon™ fibers. The architecture of the fiber used in this work is 5 harness satin with 16 thread count/inch in both warp and weft directions. Table 2.5 gives the physical properties of Hi-Nicalon™ Type S.

Table 2.5: Properties of Hi-Nicalon™ Type S [34]

Fiber Denier	1800
Density, g/cc	2.85
Composition, wt % Si:C:O	69:31:0.2
C/Si Atomic Ratio	1.05
Tex, g/km	180-210
Filament Diameter, μm (nominal)	12
Tensile Strength, GPa	2.30
Tensile Modulus, GPa	340
Oxygen Content, wt%	≤ 1.0
Sizing Amount, wt%	0.5 – 2.0

T300 carbon fiber [35] is a baseline carbon fiber known for its balance physical properties that are very similar to standard Nicalon™ SiC fiber. Plain weave 3k carbon fiber is used in this work. Table 2.6 gives the physical properties of T300 carbon fiber.

Table 2.6: Properties of T300 carbon fiber [35]

PROPERTY	ENGLISH	METRIC	METHOD
Tensile Strength	512 ksi	3,530 MPa	TY-030B-01
Tensile Modulus	33.4 Msi	230 GPa	TY-030B-01
Strain at Failure		1.5%	TY-030B-01
Density		1.76 g/cm^3	TY-030B-02
Filament Diameter		7 µm	
Yield	1K	66 g/1000m	TY-030B-03
	3K	198 g /1000m	TY-030B-03
	6K	396 g /1000m	TY-030B-03

3 MANUFACTURING PROCESS

3.1 Introduction

The manufacture of Continuous Fiber Ceramic Composites by Hand Lay-up using Polymer Infiltration Pyrolysis (PIP) consists of two steps as shown in the flow chart given later in this chapter. The first step involves impregnating/infiltrating the fiber preform with preceramic polymer and stacking them on top of each other to achieve a desired thickness, followed by compression molding (see in Figure 3.1) and curing in the hot press (see Figure 3.2).

The second step consists of pyrolyzing the cured sample, thereby converting the preceramic polymer into ceramic (in a high-temperature furnace shown later in this chapter), followed by subsequent reinfiltration/pyrolysis cycles to achieve weight convergence.

3.2 Manufacturing of CFCC Specimens for Mechanical Testing

3.2.1 Wet Lay-up of Fiber Cloths

Plain weave T300, plain weave Nicalon™, 5 harness satin Hi-Nicalon™ Type S SiC fiber cloths are used as the fiber architecture for the manufacturing of the mechanical test specimens. StarPCS™ SMP-10, SMP-730, and Polyramic® SPR-212 preceramic polymer are the matrices used in the current study. The thickness of the fibers preform was measured using a micrometer, which was approximately 0.0125'' for the plain weave T300 and Nicalon™ cloths and 0.008" for the 5-harness satin SiC cloth. The preform was cut into dimensions of 6'' x 4'' layers from the roll.

For the manufacturing of the mechanical test samples, 6 layers of plain weave for T300, 3 layers of plain weave for Nicalon™, and 10 layers of 5 harness satin were used for each plate. In this

process, initially each layer of fiber preform is properly impregnated with the preceramic polymer. Special care was taken to wet the fibers with sufficient amount of polymer for a good bonding between the laminae. After wetting the fiber preform, the wet laminae were stacked on top of each other and, subsequently, pressed using a roller until a desired thickness was obtained. Also, a foam brush was used to remove all the excess resin before and after lay-up.

3.2.2 Compression Molding and Curing

This section of the thesis explains the compression molding and curing process. To manufacture the composite plates, two appropriate aluminum plates were selected. A two-millimeter-deep and on-millimeter-deep rectangular trench with dimensions of 6" x 4" was milled out of two separate plates to serve as a mold and another plate was untouched and used as the cover plate. This mold is shown in Figure 3.1. Next, the mold was sand gritted with 220 grit paper (coarse) and then with 400 grit paper (fine) in a circular motion and degreased with acetone. A thin layer of high temperature polishing wax is applied on the plate and left for a few minutes, followed by removal of it using a lint free cloth for better surface finish on the specimens. Dry mold release agent was then sprayed on the plate for easy removal of the part after the manufacturing.

Figure 3.1: Manufactured Aluminum mold.

After initial preparation of the base plate and the cover plate, the wet lay-up stacked laminae is placed in the mold cavity and then covered with the cover plate. The mold is then put in the compression molding machine for curing and consolidation as shown in Figure 3.2 below.

Figure 3.2: Compression molding machine.

Samples are cured at the maximum temperature of 200^{o}C under uniform pressure of 120 psi.

Figure 3.3 shows the curing profile used in this work.

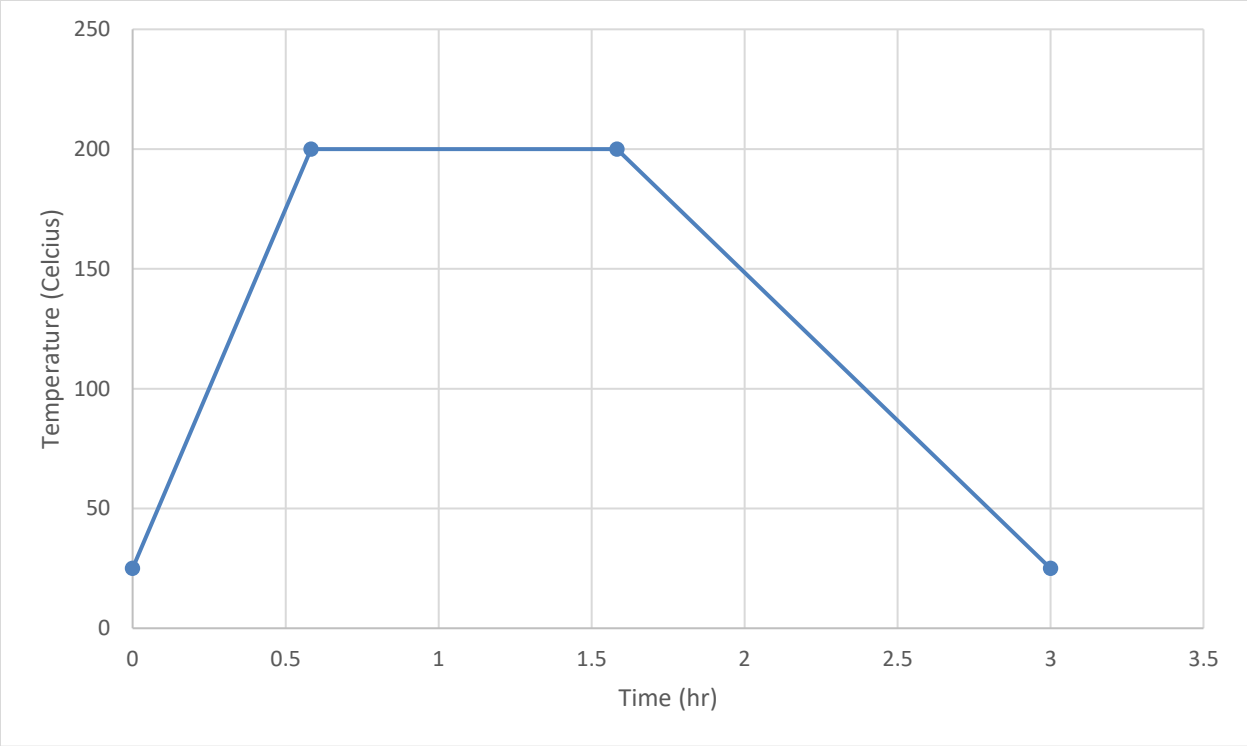

Figure 3.3: Compression molding machine cure cycle (Note: no vacuum was applied).

Before curing (B-staging) starts, pressure was applied by the compression molding top and bottom plates first and temperature was raised to a dwelling level. The temperature rise was from room temperature to 200 degrees C in ~0.5 hour, dwelled for 1 hour and cooled to room temperature. Hence, the total cycle time was 3 hours. The maximum heating rate of the Compression Molding Machine was 5 degrees C/min. After the cooling, the cured laminate is removed from the mold as shown in Figure 3.4. The consolidated green ceramic plates were then ready to be cut and weighed before densification.

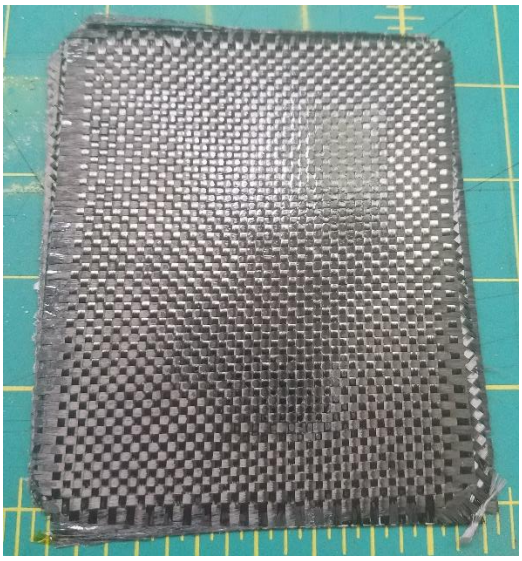

Figure 3.4: Cured green ceramic composite plate.

The edges of the manufactured plate after B-Staging were trimmed off and the samples were cut according to ASTM C 1341 [36] in required dimensions for mechanical testing (see Figure 3.5).

Figure 3.5: Cured and cut green ceramic composite beams.

At this stage, specimens are ready to be densified via Polymer Infiltration and Pyrolysis (PIP) route.

3.2.3 Pyrolysis / Infiltration / Pyrolysis (PIP)

After B-staging, cutting, and initial weighing, the cut laminates were then pyrolyzed in a high temperature furnace, as seen in Figure 3.6, in an inert environment to convert the polymer into ceramic.

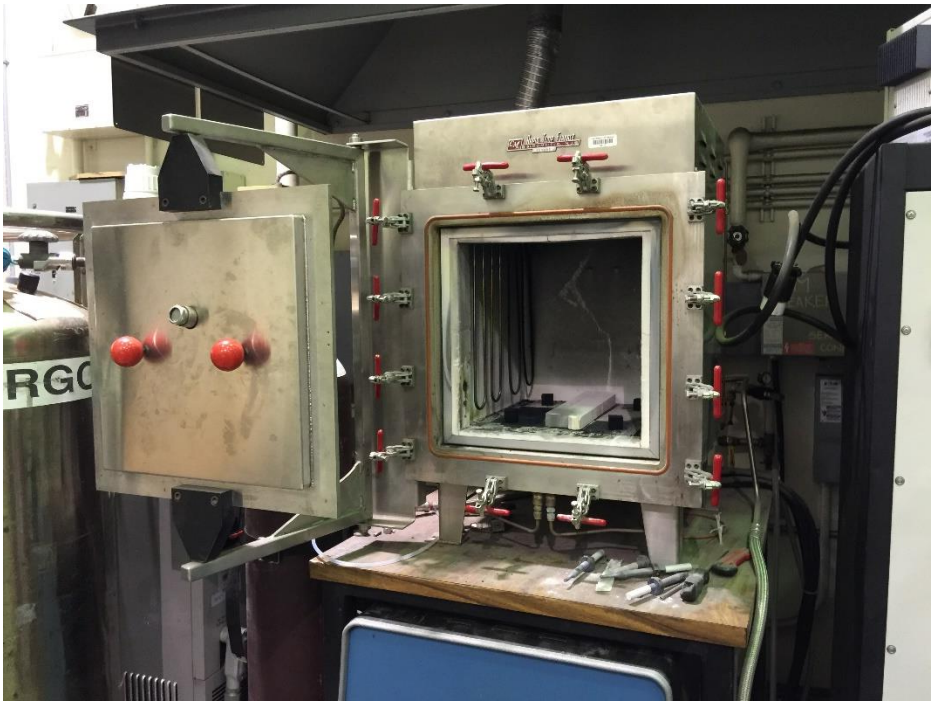

Figure 3.6: Pyrolysis high-temperature furnace.

The thermal cycle for the pyrolysis is as shown in Figure 3.7. The samples were heated from room temperature to 200°C at a heating rate of 5°C/min, ramped from 200°C to 400°C at a rate of 2°C/min, dwelled at 400°C for 1 hour, ramped from 400°C to 650°C at a rate of 2°C/min, ramped from 650°C to 1000°C at a rate of 3°C/min, dwelled at 1000°C for 1 hour. For the study

of 1500°C, it instead ramped from 650°C to 1500°C at a rate of 3°C/min, dwelled at 1500°C for 1 hour. The furnace was then allowed to cool down at a rate of 3°C/min to 250°C under inert argon gas environment. The samples were finally allowed to cool down to room temperature by natural convection. The total cycle time for each pyrolysis step was approximately 14 hours for 1000°C study and 19 hours for 1500°C study. The test samples were then removed from the furnace, weighed, and measured again.

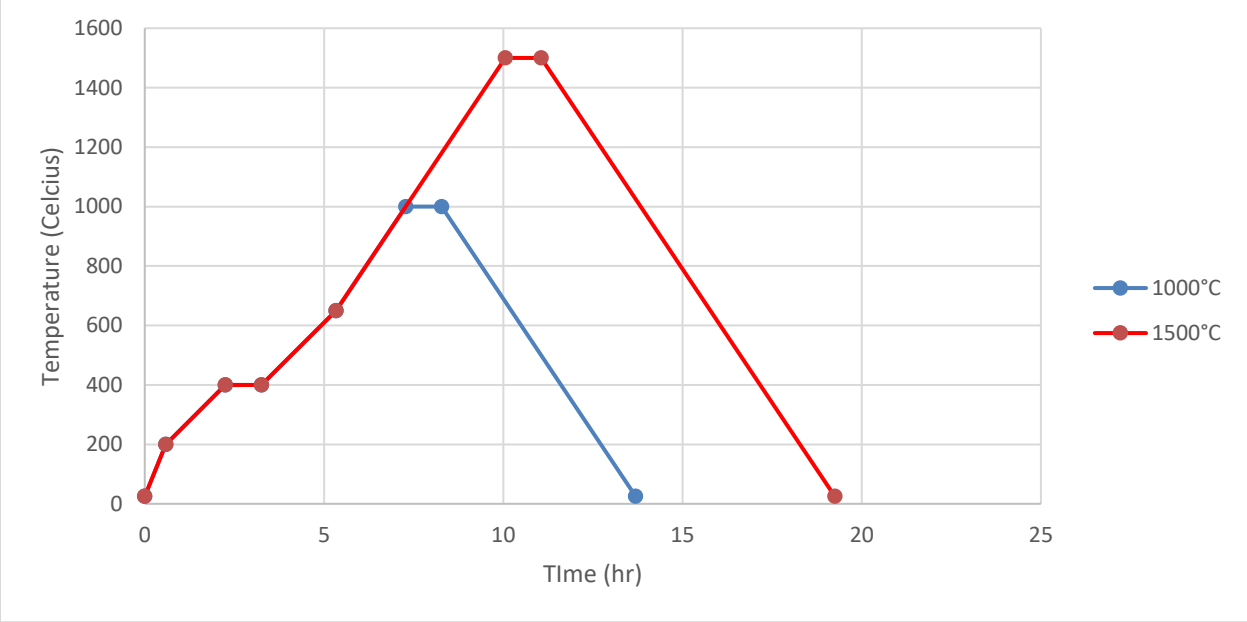

Figure 3.7: Thermal cycle for pyrolysis.

Pyrolyzed parts were immersed in preceramic polymer for reinfiltration. Reinfiltration is necessary to increase the part density and fill the voids and microcracks inside the samples created by matrix shrinkage and conversion of polymer to ceramic during the pyrolysis step. The samples were allowed to stay in the polymer until all the bubbling subsided in the reinfiltration stage, which took 6-8 hours. Once the bubbling subsided, the samples were removed from the preceramic polymer, wiped free of excess resin and placed into alumina combustion boats. The

boats were then placed inside a mechanical convection oven and cured according to the cure cycle previously outlined, without pressure. After the curing, the samples go through a pyrolysis stage in an inert environment according to the pyrolysis thermal cycle previously outlined. After this stage, the samples received their first densification, i.e., State 1. This densification cycle was repeated until the samples were fully densified. All the samples manufactured converged in weight gain according to the weight convergence criterion used. The criterion for weight gain convergence was that the last sequential weight gain of the samples should be less than 1%. The total manufacturing time for a CFCC sample was around 10 days. Figure 3.8 shows the general CFCC manufacturing methodology employed to manufacture the required test samples.

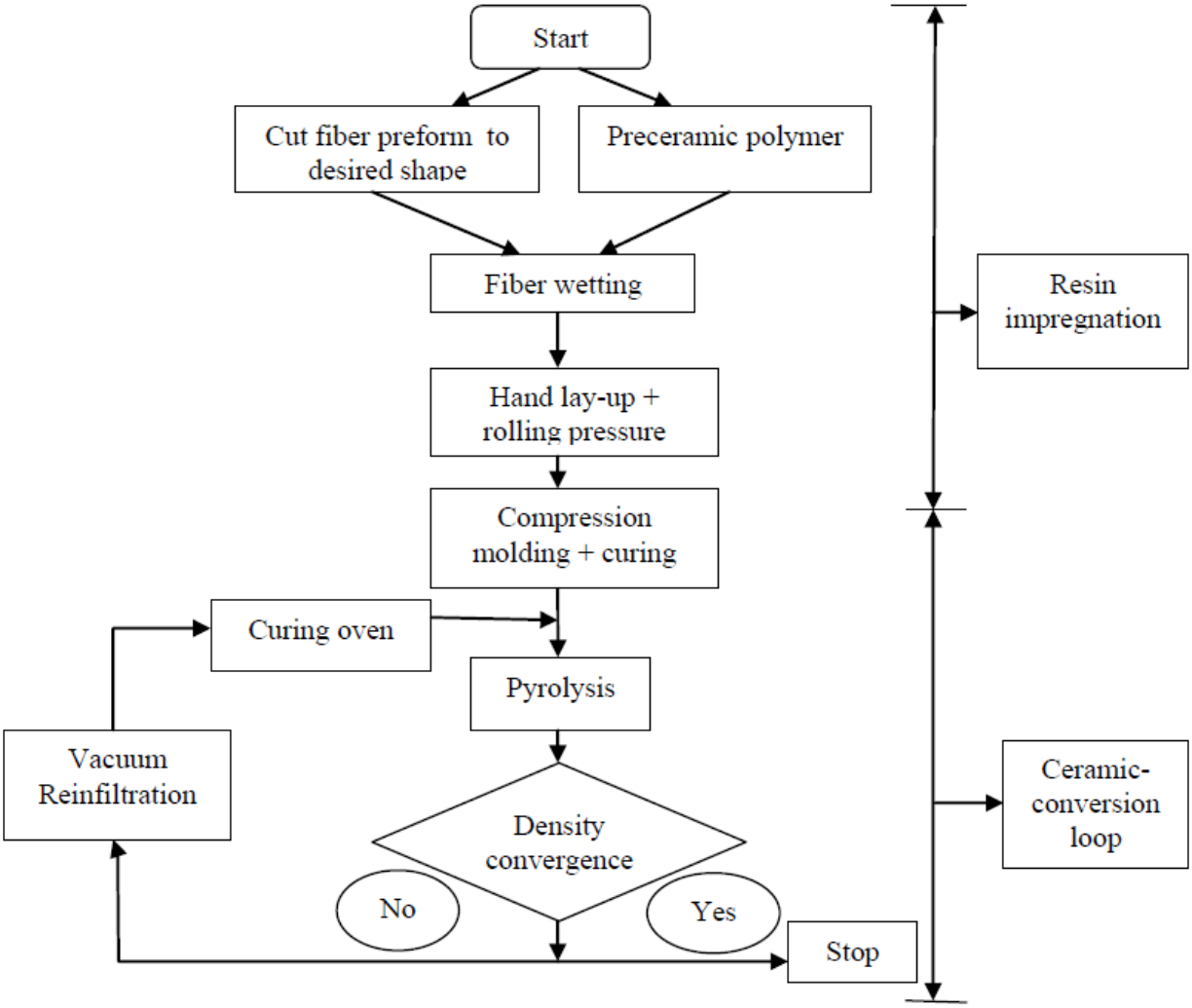

Figure 3.8: CFCC manufacturing methodology.

3.2.4 Vacuum Infiltration vs. Passive Infiltration

In this work, a forced type of polymer impregnation was employed versus the traditional passive dipping method. As shown in Figure 3.9, a Pelican® case [37] was modified to be used as a vacuum container. Articles were placed in a pool of polymer inside the vacuum container, where after proper sealing; a 90% vacuum has been achieved. The vacuum pressure inside, forces the preceramic polymer deep into the pores of the specimens to ensure proper densification and to prevent premature closure on the surface of the specimens which would result in a porous CFCC.

Figure 3.9: Modified Pelican® case used as a vacuum compartment [37].

3.3 Manufacturing Procedure for CFCCs

The general process of manufacturing continuous fiber ceramic composites can be explained by the following steps: wet lay-up, curing, and polymer pyrolysis/reinfiltration cycles. The above process was explained in detail in Section 3.2. To evaluate the effects of matrix hybridization and PIP temperatures on processing and flexural mechanical properties, 9 types of CFCCs were manufactured. The T300 laminate consisted of 6 layers of plain weave prepregged with SMP-730 and given SMP-10 hybrid matrix. The Nicalon™ laminates consisted of 3 layers of plain weave with 4 different laminates consisting of SMP-10, SPR-212, SMP-10 hybrid, and SPR-212 hybrid matrices. Both the T300 and Nicalon™ SiC fibers were only pyrolyzed at 1000°C. The Hi-Nicalon™ Type S laminates consisted of 10 layers of 5 harness satin weave with 4 different laminates consisting of SMP-10, SPR-212, SMP-10 hybrid, or SPR-212 hybrid matrices for 1000°C PIP and another set of 4 laminates consisting of the same matrices for 1500°C PIP. All laminates were cut from the fabric lot to achieve the desired thickness of 2 mm with exception of Nicalon™ laminates with a thickness of 1mm, in accordance with ASTM standards [36].

3.3.1 Manufacture of T300 CFCC

T300 CFCC consist of T300 carbon fiber and is the only fabric to be prepregged with SMP-730, based on the recommendation of the preceramic polymer supplier. The six layers of carbon fabric is wetted with SMP-10 and is stacked up using the wet lay-up technique, followed by curing using the compression molding machine. Next, the edges of the laminated composite plate are trimmed and the samples of required dimensions (based on the ASTM C 1341-06 standard) are cut using a diamond blade cutter. The cut samples are then pyrolyzed in a high temperature furnace to 1000°C in an inert argon gas environment to convert the preceramic polymer into ceramic. To convert the porous ceramic into a dense ceramic, after the first pyrolysis step, subsequent reinfiltration/pyrolysis using SPR-212 are followed as outlined previously to achieve the required dense CFCC test specimens. The manufacturing process remains the same as explained in Section 3.2.3 and is shown in Figure 3.8. The process of curing and molding the laminate to B-stage using SMP-10 then subsequently infiltrating with SPR-212 is referred to as SMP-10 hybrid and explained in Section 1.1. The T300 laminate was only pyrolyzed to 1000°C, because the excess carbon (the fabric itself) deteriorates or goes through a carbothermal decompositions and into CO or CO_2, which dissipates out of the laminate. This severely reduces the laminates mechanical properties and deteriorates or loses its physical dimensional stability in between PIP cycles to a point where the sample become untestable.

3.3.2 Manufacture of Nicalon™ CFCCs

Four different systems of CFCCs with Nicalon™ fiber reinforcements were manufactured. Two of the laminates were manufactured with pristine SMP-10 and SPR-212 while the other two used SMP-10 hybrid and SPR-212 hybrid. The manufacturing process of hybridization remains the same as explained in the section above, except the fabric was not prepregged. The Nicalon™

laminates was also only capable of 1000°C PIP and listed from the manufacturer [33] to be thermally stable to 1200°C. To verify the carbothermal decomposition, a laminate was attempted to be manufactured with 1500°C PIP, but failed mid iterations as shown in Figure 3.10. This is caused by the high oxygen content within the fabric which dissipates out of the sample as CO or CO_2, degrading the fabric.

Figure 3.10: Carbothermal decomposition of Nicalon™ laminates at 1500°C PIP.

3.3.3 Manufacture of Hi-Nicalon™ Type S

In this study, the manufacturing process remains the same as Nicalon™ laminates mentioned in Section 3.3.2 for 1000°C PIP, but another four additional laminates were manufactured for a total of eight laminates. The additional four laminates were created with the same matrices of SMP-10, SPR-212, SMP-10 hybrid, and SPR-212 hybrid to be used in 1500°C PIP. The manufacturer lists the Hi-Nicalon™ Type S [34] fabric thermally stable to 1800°C and is the only laminate to survive 1500°C PIP to be tested.

4 PROCESSING RESULTS AND DISCUSSION

4.1 Processing Results for T300 CFCCs

This section details and analyzes the processing results for continuous fiber ceramic composites manufactured with T300 carbon fiber reinforcement prepregged with SMP-730 using SMP-10 hybrid process of preceramic polymers. In this work, for each sample, a gain in weight of less than 1% from previous pyrolysis/reinfiltration cycle was considered as the convergence criterion. Nicalon™ CFCC with SMP-10 hybrid will be used as a comparison since both are manufactured with similar matrix hybridization and layers of cloth. The difference in weight for the samples after the first and the last pyrolysis/reinfiltration cycle is reported as cumulative percentage weight gain in Table 4.1.

Table 4.1: Processing results for T300 CFCC.

Specimen Type	Weight Gain (%)
T300 SMP-10 Hybrid	29.55
Nicalon™ SMP-10 Hybrid	30.86

In addition, Figure 4.1 plots the cumulative weight gain percentages of the two types of CFCCs covered in this section against pyrolysis/reinfiltration cycles. It can be seen that both have around the same total weight gain, but the rate at which the two increases in weight are different. The T300 lost a significant amount of weight after the first and second pyrolysis in comparison to the Nicalon™, which is most likely due to it being prepregged with SMP-730 before hybridization process. It then surpasses the Nicalon™ in weight gain on the third pyrolysis because of the increased porosity from initial weight drop. An unknown anomaly appears in between the third and fourth pyrolysis causing the weight gain to taper down. A possible

explanation could be because of loose ceramic grains appearing within the structures pores during the large weight gains in the third iteration and only homogenizing during the fourth.

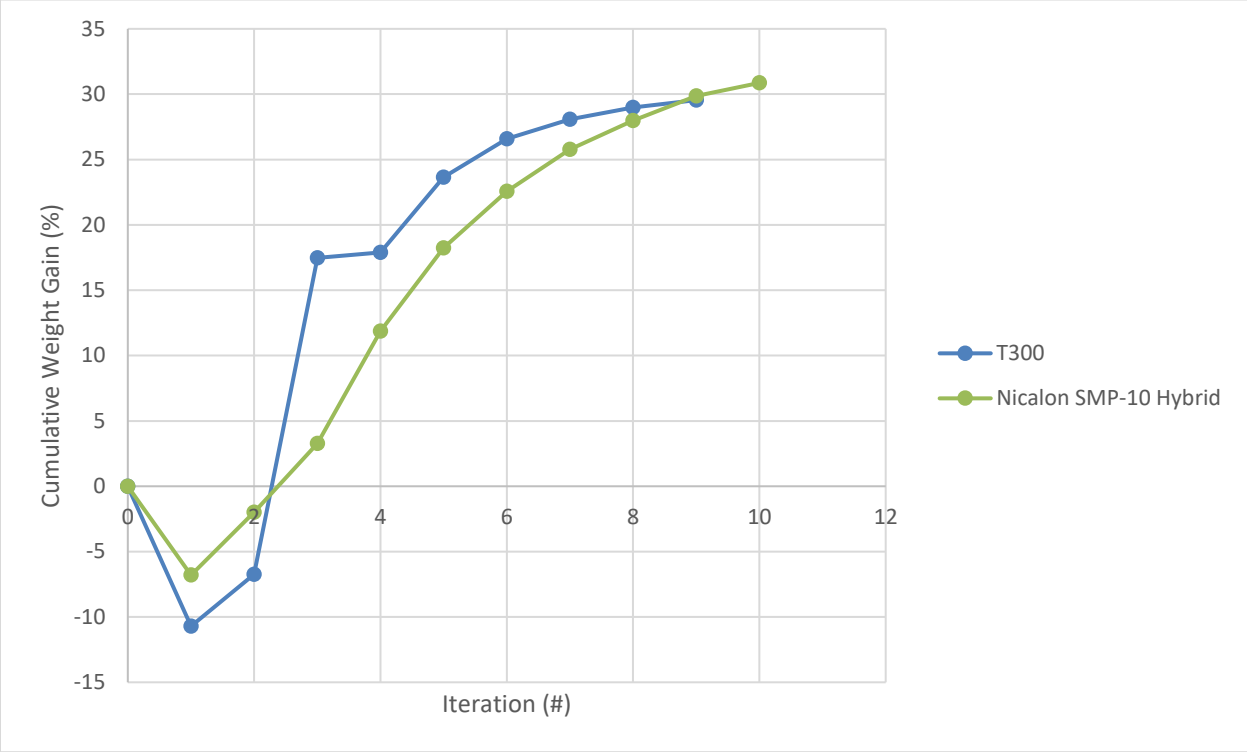

Figure 4.1: Comparison of cumulative weight gain (%) for T300 and Nicalon™ SMP-10 Hybrid after each pyrolysis cycle at 1000°C.

Furthermore, it is noted that the Nicalon™ SMP-10 hybrid took one more iteration of PIP than T300 to converge. This is also due to the T300 being prepregged with SMP-730 prior to matrix hybridization. With both the T300 carbon fiber and Nicalon™ SiC fiber reinforcement laminates converging roughly at the same pyrolysis cycle, this suggests that the matrix impregnation of both fabrics is similar.

4.2 Processing Results for Nicalon™ CFCCs

This section covers four individual sets of Nicalon™ CFCCs with SMP-10, SPR-212, SMP-10 hybrid, and SPR-212 hybrid preceramic polymers. The weight convergence criteria are the same as the section above. The reported cumulative weight gains are in Table 4.2 below.

Table 4.2: Processing results for Nicalon™ CFCCs.

Specimen Type	Weight Gain (%)
Nicalon™ SMP-10	28.08
Nicalon™ SPR-212	37.20
Nicalon™ SMP-10 Hybrid	30.86
Nicalon™ SPR-212 Hybrid	46.08

Figure 4.2 plots the cumulative weight gain percentages of the four types of Nicalon™ CFCCs against pyrolysis/reinfiltration cycles. SPR-212 pristine has a higher weight gain than SMP-10 pristine, but the same cannot be said for the hybrids. SPR-212 hybrid is molded with SPR-212 and infiltrated with SMP-10 until weight convergence, hence the majority of ceramic yield is from SMP-10 and vice versa for SMP-10 hybrid. Yet, SPR-212 hybrid, which is again, majority SMP-10, has a higher weight gain than SMP-10 hybrid. This could be attributed to SPR-212 hybrid increasing slightly in dimensions/volume compared to the other samples. SPR-212 reduces in weight more than the SMP-10 during the first iteration of pyrolysis, with the hybrids having similar results to their respective base matrix. This phenomenon could also be due to the first matrix infiltration having a larger role in overall weigh gain. An interesting note, in Figure 4.2, is that the trend/shape of the cumulative weight gain curves for SPR-212 pristine and SMP-10 hybrid (which has a majority of its matrix as SPR-212) is similar, and a similar trend can be seen for the SMP-10 pristine and SPR-212 hybrid. Also, as a note, very few samples survived PIP, because of the care needed to handle and clean 1mm thick samples.

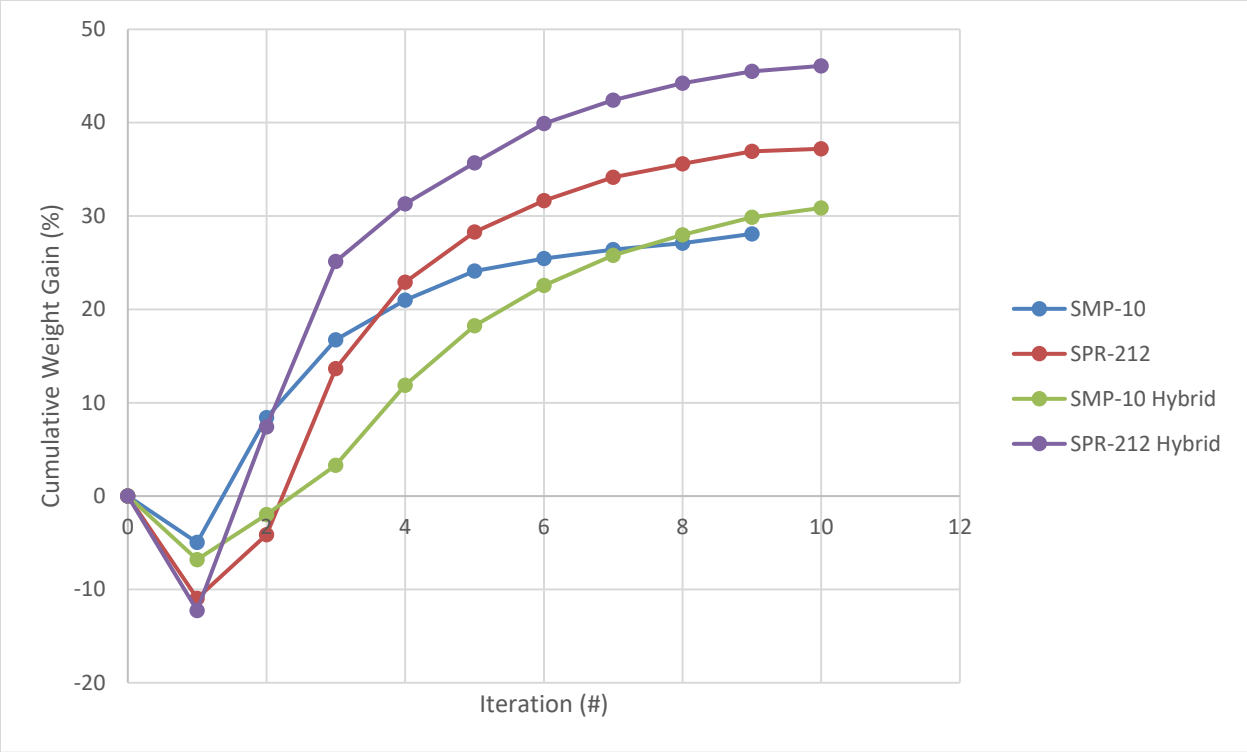

Figure 4.2: Comparison of cumulative weight gain (%) for Nicalon™ CFCCs after each pyrolysis cycle at 1000°C.

All sample weights converged at the tenth iteration, with the exception of SMP-10 converging at the ninth iteration. Therefore, all matrices completely densify and achieve complete pore closer at the same rate, based on our less than 1% cumulative weight gain convergence criterion. It is believed that the difference in cumulative weight gain is due to the difference in the characteristics of the matrices or their hybrid systems.

4.3 Processing Results for Hi-Nicalon™ Type S CFCCs at 1000°C Pyrolysis

This section covers four individual sets of Hi-Nicalon™ Type S CFCCs pyrolyzed at 1000°C with SMP-10, SPR-212, SMP-10 hybrid, and SPR-212 hybrid preceramic polymers. The weight convergence criteria are the same as the previous sections. The reported cumulative weight gains are given in Table 4.3 below.

Table 4.3: Processing results for Hi-Nicalon™ Type S at 1000°C pyrolysis.

Specimen Type	Weight Gain (%)
Hi-Nicalon™ Type S SMP-10	58.76
Hi-Nicalon™ Type S SPR-212	51.61
Hi-Nicalon™ Type S SMP-10 Hybrid	66.31
Hi-Nicalon™ Type S SPR-212 Hybrid	52.78

Figure 4.3 plots the cumulative weight gain percentages of the four types of Hi-Nicalon™ Type S CFCCs against pyrolysis/reinfiltration cycles. SMP-10 pristine has a higher weight gain than SPR-212 pristine, but vice versa for the hybrids; however, it should be noted that SPR-212 and SMP-10 hybrid (with the majority of the matrix being SPR-212) went through 8 iterations while SMP-10 and SPR-212 hybrid (with the majority of the matrix being SMP-10) went through 10 iterations. SMP-10 hybrid, which has a majority ceramic yield from SPR-212, has the highest weight gain, possibly because of its ability to infiltrate the porous structure left behind by its base SMP-10 compared to the other hybrid or pristine matrices. SMP-10 typically gains more mass due to its higher ceramic yield density, on the other hand, SPR-212 ceramic precursor has a lower viscosity than SMP-10 allowing it to completely fill internal pores and microcracks, which is evident in its quicker weight convergence. All samples lose close to the same amount of weight after the first iteration, but SMP-10 and SMP-10 hybrid lose slightly less than SPR-212 and SPR-212 hybrid. This correlates with the base matrix of the hybrids and its pristine matrix. Once again, an interesting note, in Figure 4.3, is that the trend/shape of the cumulative weight gain curves for SPR-212 pristine and SMP-10 hybrid (which has a majority of its matrix as SPR-212) is similar, and a similar trend can be seen for the SMP-10 pristine and SPR-212 hybrid.

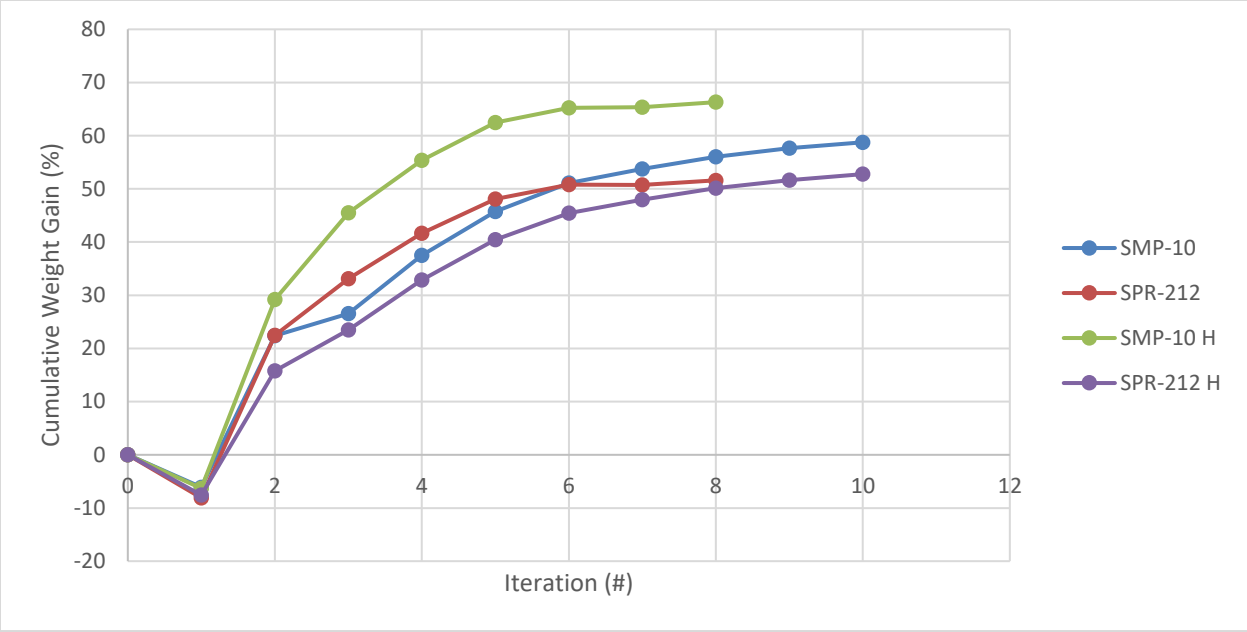

Figure 4.3: Comparison of cumulative weight gain (%) for Hi-Nicalon™ Type S CFCCs after each pyrolysis cycle at 1000°C.

As mentioned earlier, the rate of weight gain and weight convergence of SMP-10 and SPR-212 hybrid follow the same trend, with SPR-212 hybrid offset with a lower weight gain at each cycle. The lower offset of SPR-212 hybrid weight can be explained by the lower density ceramic remaining from which it was molded from. The same can be said for SPR-212 and SMP-10 hybrid, but SMP-10 hybrid has a higher weight even to SMP-10. This can be largely attributed to SPR-212s lower viscosity and possibly the molecular surface interface to SMP-10 during pyrolysis. The lower viscosity also converged two cycles quicker than its SMP-10 counterparts.

The disparity of total weight gains between Nicalon™ and Hi-Nicalon™ Type S is because of different reinforcement architectures and thickness. The Nicalon™ laminates were made out of a thicker plain weave, requiring 6 layers of cloth to attain the desired thickness of 2mm. While the Hi-Nicalon™ Types is only available in a thinner 5 harness satin weave, which required 10 layers of cloth to attain the same thickness. Therefore, a thinner and more satin fabric allowed

for a higher cumulative weight gain, most likely due to a more uniform microstructure and the fiber, and hence resin system.

4.4 Processing Results for Hi-Nicalon™ Type S CFCCs at 1500°C Pyrolysis

This section covers four individual sets of Hi-Nicalon™ Type S CFCCs pyrolyzed at 1500°C with SMP-10, SPR-212, SMP-10 hybrid, and SPR-212 hybrid preceramic polymers. The weight convergence criteria are the same as the previous sections. The reported cumulative weight gains are given inTable 2.1 Table 4.4 below.

Table 4.4: Processing results for Hi-Nicalon™ Type S at 1500°C pyrolysis.

Specimen Type	Weight Gain (%)
Hi-Nicalon™ Type S SMP-10	61.30
Hi-Nicalon™ Type S SPR-212	43.50
Hi-Nicalon™ Type S SMP-10 Hybrid	61.79
Hi-Nicalon™ Type S SPR-212 Hybrid	45.32

Figure 4.4 plots the cumulative weight gain percentages of the four types of Nicalon™ CFCCs against pyrolysis/reinfiltration cycles. Weight gain trends at 1500°C pyrolysis is similar to 1000°C pyrolysis. The only difference is the lower weights of SPR-212 and SMP-10 hybrid for 1500°C samples compared to their lower temperature pyrolysis (i.e., 1000°C) counterparts. This is due to abundant free radical silicon and carbon remaining in the amorphous SiOC ceramic left behind by SPR-212, reacting with SiC to form SiO_2, CO, and CO_2. The oxidation of the samples is likely from oxygen diffusion into the samples between pyrolysis cycles, during reinfiltration and transportation. The carbothermal decomposition forms SiO_2 around the ceramic grain boundaries allowing the sample to gain weight, giving the samples a light grey haze over black coloration. Once SiO_2 is saturated, the dissipation of CO and/or CO_2 overcome the increase

weight gains and the sample then begins to decrease in weight. High temperature thermal cycling also attributes to this decrease in weight gain by creating microcracks for oxygen to reach deeper into the samples. This is evident at last iteration where all samples begin to lose weight. The SMP-10 samples also show some evidence of oxidation from oxygen diffusion and thermal cycling. All samples converged in weight on the thirteenth iteration.

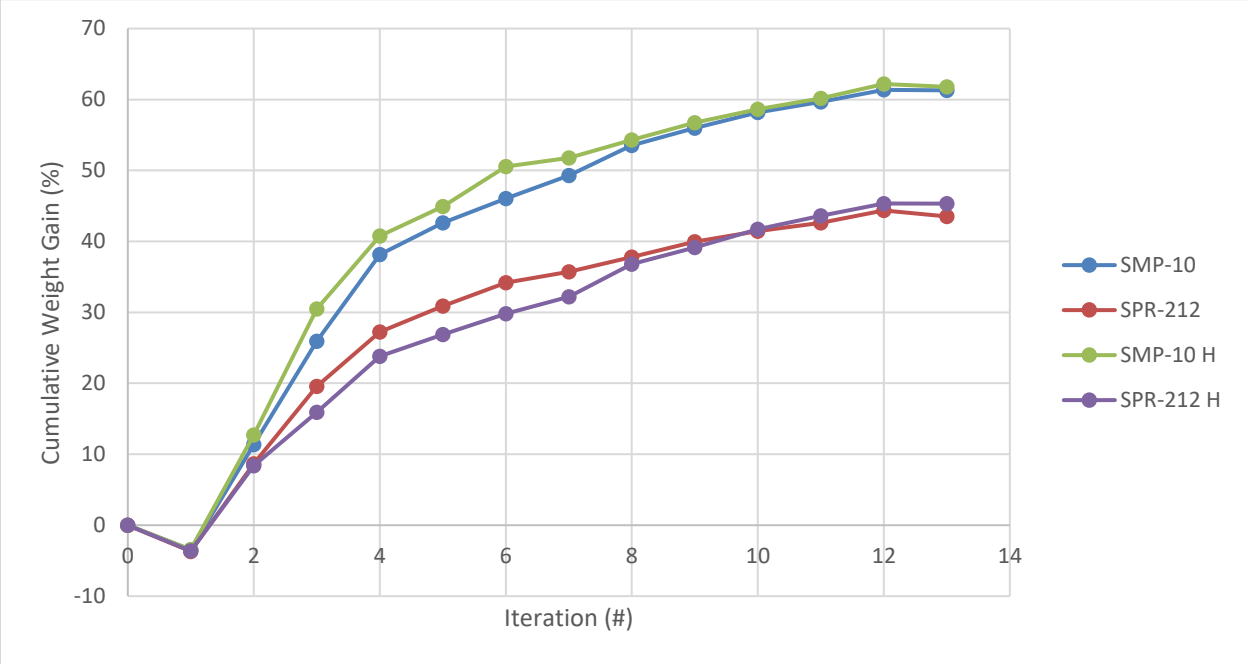

Figure 4.4: Comparison of cumulative weight gain (%) for Hi-Nicalon™ Type S CFCCs after each pyrolysis cycle at 1500°C.

5 MECHANICAL PERFORMANCES

5.1 Introduction

The main objective of this part of the study is to experimentally evaluate the mechanical performance and failure mechanism of different CFCC specimens in flexure. A four-point bend fixture was used to measure the flexural load-deflection response of CFCC specimens loaded in four-point bending. The test specimens, as seen in Figure 5.1, were selected so that they had a span to depth ratio (*L/d*) that produces tensile (at the bottom) and compressive (at the top) stresses at the outer surfaces of the sample under the bending loading. In this study, the *L/d* value is 40.0. All specimens were nominally 90 mm long, 6 mm wide, and on an average 2 mm thick, with exception of Nicalon™ specimens being 50 mm long, 3 mm wide, and 1mm thick. Seven to ten samples were used for each type of CFCC flexure test. The tests were conducted using an Instron testing machine.

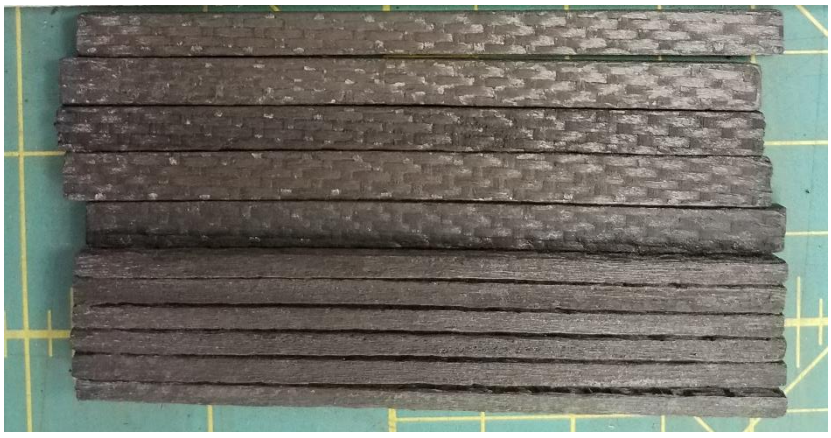

Figure 5.1: Typical manufactured CFCC test specimens.

Test method for flexural properties of continuous fiber reinforced advanced ceramic composites, ASTM C 1341 [36], a four-point bending test, is used to determine the flexural properties of the

CFCC specimens in the form of rectangular bars. Figure 5.2 shows a schematic of the four-point flexure test. The test specimen rests on two supports, the distance between which is called support span. The specimen is loaded at two points by means of two loading rollers, which are situated one third of the overall span away from the outer two support bearings (see Figure 5.2). The distance between the loading rollers, i.e., the load span is one third of the support span. The support span length was 80 mm and load span length were 26.7 mm for 2 mm thick samples. For 1 mm thick samples the support span length was 40 mm and load span length were 13.3 mm.

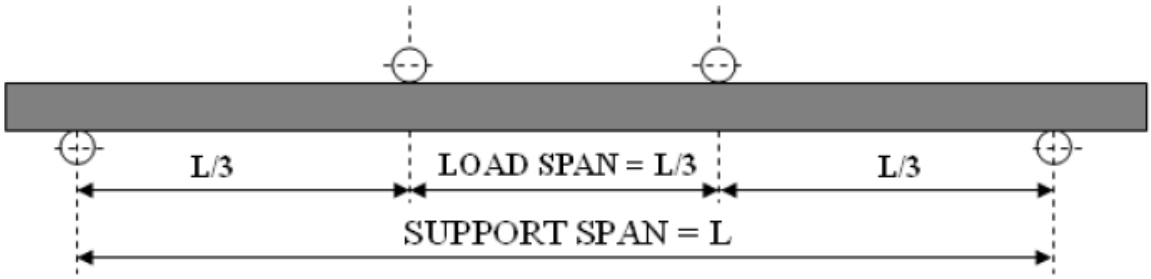

Figure 5.2: Schematic of four-point flexure test, ASTM C1341 [36].

Flexure test provides information on the strength, stiffness, and deflection/strain-to-failure of materials and structures under complex flexural stress conditions. In CFCCs, complex stress-strain behavior may develop as a result of cumulative damage processes; for example, matrix cracking, matrix/fiber debonding, fiber pull-out, fiber fracture, and delamination. This may be influenced by testing mode, testing rate, processing effects, or environmental influences. Some of these effects may be consequences of stress corrosion or sub-critical (slow) crack growth, which can be minimized by testing at sufficiently rapid rates. In this study, the test rate was 0.59 mm/sec [36]. The maximum stress in the outer surface at the point of maximum stress, i.e., flexural strength (S) can be calculated using the maximum load and deflection obtained from the four-point flexure test, and is given in Equation (1) [36]:

$$S = \frac{PL}{bd^2} \tag{1}$$

where, *P* is the maximum load in the flexure test in Newton (*N*), *b* is the specimen width in mm, *d* is the specimen thickness at the point of break in mm, and *L* is the length of the specimen in mm. Equation (2) gives the flexural modulus of elasticity, *E*, for samples tested in four-point flexure [36]:

$$E = \frac{0.21mL^3}{bd^3} \tag{2}$$

where, *m* is the slope of tangent to the initial straight-line portion of the load-deflection curve (*N/mm*). Similarly, the maximum strain-to-failure was calculated using Equation (3).

$$\varepsilon = 4.7\left(\frac{Db}{L^2}\right) \tag{3}$$

where, *D* is the deflection in *mm*. Toughness refers to the amount of energy per unit volume that a material can absorb up to failure and is the area below the stress-strain curve up to the point of failure. As seen in Equation (4), toughness was calculated using Equations (1) and (3).

$$\frac{energy}{volume} = \int_0^{\varepsilon f} \sigma.\delta\varepsilon = \frac{2.35PD}{bdL} \tag{4}$$

Four-point bending test was chosen to quantify the performance of the developed CFCCs as shown in Figure 5.3. The four-point geometry is known to produce more reliable statistical data when compared with three-point bending test, particularly for brittle materials [26]. For obtaining a valid flexural strength by four-point bending test, a high support span/thickness (*L/d*) ratio of about 40 was used to prevent shear failure and invalidation of the tests.

Figure 5.3: Four-point bending test fixture.

The primary reason that four-point bending test [36] is preferred over three-point bending test [36] for brittle materials, is that for three-point bending test, the moment diagram is maximum under the loading point (see Figure 5.4) and this causes stress concentrations under maximum stress that could lead to a premature failure.

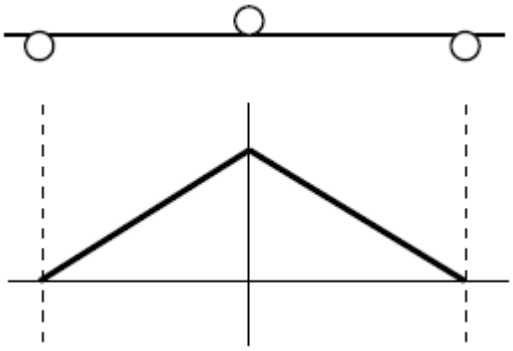

Figure 5.4: Moment diagram for 3-point bending test.

Whereas, in case of four-point bending, the stress concentrations of three-point bending at the potential failure location (i.e., mid-span) does not exist and the mid-span (i.e., where the stress is maximum) is not directly under the loading. In addition, in the four-point bending test, the moment diagram is maximum and constant in between the load span (see Figure 5.5), leading to more distributed stress in between the supports with lower stress at the mid-span and higher

stress in between the supports (as compared to the three-point bending test) and hence more of the specimen's cracks in between the supports are subjected to higher stresses, on the average, and hence a more reliable failure may occur in this case for brittle material.

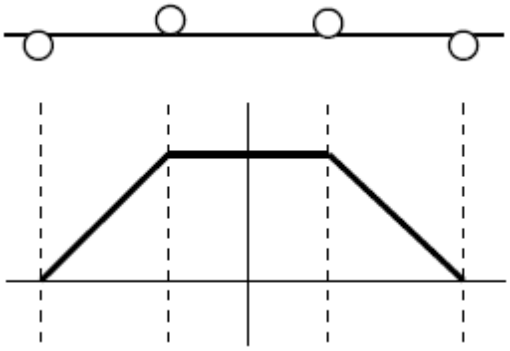

Figure 5.5: Moment diagram for 4-point bending test.

All the tested samples fractured inside the uniformly stressed region of flexure specimen (i.e., in between the inner loading points of the fixture), eliminating uncertainties about failures due to stress concentrations outside the uniform loading region as well as the shear failure of the specimen. This is evident from the optical microscopy pictures of the failed samples shown in the following sections.

5.2 Four-point Flexure Tests, Results, and Discussion for the T300 CFCCs

This section reports and analyzes the results of the four-point bending tests for T300 CFCCs. These samples were used to compare standard T300 carbon fiber against SiC fibers in a CFCC with similar manufacturing processes. Total of six specimens were tested using Instron testing machine. The load-deflection curves for T300 test specimens are shown in Figure 5.6.

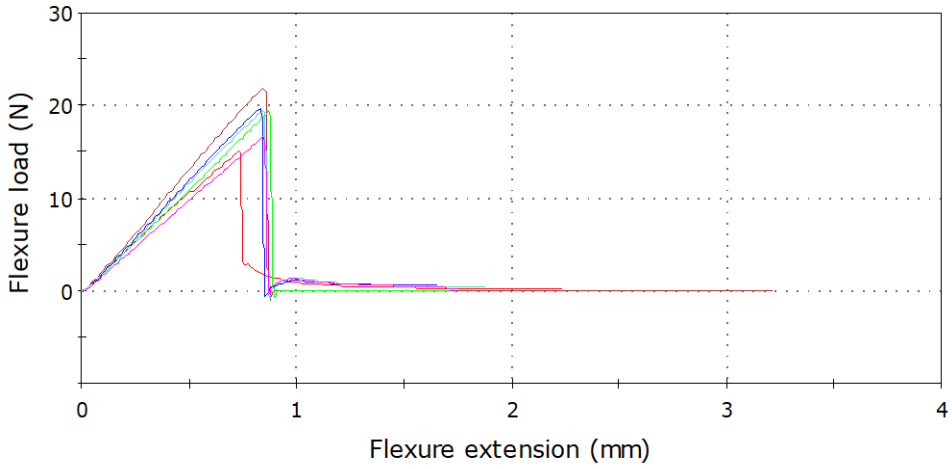

Figure 5.6: Load-deflection curves obtained for T300 CFCCs from 4-point bending test.

T300 test specimens showed very uniform pattern to failure, demonstrating the uniform quality of the CFCCs and accuracy of the test. All specimens failed within the uniform loading region (i.e., in between the inner loading points of the fixture) as predicted (e.g., see Figure 5.7 and Figure 5.8). It should be noted that the main focus in this work was on the systematic studies of the Nicalon™ fibers with various preceramic polymers, such as SMP-10, SPR-212, SMP-10 hybrid, and SPR-212 hybrid. However, we wanted to perform a limited study on the T300-CFCC and compare the results with corresponding Nicalon™ CFCC, and hence we picked T300 with SMP-10 hybrid due to SMP-10 hybrid promising results that we obtained in our Nicalon™ preceramic polymer studies. Table 5.1 reports the average maximum load, maximum deflection (D) of the beam center at maximum load, and the thickness (d) at the point of break from the four-point bending test for T300 carbon fiber and SMP-10 hybrid preceramic polymer mechanical test specimens. The standard deviations of load and deflection is given in parentheses.

Figure 5.7: Optical micrograph of T300 CFCC mid-span failure.

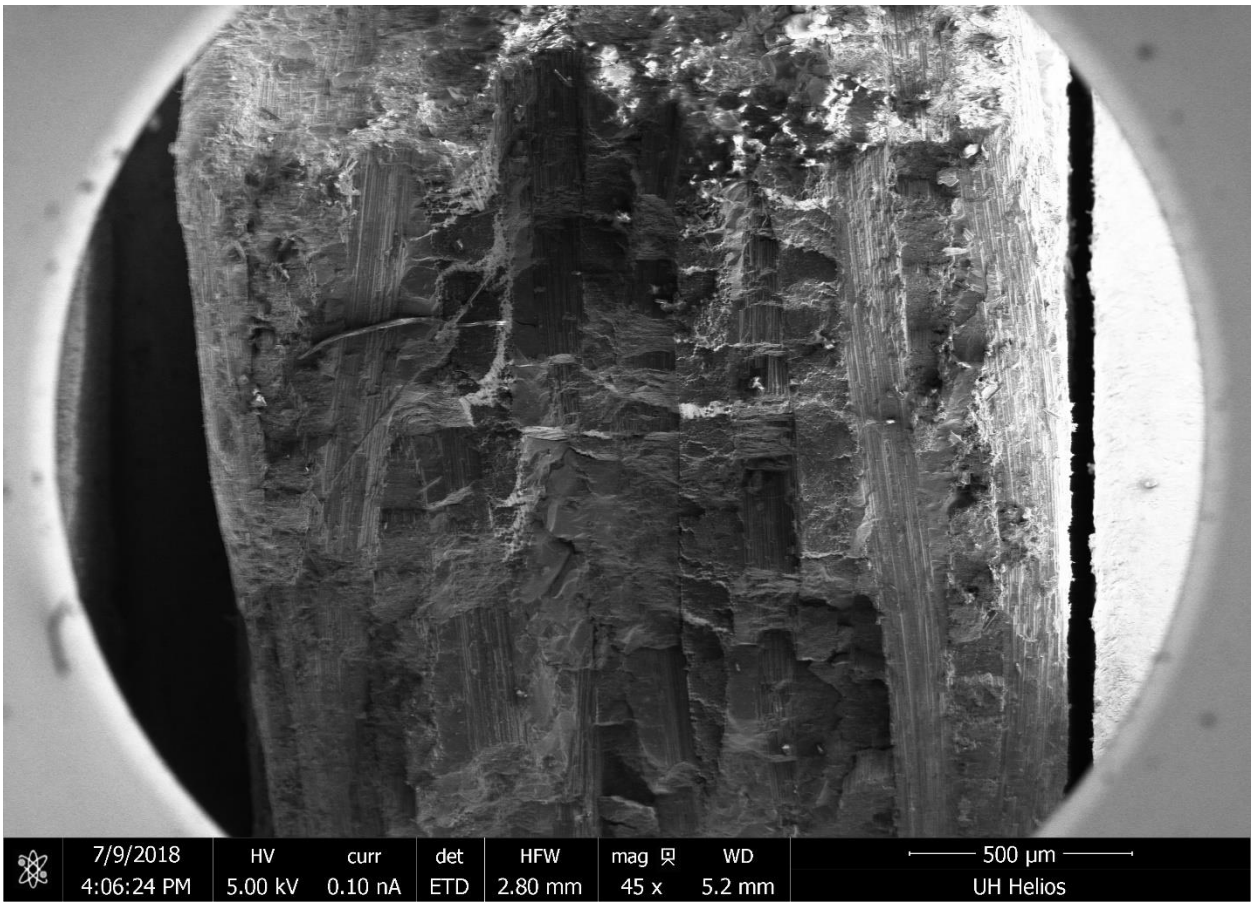

Figure 5.8: SEM of T300 fracture surface.

Table 5.1: Four-point bending test results for T300-SMP-10 hybrid CFCC specimens; standard deviations are given in parentheses.

Specimen	***d* [mm]**	**Load [*N*]**	***D* [mm]**
T300	2.00	19.41 (1.85)	0.949 (0.0198)

Using Equations (1) through (4) the flexural strength, modulus, strain to failure, and toughness for all samples were calculated, respectively, and are reported in Table 5.2 with their standard deviations in parentheses. Same trend as the load at failure is also observed for the flexural strength of the specimens.

Table 5.2: Mechanical properties from 4-point bending test results for T300-SMP-10 hybrid CFCC; standard deviations are given in parentheses.

Specimen Type	Flexural Strength [MPa]	Elastic Modulus [GPa]	Strain-to-failure [mm/mm]	Toughness [MJ/m^3]
T300	63.96 (3.88)	53.12 (2.87)	0.00139 (0.0000344)	44.55 (3.73)

T300 carbon fiber with SMP-10 hybrid successfully created a CFCC with reasonable mechanical performance, and the comparison with Nicalon™ SMP-10 hybrid will be discussed in a later section below.

5.3 Four-point Flexure Tests, Results, and Discussion for the Nicalon™ CFCCs

Only in this study, i.e., Nicalon™ fiber CFCCs, the thickness was about 1 mm due to our initial studies performed in this area. Although, the dimensions were still in accordance with the ASTM C1341 [36], during this study we realized that a 2-mm thick sample, is more suitable for such CFCCs studies. Therefore, although for the Nicalon™ fiber CFCCs studies, the original sample size was around 7; however, not all of the samples survived the initial phases of four-point bending tests. More specifically, the CFCCs made with SMP-10 and SPR-212 (where the majority of the matrix is SMP-10) failed prematurely, as explained in the following.

5.3.1 Four-point Flexure Tests, Results, and Discussion for the Nicalon™ CFCCs with SMP-10

This section reports and analyzes the results of the four-point bending test for Nicalon™ CFCCs with SMP-10 preceramic polymer. Originally 7 specimens were manufactured, but only two survived to testing and averaged in this study as discussed before. Figure 5.10 gives the quality of these samples showing that the parts were free of voids. Four-point bending test was chosen to quantify the mechanical performance of Nicalon™ CFCCs with SMP-10 as shown in Figure

5.3Figure 5.5. All the test parameters such as support span/thickness (*L/d*) ratio, loading rate and dimensions of the specimen remained the same as described in previous sections. Figure 5.9 shows the load-deflection curves obtained in the four-point bending test. The strain was later calculated at the mid-span of the test specimen and using strain gages as suggested in the ASTM standard [36]. The failure load is at the peak in Figure 5.9.

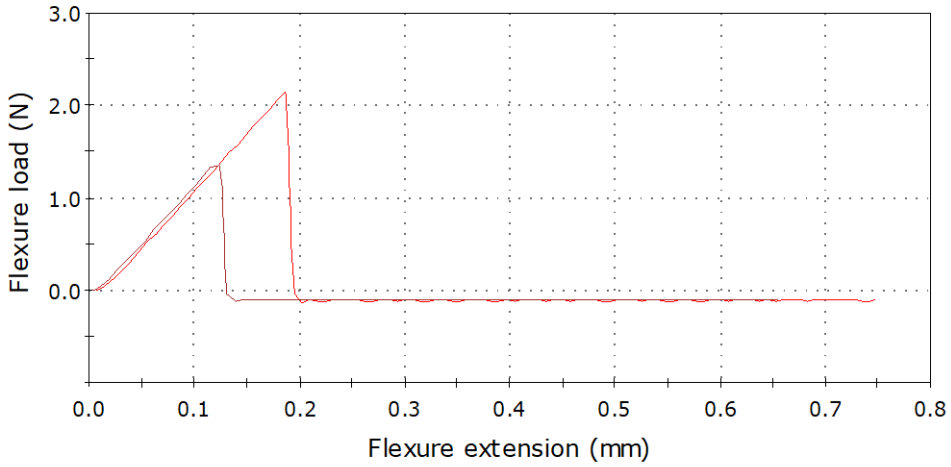

Figure 5.9: Load-deflection curve obtained for Nicalon™ CFCCs with SMP-10 from 4-point bending test.

With such few samples we assume the samples are of valid quality (see Figure 5.10 for the quality of the manufactured test, showing that the samples are void free) CFCCs and are accurate tests. All the tested samples fractured inside the uniform loading region of flexure specimen, eliminating uncertainties about failures due to stress concentrations outside the uniform loading region as well as the shear failure of the specimen.

Table 5.3 reports the average maximum load (*N*), maximum deflection (*D*) of the beam center at maximum load, and the thickness (*d*) at the point of break from the four-point bending test for

Nicalon™ SMP-10 CFCCs. The standard deviation of load and deflection is given in parentheses.

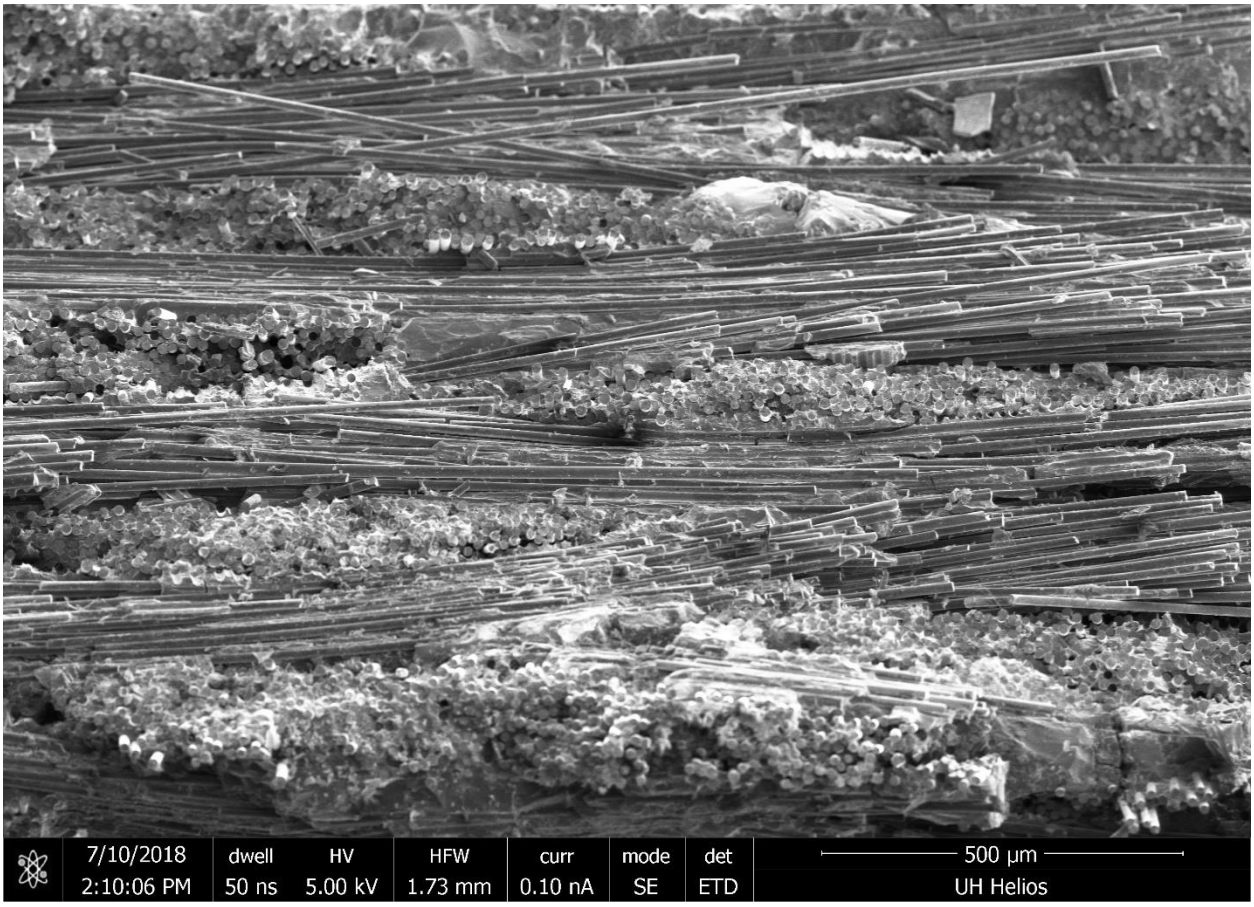

Figure 5.10: SEM of Nicalon™ SMP-10 at fracture with no voids.

Table 5.3: Four-point bending test results for Nicalon™ with SMP-10 specimens; standard deviations are given in parentheses.

Specimen	***d* [mm]**	**Load [*N*]**	***D* [mm]**
Nicalon™ SMP-10	0.823	1.74 (0.562)	0.174 (0.0443)

Using Equations (1) through (4) the flexural strength, modulus, strain to failure, and toughness for all samples were calculated, respectively, and are reported in Table 5.4 with their standard deviations in parentheses.

Table 5.4: Mechanical properties from 4-point bending test results for Nicalon™ with SMP-10; standard deviations are given in parentheses.

Specimen Type	Flexural Strength [MPa]	Elastic Modulus [GPa]	Strain-to-failure [mm/mm]	Toughness [MJ/m^3]
Nicalon™ SMP-10	38.87 (11.3)	61.79 (3.78)	0.000633 (0.000165)	14.56 (6.11)

SMP-10 is an industry standard preceramic polymer therefore, Nicalon™ SMP-10 CFCCs will be used as a baseline to compare the other Nicalon™ preceramic polymers in a later section below.

5.3.2 Four-point Flexure Tests, Results, and Discussion for the Nicalon™ CFCCs with SPR-212

This section reports and analyzes the results of the four-point bending test for Nicalon™ CFCCs with SPR-212 preceramic polymer. Seven different specimens underwent four-point bending tests to quantify their mechanical performance, similar to the previous cases. Once again, test parameters remain unchanged. Figure 5.11 demonstrates the load-deflection curves obtained in the four-point bending test for seven specimens of Nicalon™ SPR-212.

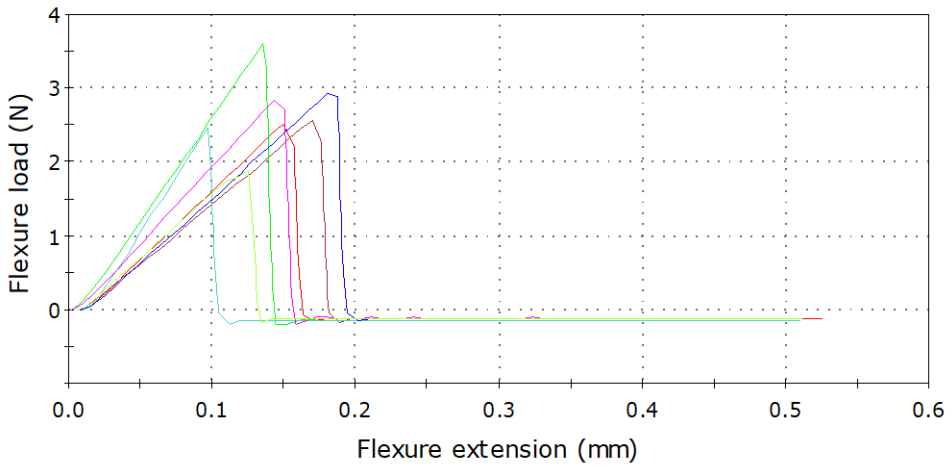

Figure 5.11: Load-deflection curve obtained for Nicalon™ CFCCs with SPR-212 from 4-point bending test.

All specimens failed within the uniform loading region, i.e., in between loading supports. Table 5.5 reports the average maximum load (*N*), maximum deflection (*D*) of the beam center at maximum load, and the thickness (*d*) at the point of break from the four-point bending test for Nicalon™ SPR-212 CFCCs. The standard deviation of load and deflection is given in parentheses.

Table 5.5: Four-point bending test results for Nicalon™ with SPR-212 specimens; standard deviations are given in parentheses.

Specimen	***d* [mm]**	**Load [*N*]**	***D* [mm]**
Nicalon™ SPR-212	1.03	2.68 (0.527)	0.202 (0.0277)

An increase of load and deflection was observed compared to Nicalon™ with SMP-10, but this is due to the samples higher average thickness. Equations (1) through (4) were used to calculate the mechanical properties of the Nicalon™ SPR-212 CFCCs in a similar fashion as the previous cases above. Averaged properties are reported in Table 5.6 below with standard deviations in parentheses.

Table 5.6: Mechanical properties from 4-point bending test results for Nicalon™ with SPR-212; standard deviations are given in parentheses.

Specimen Type	Flexural Strength [MPa]	Elastic Modulus [GPa]	Strain-to-failure [mm/mm]	Toughness [MJ/m^3]
Nicalon™ SPR-212	39.97 (6.08)	54.65 (10.8)	0.000720 (0.000127)	16.20 (3.56)

Nicalon™ SPR-212 has a marginally higher flexural strength with a larger improvement in strain-to-failure and toughness than the baseline Nicalon™ SMP-10. It is only lower in stiffness. The differences are attributed to the differences between SiC and SiOC ceramic matrices.

5.3.3 Four-point Flexure Tests, Results, and Discussion for the Nicalon™ CFCCs with SMP-10 Hybrid

This section reports and analyzes the results of the four-point bending test for Nicalon™ CFCCs with SMP-10 hybrid preceramic polymers. Eight different specimens underwent four-point bending tests to quantify their mechanical performance, similar to the previous cases. Once again, test parameters remain unchanged. Figure 5.12 demonstrates the load-deflection curves obtained in the four-point bending test for eight specimens of Nicalon™ SMP-10 hybrid.

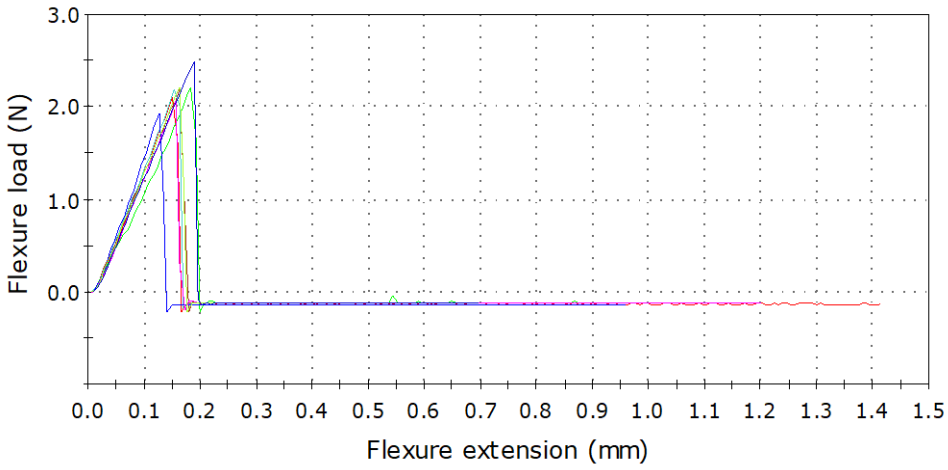

Figure 5.12: Load-deflection curve obtained for Nicalon™ CFCCs with SMP-10 hybrid from 4-point bending test.

All specimens failed within the uniform loading region, in between loading supports. Table 5.7 reports the average maximum load (*N*), maximum deflection (*D*) of the beam center at maximum load, and the thickness (*d*) at the point of break from the four-point bending test for Nicalon™ SMP-10 hybrid CFCCs. The standard deviation of load and deflection is given in parentheses.

Table 5.7: Four-point bending test results for Nicalon™ with SMP-10 hybrid specimens; standard deviations are given in parentheses.

Specimen	*d* [mm]	Load [*N*]	*D* [mm]
Nicalon™ SMP-10 Hybrid	0.865	2.17 (0.160)	0.213 (0.0196)

There is a small increase in load and deflection compared to Nicalon™ SMP-10. Table 5.8 reports calculated mechanical properties of the Nicalon™ SMP-10 hybrid CFCCs. Equations (1) through (4) were utilized in a similar manner as described previously. Properties were averaged, and standard deviations are given in parentheses.

Table 5.8: Mechanical properties from 4-point bending test results for Nicalon™ with SMP-10 hybrid; standard deviations are given in parentheses.

Specimen Type	Flexural Strength [MPa]	Elastic Modulus [GPa]	Strain-to-failure [mm/mm]	Toughness [MJ/m^3]
Nicalon™ SMP-10 Hybrid	40.14 (7.24)	61.11 (13.9)	0.000694 (0.000079)	18.48 (3.02)

Nicalon™ SMP-10 hybrid out performs Nicalon™ with pristine SMP-10 in every property. It is only marginally less in stiffness, but within error. It also has better performance than its SPR-212 counterpart.

5.3.4 Four-point Flexure Tests, Results, and Discussion for the Nicalon™ CFCCs with SPR-212 Hybrid

This section reports and analyzes the results of the four-point bending test for Nicalon™ CFCCs with SPR-212 hybrid preceramic polymers. Originally seven different specimens were prepared, but only two survived and underwent four-point bending tests to quantify their mechanical performance, similar to the previous cases. Figure 5.13 gives the quality of these samples showing that the parts were free of voids. Once again, test parameters remain unchanged. Figure 5.14 demonstrates the load-deflection curves obtained in the four-point bending test for two specimens of Nicalon™ SPR-212 hybrid.

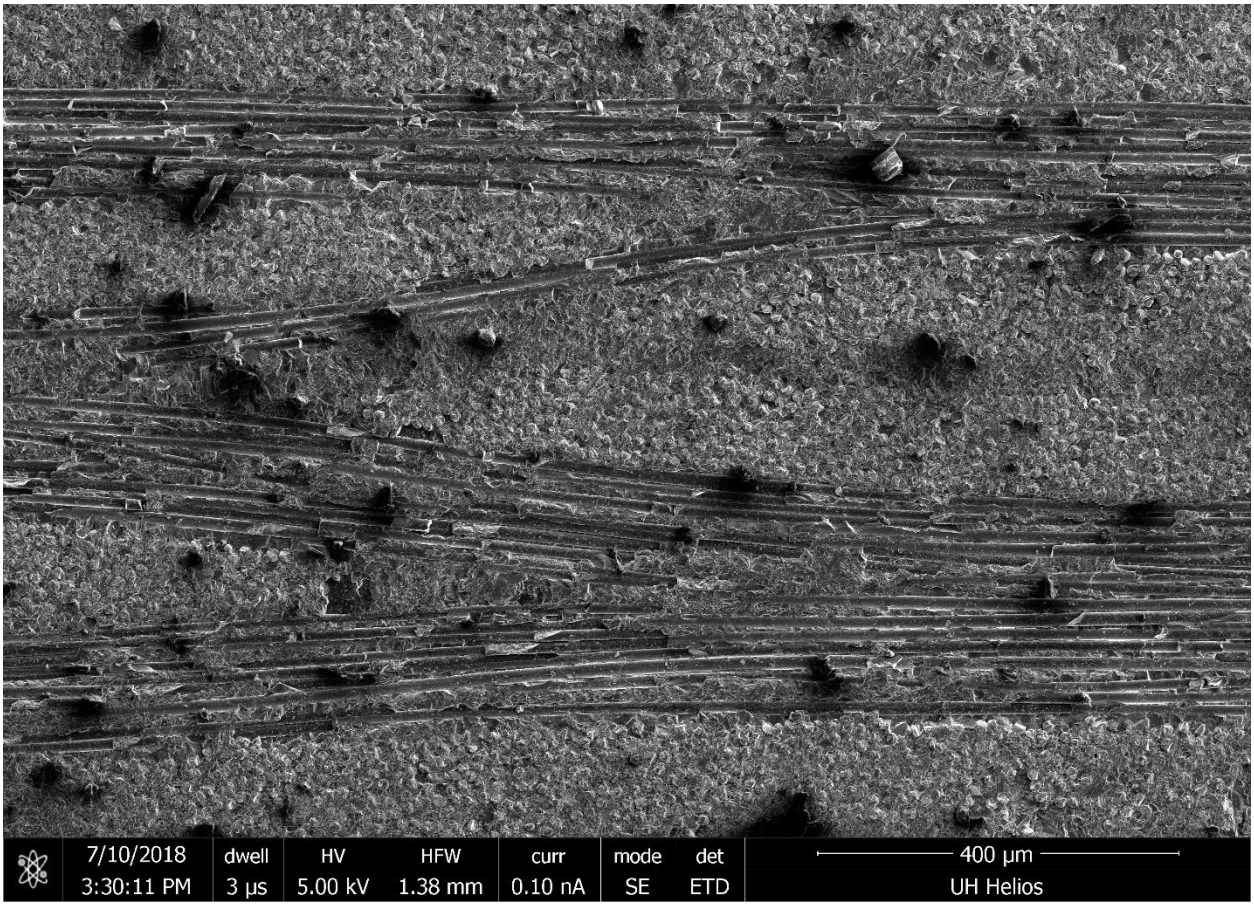

Figure 5.13: SEM of Nicalon™ SPR-212 with no voids.

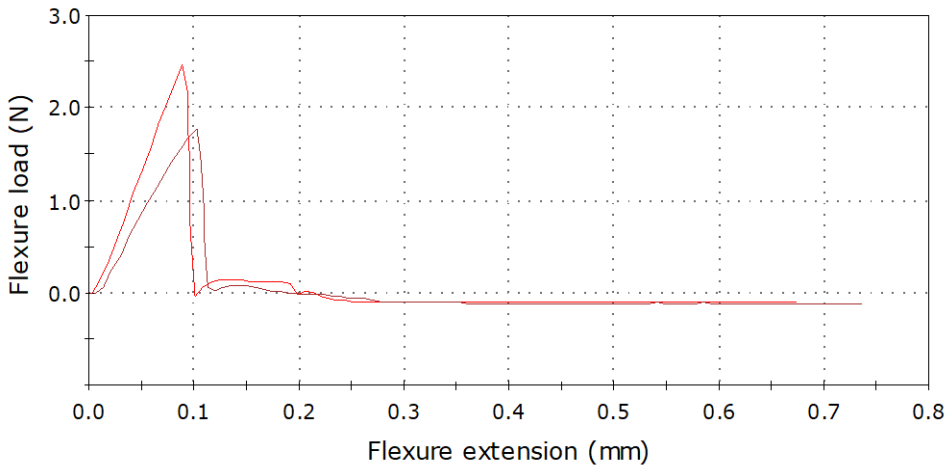

Figure 5.14: Load-deflection curve obtained for Nicalon™ CFCCs with SPR-212 hybrid from 4-point bending test.

All specimens failed within the uniform loading region, in between loading supports. Table 5.9 reports the average maximum load (*N*), maximum deflection (*D*) of the beam center at maximum load, and the thickness (*d*) at the point of break from the four-point bending test for Nicalon™ SPR-212 hybrid CFCCs. The standard deviation of load and deflection is given in parentheses.

Table 5.9: Four-point bending test results for Nicalon™ with SPR-212 hybrid specimens; standard deviations are given in parentheses.

Specimen	*d* [mm]	Load [*N*]	*D* [mm]
Nicalon™ SPR-212 Hybrid	1.07	2.11 (0.490)	0.115 (0.00896)

Table 5.10 reports calculated mechanical properties of the Nicalon™ SPR-212 hybrid CFCCs. Equations (1) through (4) were utilized in a similar manner as described previously. Properties were averaged, and standard deviations are given in parentheses.

Table 5.10: Mechanical properties from 4-point bending test results for Nicalon™ with SPR-212 hybrid; standard deviations are given in parentheses.

Specimen Type	Flexural Strength [MPa]	Elastic Modulus [GPa]	Strain-to-failure [mm/mm]	Toughness [MJ/m^3]
Nicalon™ SPR-212 Hybrid	22.71 (0.871)	56.11 (1.22)	0.000510 (0.00000113)	5.80 (0.234)

Nicalon™ SPR-212 hybrid is the worst performer for the Nicalon™ tests.

5.4 Four-point Flexure Tests, Results, and Discussion for the Hi-Nicalon™ Type S CFCCs at 1000°C Pyrolysis

5.4.1 Four-point Flexure Tests, Results, and Discussion for the Hi-Nicalon™ Type S CFCCs at 1000°C Pyrolysis with SMP-10

This section reports and analyzes the results of the four-point bending test for Hi-Nicalon™ Type S CFCCs with SMP-10 preceramic polymer, pyrolyzed at 1000°C. Eight different specimens underwent four-point bending tests to quantify their mechanical performance, similar to the previous cases. Once again, test parameters remain unchanged. Figure 5.15 demonstrates the load-deflection curves obtained in the four-point bending test for eight specimens of Hi-Nicalon™ Type S SMP-10.

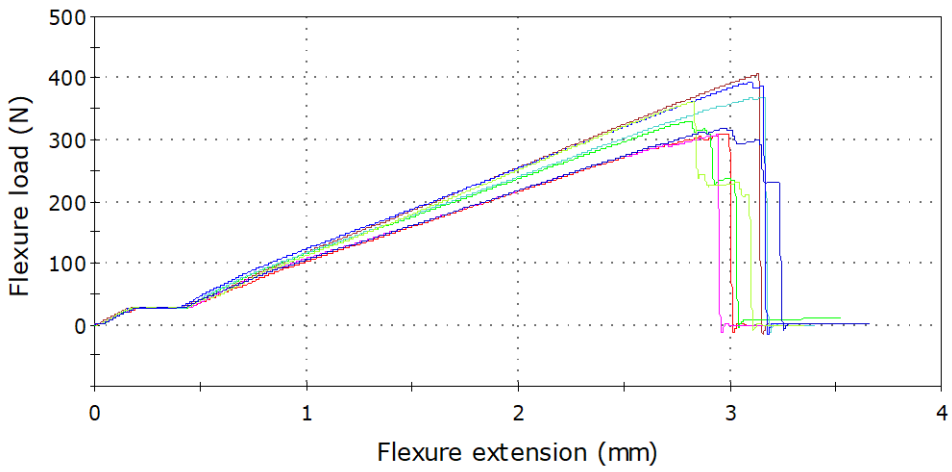

Figure 5.15: Load-deflection curve obtained for Hi-Nicalon™ Type S CFCCs with SMP-10 pyrolyzed at 1000°C, from 4-point bending test.

The curves for the specimens were shifted and rezeroed to compensate for the toe at the beginning of the tests, according to ASTM C1341 [36]. All specimens failed within the uniform loading region, in between loading supports. Table 5.11 reports the average maximum load (*N*), maximum deflection (*D*) of the beam center at maximum load, and the thickness (*d*) at the point of break from the four-point bending test for Hi-Nicalon™ Type S SMP-10 CFCCs. The standard deviation of load and deflection is given in parentheses.

Table 5.11: Four-point bending test results for Hi-Nicalon™ Type S with SMP-10 specimens pyrolyzed at 1000°C; standard deviations are given in parentheses.

Specimen	*d* [mm]	Load [*N*]	*D* [mm]
Hi-Nicalon™ Type S SMP-10	2.25	350 (38.4)	3.05 (0.179)

Table 5.12 reports calculated mechanical properties of the Hi-Nicalon™ Type S SMP-10 CFCCs. Equations (1) through (4) were utilized in a similar manner as described previously. Properties were averaged, and standard deviations are given in parentheses.

Table 5.12: Mechanical properties from 4-point bending test results for Hi-Nicalon™ Type S with SMP-10 pyrolyzed at 1000°C; standard deviations are given in parentheses.

Specimen Type	Flexural Strength [MPa]	Elastic Modulus [GPa]	Strain-to-failure [mm/mm]	Toughness [MJ/m^3]
Hi-Nicalon™ Type S SMP-10	431.0 (28.9)	88.04 (8.46)	0.00725 (0.000360)	1391 (160)

Again, SMP-10 is an industry standard preceramic polymer, therefore Hi-Nicalon™ Type S with SMP-10 will be a baseline for comparison. The comparison between the other Hi-Nicalon™ Type S specimens will be discussed in a later section below.

5.4.2 Four-point Flexure Tests, Results, and Discussion for the Hi-Nicalon™ Type S CFCCs at 1000°C Pyrolysis with SPR-212

This section reports and analyzes the results of the four-point bending test for Hi-Nicalon™ Type S CFCCs with SPR-212 preceramic polymer, pyrolyzed at 1000°C. Nine different specimens underwent four-point bending tests to quantify their mechanical performance, similar to the previous cases. Once again, test parameters remain unchanged. Figure 5.16 demonstrates the load-deflection curves obtained in the four-point bending test for nine specimens of Hi-Nicalon™ Type S SPR-212.

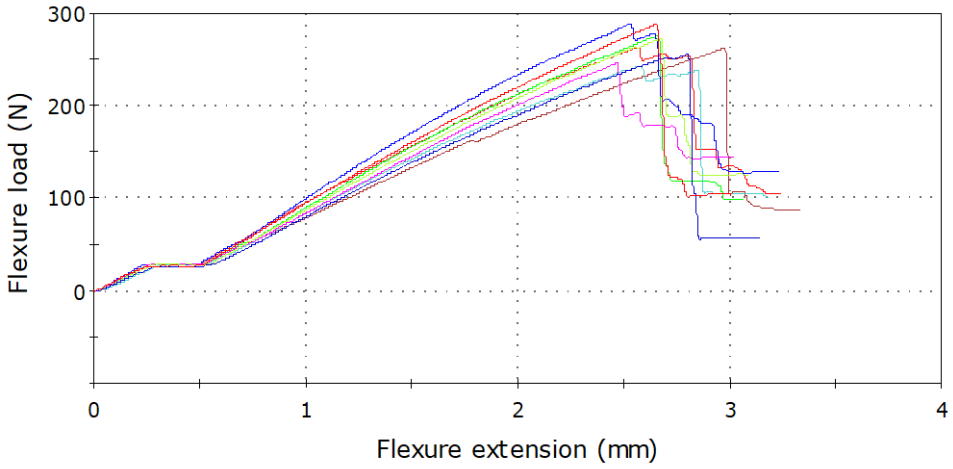

Figure 5.16: Load-deflection curve obtained for Hi-Nicalon™ Type S CFCCs with SPR-212 pyrolyzed at 1000°C, from 4-point bending test.

The curves for the specimens were shifted and rezeroed to compensate for the toe at the beginning of the tests, according to ASTM C1341 [36]. All specimens failed within the uniform loading region, in between loading supports. Table 5.13 reports the average maximum load (*N*), maximum deflection (*D*) of the beam center at maximum load, and the thickness (*d*) at the point of break from the four-point bending test for Hi-Nicalon™ Type S SPR-212 CFCCs. The standard deviation of load and deflection is given in parentheses.

Table 5.13: Four-point bending test results for Hi-Nicalon™ Type S with SPR-212 specimens pyrolyzed at 1000°C; standard deviations are given in parentheses.

Specimen	*d* [mm]	Load [*N*]	*D* [mm]
Hi-Nicalon™ Type S SPR-212	2.09	266 (16.5)	2.64 (0.0923)

Table 5.14 reports calculated mechanical properties of the Hi-Nicalon™ Type S SPR-212 CFCCs. Equations (1) through (4) were utilized in a similar manner as described previously. Properties were averaged, and standard deviations are given in parentheses.

Table 5.14: Mechanical properties from 4-point bending test results for Hi-Nicalon™ Type S with SPR-212 pyrolyzed at 1000°C; standard deviations are given in parentheses.

Specimen Type	Flexural Strength [MPa]	Elastic Modulus [GPa]	Strain-to-failure [mm/mm]	Toughness [MJ/m^3]
Hi-Nicalon™ Type S SPR-212	366.5 (17.0)	72.59 (5.30)	0.00600 (0.000199)	977.3 (64.5)

Unlike the Nicalon™ study, Hi-Nicalon™ Type S SPR-212 performs worst in all mechanical properties compared to Hi-Nicalon™ Type S SMP-10. This is believed to be due to the difference in fabric to matrix interface between the two different fabrics, and will be discussed in later sections

5.4.3 Four-point Flexure Tests, Results, and Discussion for the Hi-Nicalon™ Type S CFCCs at 1000°C Pyrolysis with SMP-10 Hybrid

This section reports and analyzes the results of the four-point bending test for Hi-Nicalon™ Type S CFCCs with SMP-10 hybrid preceramic polymers, pyrolyzed at 1000°C. Ten different specimens underwent four-point bending tests to quantify their mechanical performance, similar to the previous cases. Once again, test parameters remain unchanged. Figure 5.17 demonstrates

the load-deflection curves obtained in the four-point bending test for ten specimens of Hi-Nicalon™ Type S SMP-10 hybrid.

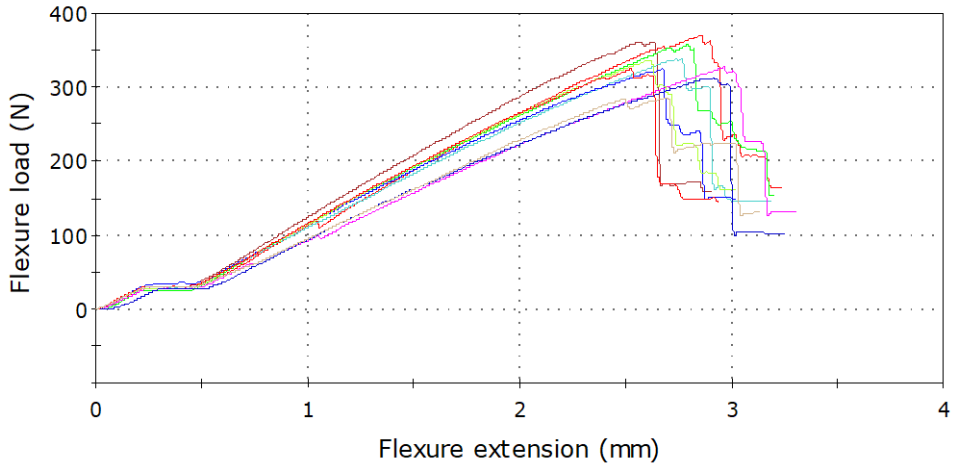

Figure 5.17: Load-deflection curve obtained for Hi-Nicalon™ Type S CFCCs with SMP-10 hybrid pyrolyzed at 1000°C, from 4-point bending test.

The curves for the specimens were shifted and rezeroed to compensate for the toe at the beginning of the tests, according to ASTM C1341 [36]. All specimens failed within the uniform loading region, in between loading supports. Table 5.15 reports the average maximum load (*N*), maximum deflection (*D*) of the beam center at maximum load, and the thickness (*d*) at the point of break from the four-point bending test for Hi-Nicalon™ Type S SMP-10 hybrid CFCCs. The standard deviation of load and deflection is given in parentheses.

Table 5.15: Four-point bending test results for Hi-Nicalon™ Type S with SMP-10 hybrid specimens pyrolyzed at 1000°C; standard deviations are given in parentheses.

Specimen	***d* [mm]**	**Load [*N*]**	***D* [mm]**
Hi-Nicalon™ Type S SMP-10 Hybrid	2.40	334 (25.0)	2.79 (0.159)

Table 5.16 reports calculated mechanical properties of the Hi-Nicalon™ Type S SMP-10 hybrid CFCCs. Equations (1) through (4) were utilized in a similar manner as described previously. Properties were averaged, and standard deviations are given in parentheses.

Table 5.16: Mechanical properties from 4-point bending test results for Hi-Nicalon™ Type S with SMP-10 hybrid pyrolyzed at 1000°C; standard deviations are given in parentheses.

Specimen Type	Flexural Strength [MPa]	Elastic Modulus [GPa]	Strain-to-failure [mm/mm]	Toughness [MJ/m^3]
Hi-Nicalon™ Type S SMP-10 Hybrid	377.8 (9.53)	68.45 (3.45)	0.00693 (0.000332)	1164 (74.3)

Hi-Nicalon™ Type S SMP-10 hybrid has improvements in every mechanical property compared to Hi-Nicalon™ Type S SPR-212. The only exception is stiffness, but it is within the margin of error. This demonstrates that the molding of the laminate with SMP-10 can increase its properties in SMP-10 hybrid compared to SPR-212.

5.4.4 Four-point Flexure Tests, Results, and Discussion for the Hi-Nicalon™ Type S CFCCs at 1000°C Pyrolysis with SPR-212 Hybrid

This section reports and analyzes the results of the four-point bending test for Hi-Nicalon™ Type S CFCCs with SPR-212 hybrid preceramic polymers, pyrolyzed at 1000°C. Ten different specimens underwent four-point bending tests to quantify their mechanical performance, similar to the previous cases. Once again, test parameters remain unchanged. Figure 5.18 demonstrates the load-deflection curves obtained in the four-point bending test for ten specimens of Hi-Nicalon™ Type S SPR-212 hybrid.

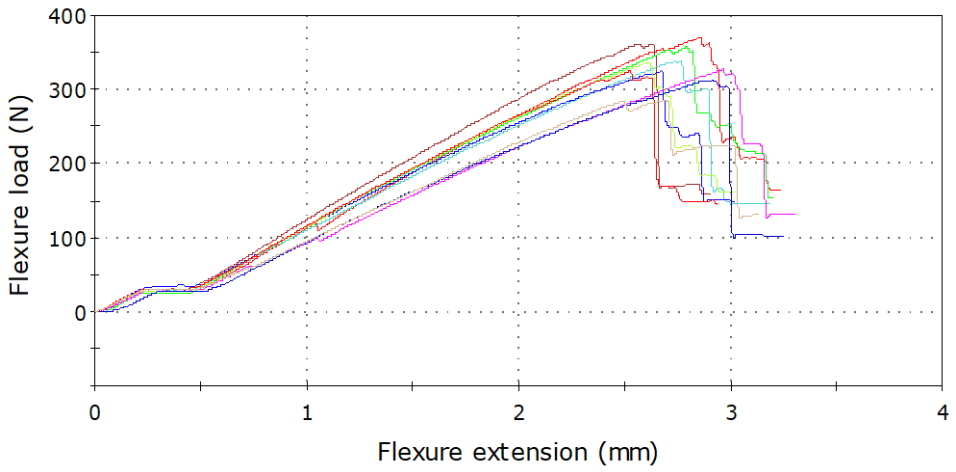

Figure 5.18: Load-deflection curve obtained for Hi-Nicalon™ Type S CFCCs with SPR-212 hybrid pyrolyzed at 1000°C, from 4-point bending test.

The curves for the specimens were shifted and rezeroed to compensate for the toe at the beginning of the tests, according to ASTM C1341 [36]. All specimens failed within the uniform loading region, in between loading supports. Table 5.17 reports the average maximum load (*N*), maximum deflection (*D*) of the beam center at maximum load, and the thickness (*d*) at the point of break from the four-point bending test for Hi-Nicalon™ Type S SPR-212 hybrid CFCCs. The standard deviation of load and deflection is given in parentheses.

Table 5.17: Four-point bending test results for Hi-Nicalon™ Type S with SPR-212 hybrid specimens pyrolyzed at 1000°C; standard deviations are given in parentheses.

Specimen	***d* [mm]**	**Load [*N*]**	***D* [mm]**
Hi-Nicalon™ Type S SPR-212 Hybrid	2.13	327 (31.4)	2.82 (0.156)

Table 5.18 reports calculated mechanical properties of the Hi-Nicalon™ Type S SPR-212 hybrid CFCCs. Equations (1) through (4) were utilized in a similar manner as described previously. Properties were averaged, and standard deviations are given in parentheses.

Table 5.18: Mechanical properties from 4-point bending test results for Hi-Nicalon™ Type S with SPR-212 hybrid pyrolyzed at 1000°C; standard deviations are given in parentheses.

Specimen Type	Flexural Strength [MPa]	Elastic Modulus [GPa]	Strain-to-failure [mm/mm]	Toughness [MJ/m^3]
Hi-Nicalon™ Type S SPR-212 Hybrid	428.5 (19.6)	93.91 (6.67)	0.00649 (0.000340)	1237 (117)

Hi-Nicalon™ Type S SPR-212 hybrid has higher stiffness than Hi-Nicalon™ Type S SMP-10, but this is within the margin of error. The other mechanical properties are a blend between SMP-10 and SPR-212 counterparts.

5.5 Four-point Flexure Tests, Results, and Discussion for the Hi-Nicalon™ Type S CFCCs at 1500°C Pyrolysis

5.5.1 Four-point Flexure Tests, Results, and Discussion for the Hi-Nicalon™ Type S CFCCs at 1500°C Pyrolysis with SMP-10

This section reports and analyzes the results of the four-point bending test for Hi-Nicalon™ Type S CFCCs with SMP-10 preceramic polymer, pyrolyzed at 1500°C. Nine different specimens underwent four-point bending tests to quantify their mechanical performance, similar to the previous cases. Once again, test parameters remain unchanged. Figure 5.19 demonstrates the load-deflection curves obtained in the four-point bending test for nine specimens of 1500°C Hi-Nicalon™ Type S SMP-10.

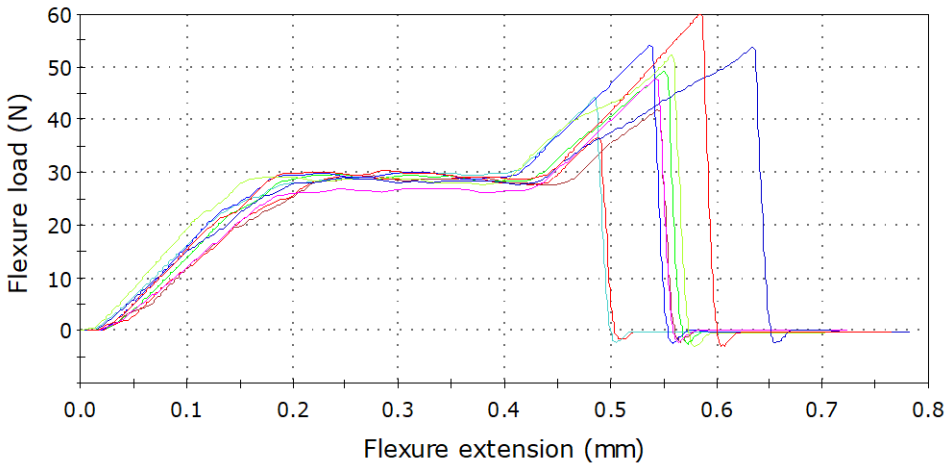

Figure 5.19: Load-deflection curve obtained for Hi-Nicalon™ Type S CFCCs with SMP-10 pyrolyzed at 1500°C, from 4-point bending test.

The curves for the specimens were shifted and rezeroed to compensate for the toe at the beginning of the tests, according to ASTM C1341 [36]. All specimens failed within the uniform loading region, in between loading supports. Table 5.19 reports the average maximum load (*N*), maximum deflection (*D*) of the beam center at maximum load, and the thickness (*d*) at the point of break from the four-point bending test for 1500°C Hi-Nicalon™ Type S SMP-10 CFCCs. The standard deviation of load and deflection is given in parentheses.

Table 5.19: Four-point bending test results for Hi-Nicalon™ Type S with SMP-10 specimens pyrolyzed at 1500°C; standard deviations are given in parentheses.

Specimen	***d* [mm]**	**Load [*N*]**	***D* [mm]**
1500°C Hi-Nicalon™ Type S SMP-10	1.80	48.9 (7.13)	0.297 (0.0281)

It can be observed that the thickness is not the desired 2 mm. This is believed to be due to a higher carbothermal decomposition and chemical shrinkage of the matrix at higher pyrolysis temperature of 1500ºC. Table 5.20 reports calculated mechanical properties of the 1500°C Hi-Nicalon™ Type S SMP-10 CFCCs. Equations (1) through (4) were utilized in a similar manner

as described previously. Properties were averaged, and standard deviations are given in parentheses.

Table 5.20: Mechanical properties from 4-point bending test results for Hi-Nicalon™ Type S with SMP-10 pyrolyzed at 1500°C; standard deviations are given in parentheses.

Specimen Type	Flexural Strength [MPa]	Elastic Modulus [GPa]	Strain-to-failure [mm/mm]	Toughness [MJ/m^3]
1500°C Hi-Nicalon™ Type S SMP-10	87.65 (7.52)	160.6 (16.6)	0.000611 (0.0000689)	23.88 (3.97)

Once again, this SMP-10 specimen will be used for a baseline comparison between the other 1500°C pyrolyzed specimens, which will be discussed in a later section below.

5.5.2 Four-point Flexure Tests, Results, and Discussion for the Hi-Nicalon™ Type S CFCCs at 1500°C Pyrolysis with SPR-212

This section reports and analyzes the results of the four-point bending test for Hi-Nicalon™ Type S CFCCs with SPR-212 preceramic polymer, pyrolyzed at 1500°C. Nine different specimens underwent four-point bending tests to quantify their mechanical performance, similar to the previous cases. Once again, test parameters remain unchanged. Figure 5.20 demonstrates the load-deflection curves obtained in the four-point bending test for nine specimens of 1500°C Hi-Nicalon™ Type S SPR-212.

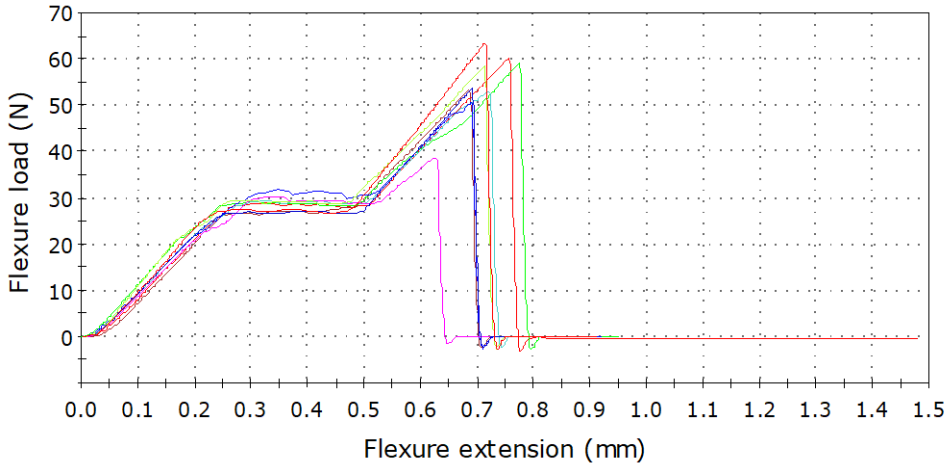

Figure 5.20: Load-deflection curve obtained for Hi-Nicalon™ Type S CFCCs with SPR-212 pyrolyzed at 1500°C, from 4-point bending test.

The curves for the specimens were shifted and rezeroed to compensate for the toe at the beginning of the tests, according to ASTM C1341 [36]. All specimens failed within the uniform loading region, in between loading supports. Table 5.21 reports the average maximum load (*N*), maximum deflection (*D*) of the beam center at maximum load, and the thickness (*d*) at the point of break from the four-point bending test for 1500°C Hi-Nicalon™ Type S SPR-212 CFCCs. The standard deviation of load and deflection is given in parentheses.

Table 5.21: Four-point bending test results for Hi-Nicalon™ Type S with SPR-212 specimens pyrolyzed at 1500°C; standard deviations are given in parentheses.

Specimen	***d* [mm]**	**Load [*N*]**	***D* [mm]**
1500°C Hi-Nicalon™ Type S SPR-212	1.66	54.5 (7.20)	0.479 (0.0362)

Again, the reduction of thickness from the desired 2 mm is believed to be due to a higher carbothermal decomposition and chemical shrinkage of the matrix at higher pyrolysis temperature of 1500°C. It should also be noted that the reduction of thickness, in this case, is more severe than its SMP-10 counterpart. Table 5.22 reports calculated mechanical properties of the 1500°C Hi-Nicalon™ Type S SPR-212 CFCCs. Equations (1) through (4) were utilized in a

similar manner as described previously. Properties were averaged, and standard deviations are given in parentheses.

Table 5.22: Mechanical properties from 4-point bending test results for Hi-Nicalon™ Type S with SPR-212 pyrolyzed at 1500°C; standard deviations are given in parentheses.

Specimen Type	Flexural Strength [MPa]	Elastic Modulus [GPa]	Strain-to-failure [mm/mm]	Toughness [MJ/m^3]
1500°C Hi-Nicalon™ Type S SPR-212	100.8 (9.59)	121.4 (10.4)	0.000932 (0.0000764)	41.94 (6.44)

Hi-Nicalon™ Type S SPR-212 pyrolyzed at 1500°C has significantly greater mechanical properties than the 1500°C SMP-10 baseline. It is only weaker in stiffness in comparison.

5.5.3 Four-point Flexure Tests, Results, and Discussion for the Hi-Nicalon™ Type S CFCCs at 1500°C Pyrolysis with SMP-10 Hybrid

This section reports and analyzes the results of the four-point bending test for Hi-Nicalon™ Type S CFCCs with SMP-10 hybrid preceramic polymers, pyrolyzed at 1500°C. Seven different specimens underwent four-point bending tests to quantify their mechanical performance, similar to the previous cases. Once again, test parameters remain unchanged. Figure 5.21 demonstrates the load-deflection curves obtained in the four-point bending test for seven specimens of 1500°C Hi-Nicalon™ Type S SMP-10 hybrid.

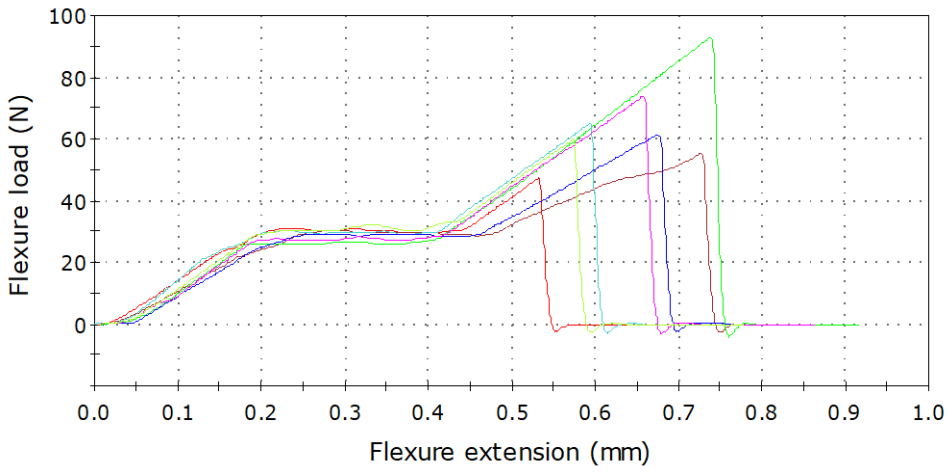

Figure 5.21: Load-deflection curve obtained for Hi-Nicalon™ Type S CFCCs with SMP-10 hybrid pyrolyzed at 1500°C, from 4-point bending test.

The curves for the specimens were shifted and rezeroed to compensate for the toe at the beginning of the tests, according to ASTM C1341 [36]. All specimens failed within the uniform loading region, in between loading supports. Table 5.23 reports the average maximum load (*N*), maximum deflection (*D*) of the beam center at maximum load, and the thickness (*d*) at the point of break from the four-point bending test for 1500°C Hi-Nicalon™ Type S SMP-10 hybrid CFCCs. The standard deviation of load and deflection is given in parentheses.

Table 5.23: Four-point bending test results for Hi-Nicalon™ Type S with SMP-10 hybrid specimens pyrolyzed at 1500°C; standard deviations are given in parentheses.

Specimen	***d* [mm]**	**Load [*N*]**	***D* [mm]**
1500°C Hi-Nicalon™ Type S SMP-10 Hybrid	2.07	65.0 (14.8)	0.427 (0.103)

Table 5.24 reports calculated mechanical properties of the 1500°C Hi-Nicalon™ Type S SMP-10 hybrid CFCCs. Equations (1) through (4) were utilized in a similar manner as described previously. Properties were averaged, and standard deviations are given in parentheses.

Table 5.24: Mechanical properties from 4-point bending test results for Hi-Nicalon™ Type S with SMP-10 hybrid pyrolyzed at 1500°C; standard deviations are given in parentheses.

Specimen Type	Flexural Strength [MPa]	Elastic Modulus [GPa]	Strain-to-failure [mm/mm]	Toughness [MJ/m^3]
1500°C Hi-Nicalon™ Type S SMP-10 Hybrid	90.09 (18.0)	105.9 (11.4)	0.000961 (0.000222)	39.70 (16.3)

Although the thickness did not shrink in this case, the data is more sporadic in the load-deflection graph, see Figure 5.21, which created a relatively large standard deviations for this case. This could be attributed to the nature of the hybridization for this case, and how various polymers interact with each other.

5.5.4 Four-point Flexure Tests, Results, and Discussion for the Hi-Nicalon™ Type S CFCCs at 1500°C Pyrolysis with SPR-212 Hybrid

This section reports and analyzes the results of the four-point bending test for Hi-Nicalon™ Type S CFCCs with SPR-212 hybrid preceramic polymers, pyrolyzed at 1500°C. Nine different specimens underwent four-point bending tests to quantify their mechanical performance, similar to the previous cases. Once again, test parameters remain unchanged. Figure 5.22 demonstrates the load-deflection curves obtained in the four-point bending test for nine specimens of 1500°C Hi-Nicalon™ Type S SPR-212 hybrid.

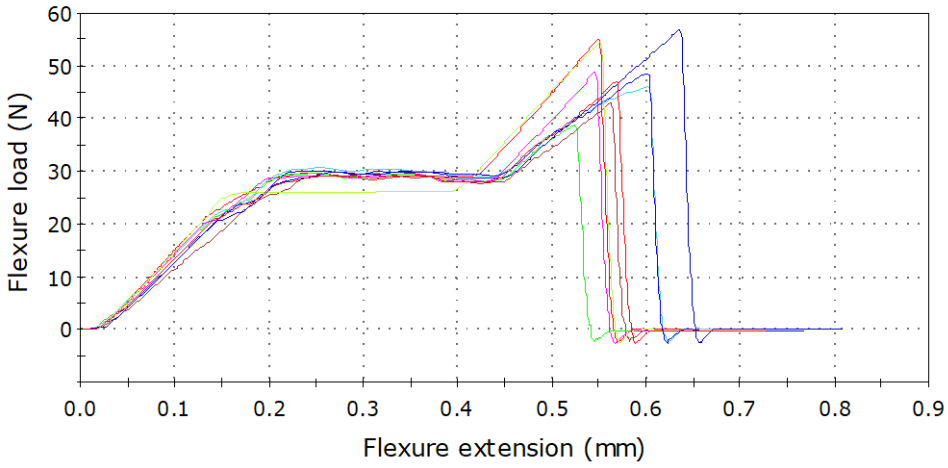

Figure 5.22: Load-deflection curve obtained for Hi-Nicalon™ Type S CFCCs with SPR-212 hybrid pyrolyzed at 1500°C, from 4-point bending test.

The curves for the specimens were shifted and rezeroed to compensate for the toe at the beginning of the tests, according to ASTM C1341 [36]. All specimens failed within the uniform loading region, in between loading supports. Table 5.25 reports the average maximum load (*N*), maximum deflection (*D*) of the beam center at maximum load, and the thickness (*d*) at the point of break from the four-point bending test for 1500°C Hi-Nicalon™ Type S SPR-212 hybrid CFCCs. The standard deviation of load and deflection is given in parentheses.

Table 5.25: Four-point bending test results for Hi-Nicalon™ Type S with SPR-212 hybrid specimens pyrolyzed at 1500°C; standard deviations are given in parentheses.

Specimen	***d* [mm]**	**Load [*N*]**	***D* [mm]**
1500°C Hi-Nicalon™ Type S SPR-212 Hybrid	1.65	48.7 (5.95)	0.344 (0.0456)

Once again, the reduction of thickness from the desired 2 mm is believed to be due to a higher carbothermal decomposition and chemical shrinkage of the matrix at higher pyrolysis temperature of 1500°C and is in the order of the case with SPR-212. Table 5.26 reports calculated mechanical properties of the 1500°C Hi-Nicalon™ Type S SPR-212 hybrid CFCCs.

Equations (1) through (4) were utilized in a similar manner as described previously. Properties were averaged, and standard deviations are given in parentheses.

Table 5.26: Mechanical properties from 4-point bending test results for Hi-Nicalon™ Type S with SPR-212 hybrid pyrolyzed at 1500°C; standard deviations are given in parentheses.

Specimen Type	Flexural Strength [MPa]	Elastic Modulus [GPa]	Strain-to-failure [mm/mm]	Toughness [MJ/m^3]
1500°C Hi-Nicalon™ Type S SPR-212 Hybrid	92.34 (10.4)	159.0 (15.6)	0.000670 (0.0000833)	27.65 (5.65)

Hi-Nicalon™ Type S SPR-212 hybrid, being majority SMP-10 ceramic yield, has very close mechanical properties to its SMP-10 baseline counterpart. Most of its mechanical properties have a marginal improvement from its SPR-212 base matrix.

5.6 Discussion on the Comparison of the Results for Nicalon™ CFCCs

Nicalon™ SPR-212 had higher flexural strength, strain-to-failure, and toughness but lower modulus of elasticity than the baseline Nicalon™ SMP-10. Nicalon™ SMP-10 hybrid (that had a majority of its matrix as SPR-212) had also all mechanical properties higher than the baseline, with modulus of elasticity within margin of error. This is believed to be due to a strong base matrix of SMP-10 with low viscosity SPR-212 to fill in the microcracks and pore during further infiltration. Nicalon™ SPR-212 hybrid (that had a majority of its matrix as SMP-10) had the lowest mechanical properties in this study. Table 5.27 reports the mechanical properties of all four types of Nicalon™ CFCCs studied in this research.

Table 5.27: Compiled mechanical properties for all four types of Nicalon™ CFCCs; standard deviations are given in parentheses.

Specimen Type	Flexural Strength [MPa]	Elastic Modulus [GPa]	Strain-to-failure [mm/mm]	Toughness [MJ/m^3]
Nicalon™ SMP-10	38.87 (11.3)	61.79 (3.78)	0.000633 (0.000165)	14.56 (6.11)
Nicalon™ SPR-212	39.97 (6.08)	54.65 (10.8)	0.000720 (0.000127)	16.20 (3.56)
Nicalon™ SMP-10 Hybrid	40.14 (7.24)	61.11 (13.9)	0.000694 (0.000079)	18.48 (3.02)
Nicalon™ SPR-212 Hybrid	22.71 (0.871)	56.11 (1.22)	0.000510 (0.00000113)	5.80 (0.234)

Figure 5.23a compares the flexural strengths of all four types of Nicalon™ CFCCs as listed in Table 5.27. Percentages of improvements in strength compared to the base Nicalon™ SMP-10 CFCCs are given in Figure 5.23b.

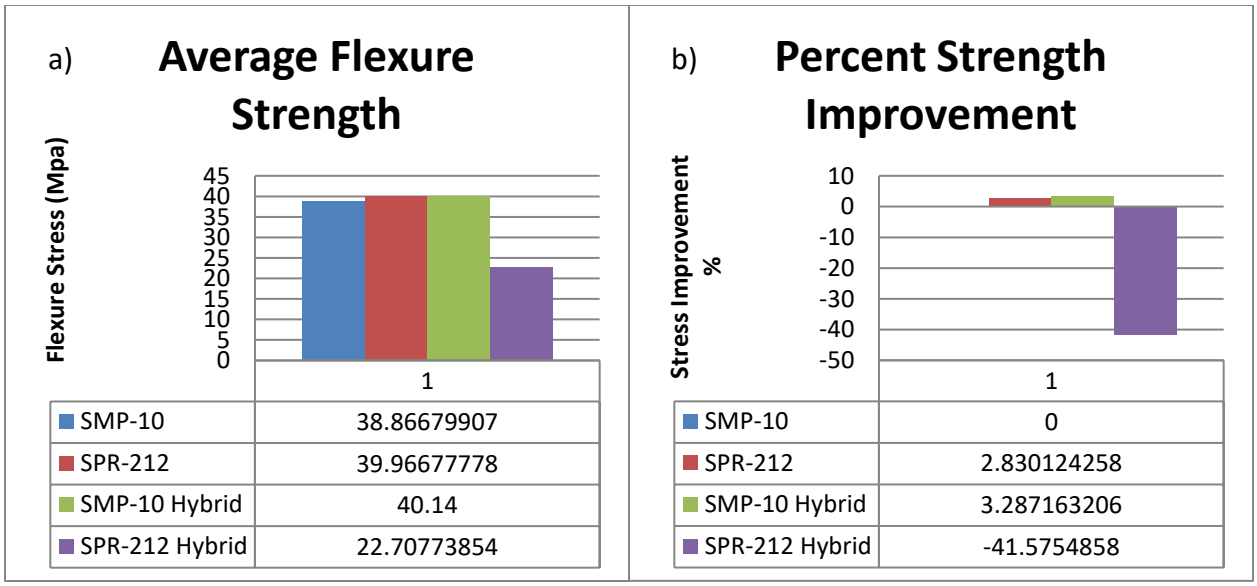

Figure 5.23: Flexural strength comparison for all four types of Nicalon™ CFCCs, a) Flexural strengths in MPa, and b) percent improvements in flexural strength compared to Nicalon™ SMP-10 CFCCs.

The highest flexural strength was demonstrated by SMP-10 hybrid with SPR-212 slightly behind it. A 3.3% increase in flexural strength compared to the baseline SMP-10 was achieved. Figure

5.24a compares the toughness calculated for each type of Nicalon™ CFCCs. Figure 5.24b demonstrates the percentages of improvements in toughness that were achieved compared to the baseline Nicalon™ SMP-10 CFCCs.

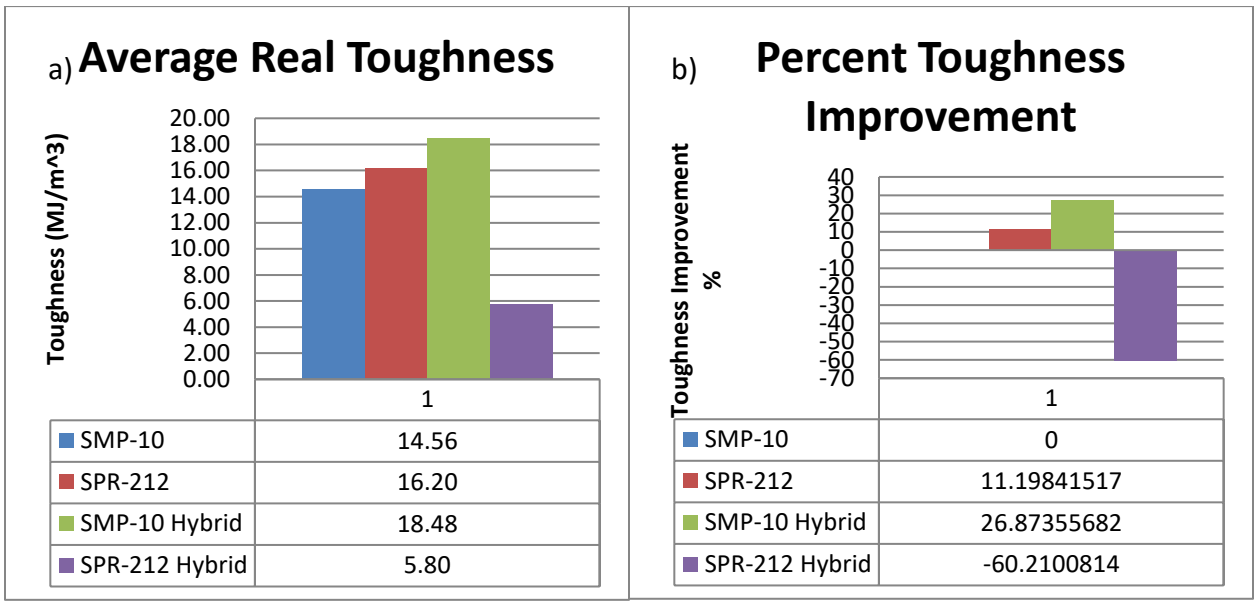

Figure 5.24: Toughness comparison for all four types of Nicalon™ CFCCs, a) Toughness in MJ/m^2, and b) Percent improvements in toughness compared to Nicalon™ SMP-10 CFCCs.

SPR-212 has a higher toughness of 11% over the baseline, but SMP-10 hybrid has the highest at 27%. SPR-212 hybrid has a very poor performance. Figure 5.25a compares the values derived for modulus of elasticity for all four types of Nicalon™ CFCCs studied in this work. Figure 5.25b demonstrates the percentages of improvements in modulus of elasticity compared to baseline Nicalon™ SMP-10 CFCCs.

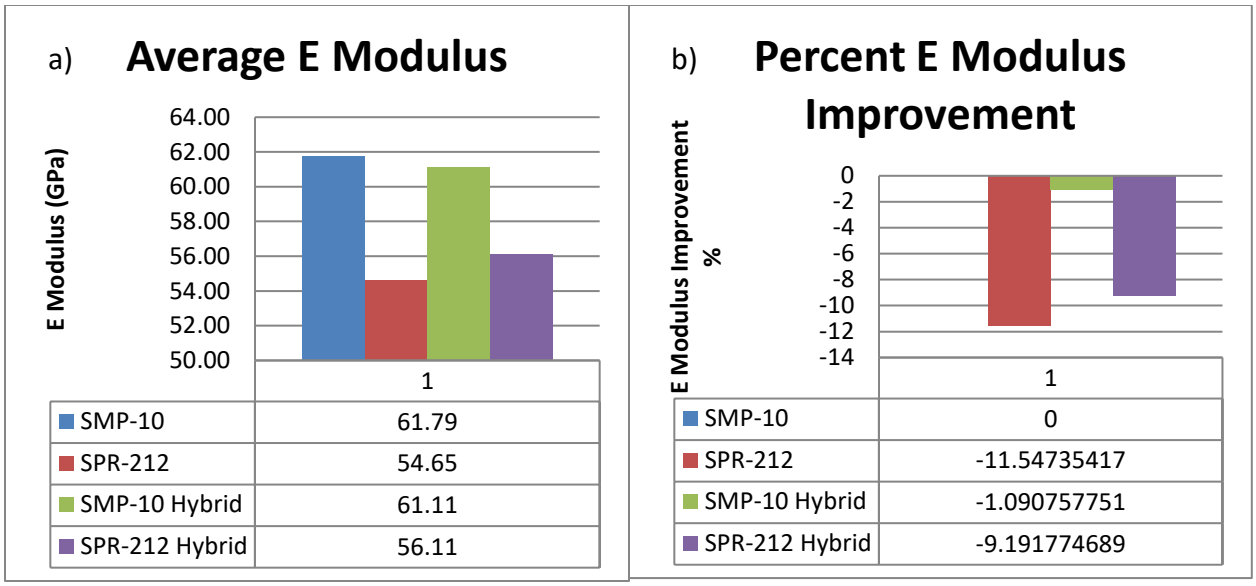

Figure 5.25: Elastic moduli comparison for all four types of Nicalon™ CFCCs, a) Elastic moduli in GPa, and b) Percent improvements in elastic moduli compared to Nicalon™ SMP-10 CFCCs

The baseline SMP-10 has the highest stiffness of all the specimens. SPR-212 has the lowest stiffness of 9% below baseline, but SMP-10 is within margin of error of SMP-10. Figure 5.26a compares the amount of strain in mm/mm the CFCCs underwent up to failure point with Figure 5.26b comparing to the baseline in percent improvement.

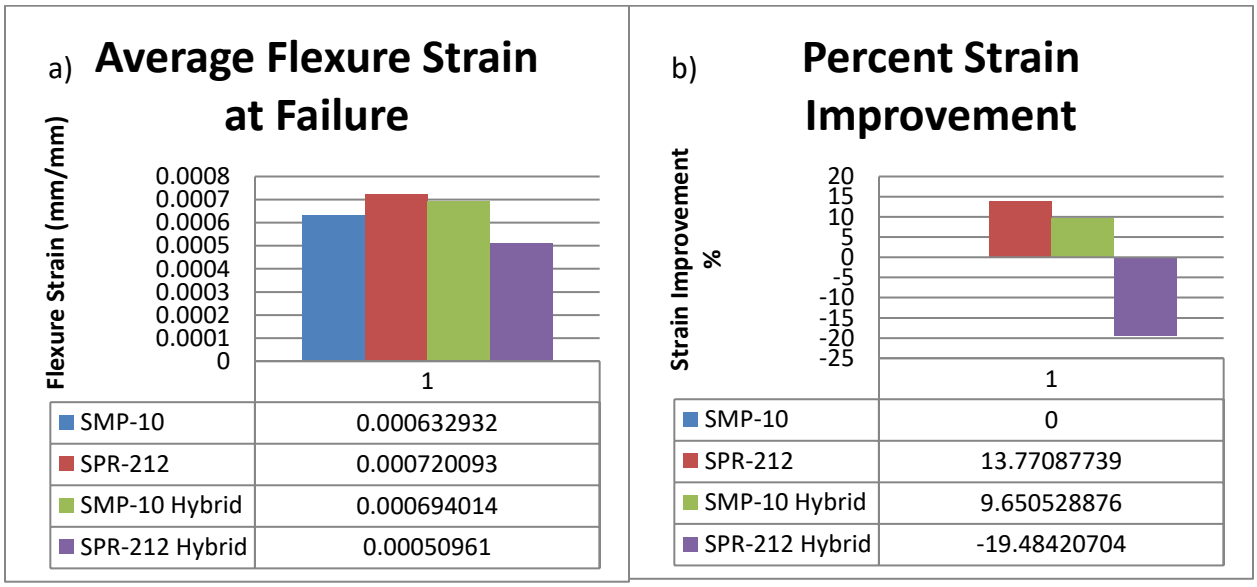

Figure 5.26: Strain-to-failure for all four types of Nicalon™ CFCCs, a) Strain-to-failure in mm/mm, and b) Percent improvements in strain-to-failure compared to Nicalon™ SMP-10 CFCCs.

Similarly, Figure 5.27a shows the deflection to failure in mm for all four types of Nicalon™ CFCCs studied in this work with Figure 5.27b comparing to the baseline in percent improvement.

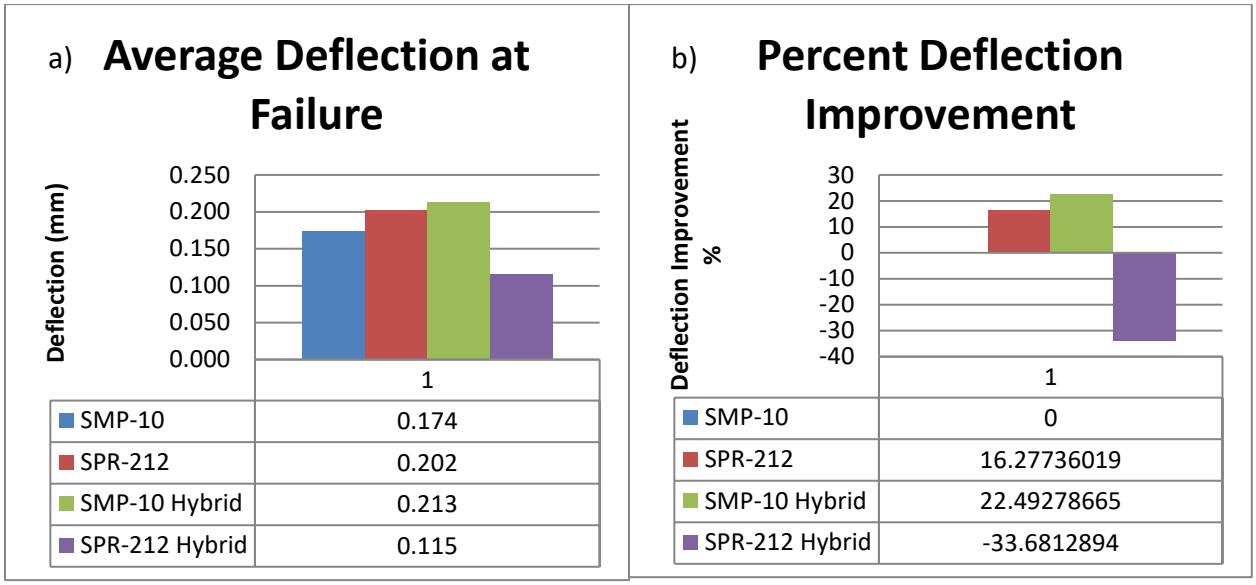

Figure 5.27: Deflection to failure for all four types of Nicalon™ CFCCs, a) Deflection to failure in mm, and b) Percent improvements in deflection to failure compared to Nicalon™ SMP-10 CFCCs.

***Nicalon™ Fiber CFCCs Conclusions**: These results show that overall, Nicalon™ SMP-10 hybrid CFCC had the best performance in terms of Strength, Modulus, Strain-to-failure, failure deflection, and Toughness followed by Nicalon™ SMP-10 hybrid CFCC.*

5.7 Discussion on the Comparison of the Results for T300 CFCCs

T300 CFCCs were performed to mainly compare the performance of the CFCCs made with Nicalon™ fiber compared with those made with T300 carbon fiber. The following compares the best performing cases for each, i.e., their CFCCs made with SMP-10 hybrid. T300 SMP-10 hybrid outperformed Nicalon™ SMP-10 hybrid in every mechanical property except stiffness, despite T300 fabric having a higher tensile modulus than Nicalon™ fiber. The decrease in

stiffness is likely due to the high pyrolysis temperature of 1000°C and thermal cycling having an annealing effect on the carbon fabric; however, the lower stiffness of T300 SMP-10 hybrid is within the margin of error of the Nicalon™ SMP-10 hybrid modulus in terms of standard deviation (see Table 5.28). The T300 had a noticeable strength increase, but its toughness had the largest increase compared to its counterpart. This is caused by the difference of the base fabric strength and toughness, and is reflected in its strength, strain, and deflection at failure.

Table 5.28: Compiled mechanical properties for T300 and Nicalon™ SMP-10 Hybrid CFCCs; standard deviations are given in parentheses.

Specimen Type	Flexural Strength [MPa]	Elastic Modulus [GPa]	Strain-to-failure [mm/mm]	Toughness [MJ/m^3]
T300 SMP-10 Hybrid	63.96 (3.88)	53.12 (2.87)	0.00139 (0.0000344)	44.55 (3.73)
Nicalon™ SMP-10 Hybrid	40.14 (7.24)	61.11 (13.9)	0.000694 (0.000079)	18.48 (3.02)

Figure 5.28a compares the flexural strengths of T300 and Nicalon™ SMP-10 hybrid CFCCs as listed in Table 5.28. Percentages of improvements in strength compared to the base Nicalon™ SMP-10 hybrid CFCCs are given in Figure 5.28b.

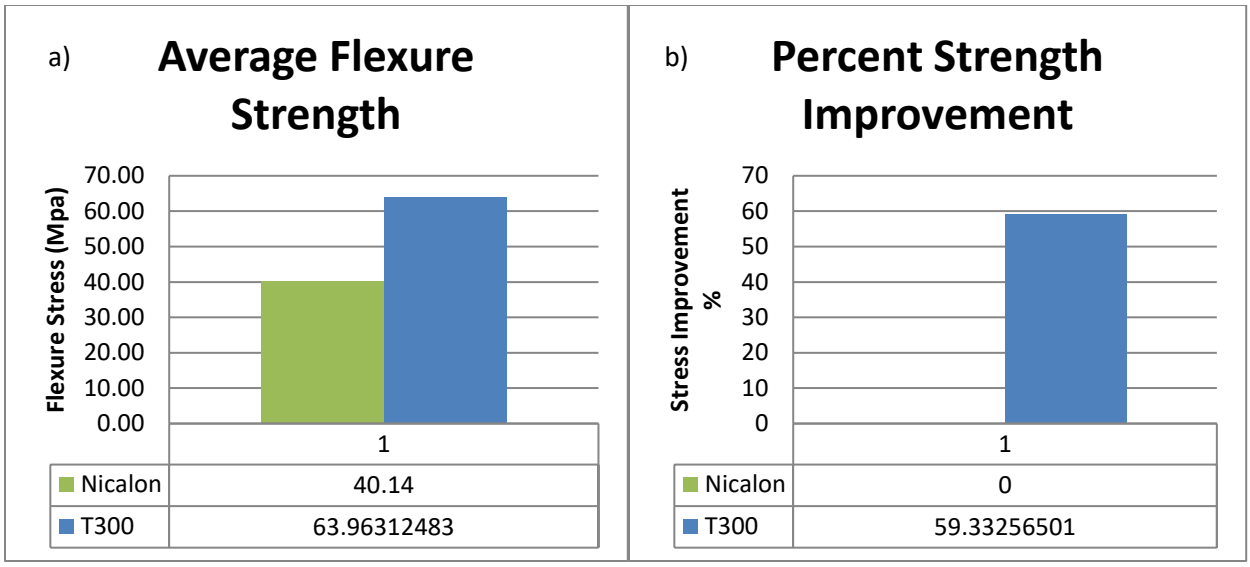

Figure 5.28: Flexural strength comparison for T300 and Nicalon™ SMP-10 Hybrid CFCCs, a) Flexural strengths in MPa, and b) percent improvements in flexural strength compared to Nicalon™ SMP-10 SMP-10 Hybrid CFCCs.

The highest flexural strength was demonstrated by T300 SMP-10 hybrid. A 59% increase in flexural strength compared to the baseline Nicalon™ SMP-10 hybrid was achieved.

Figure 5.29a compares the toughness calculated for T300 and Nicalon™ SMP-10 hybrid CFCCs. Figure 5.29b demonstrates the percentages of improvements in toughness that were achieved compared to the baseline Nicalon™ SMP-10 hybrid CFCCs.

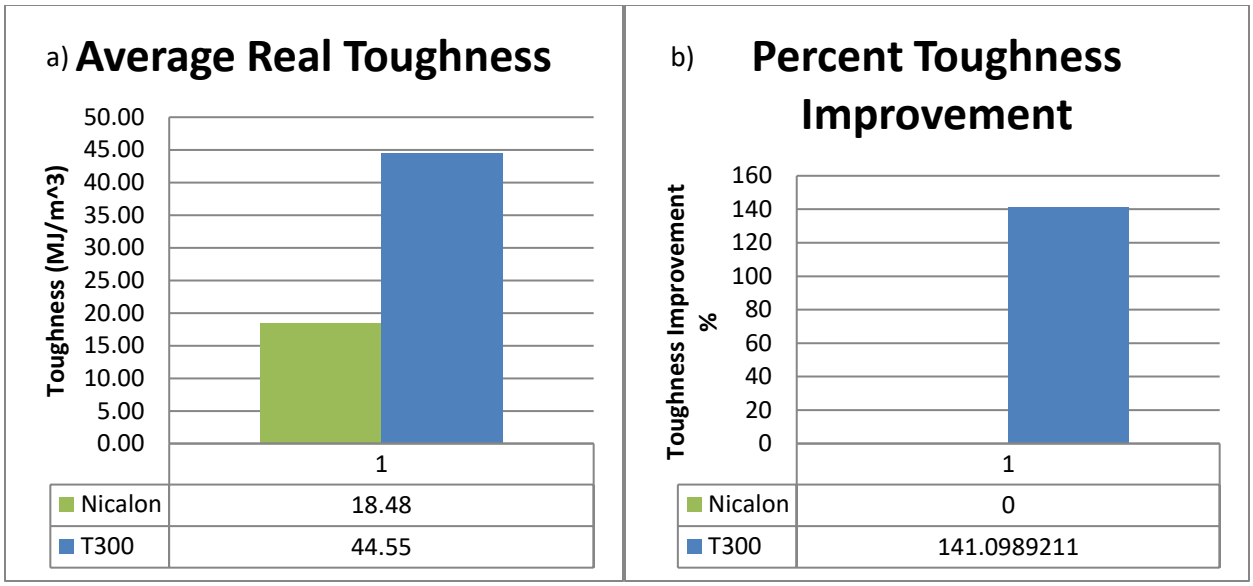

Figure 5.29: Toughness comparison for T300 and Nicalon™ SMP-10 Hybrid CFCCs, a) Toughness in MJ/m^2, and b) Percent improvements in toughness compared to Nicalon™ SMP-10 Hybrid CFCCs.

The T300 SMP-10 hybrid has a substantial different in toughness than its Nicalon™ SMP-10 hybrid counterpart, with a 141% improvement.

Figure 5.30a compares the values derived for modulus of elasticity for T300 and Nicalon™ SMP-10 hybrid CFCCs studied in this work. Figure 5.30b demonstrates the percentages of improvements in modulus of elasticity compared to baseline Nicalon™ SMP-10 hybrid CFCCs. T300 SMP-10 hybrid is lower in stiffness than it Nicalon™ SMP-10 hybrid counterpart, with a decrease of 13%.

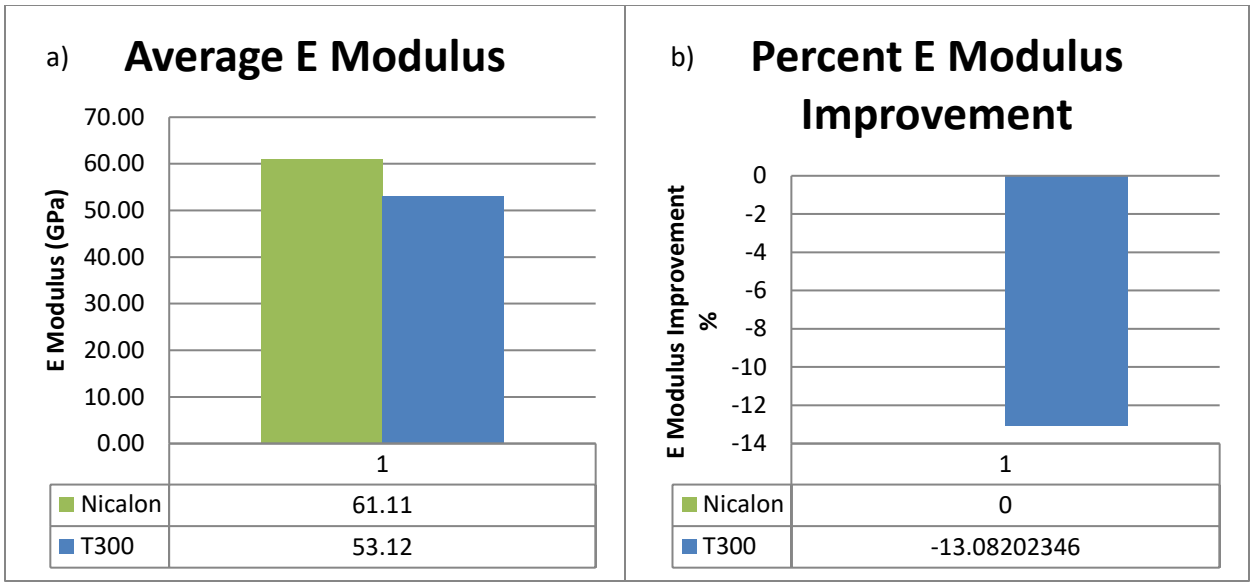

Figure 5.30: Elastic moduli comparison for all T300 and Nicalon™ SMP-10 Hybrid CFCCs, a) Elastic moduli in GPa, and b) Percent improvements in elastic moduli compared to Nicalon™ SMP-10 Hybrid CFCCs.

***Nicalon™ & T300 Fiber CFCCs Comparison Conclusions**: These results show that T300 SMP-10 hybrid CFCC had clearly better performances in terms of Strength, Strain-to-failure, and Toughness compared with Nicalon™ SMP-10 hybrid CFCC; however, in terms of modulus, Nicalon™ SMP-10 hybrid CFCC performed somewhat better.*

5.8 Discussion on the Comparison of the Results for Hi-Nicalon™ Type S CFCCs pyrolyzed at 1000°C

The Hi-Nicalon™ Type S specimens do not follow similar mechanical property trends as standard Nicalon™ specimens. This is caused by the difference in atomic composition, where Hi-Nicalon™ Type S has a lower amount of free carbon atoms and is evident in the fibers data sheet [34] with an increase in modulus but decrease in strength compared to the standard Nicalon™ fabric. Although the Hi-Nicalon™ Type S fabric has lower strength compared to the standard Nicalon™ fabric, all mechanical properties of Hi-Nicalon™ Type S CFCCs are much

greater in performance. The possible cause is perhaps due to fabric to matrix interface of the atomically balanced silicon to carbon ratio of the Hi-Nicalon™ Type S fabric to SiC ceramic form from the preceramic polymers. SMP-10 had the highest performance in all mechanical properties and the use of any SPR-212 reduced its performance. This is observed with SPR-212 hybrid, where the base matrix of SPR-212 reduced its performance in all properties. SMP-10 hybrid (with a majority of the matrix being SPR-212) also followed this trend with its slightly higher mechanical properties over pristine SPR-212. Table 5.27 reports the mechanical properties of all four types of Hi-Nicalon™ Type S CFCCs studied in this research at 1000ºC pyrolysis.

Table 5.29: Compiled mechanical properties for all four types of Hi-Nicalon™ Type S CFCCs pyrolyzed at 1000°C; standard deviations are given in parentheses.

Specimen Type	**Flexural Strength [MPa]**	**Elastic Modulus [GPa]**	**Strain-to-failure [mm/mm]**	**Toughness [MJ/m^3]**
Hi-Nicalon™ Type S SMP-10	431.0 (28.9)	88.04 (8.46)	0.00725 (0.000360)	1391 (160)
Hi-Nicalon™ Type S SPR-212	366.5 (17.0)	72.59 (5.30)	0.00600 (0.000199)	977.3 (64.5)
Hi-Nicalon™ Type S SMP-10 Hybrid	377.8 (9.53)	68.45 (3.45)	0.00693 (0.000332)	1164 (74.3)
Hi-Nicalon™ Type S SPR-212 Hybrid	428.5 (19.6)	93.91 (6.67)	0.00649 (0.000340)	1237 (117)

Figure 5.31 Figure 5.31a compares the flexural strengths of all four types of Hi-Nicalon™ Type S CFCCs pyrolyzed at 1000°C as listed in Table 5.29. Percentages of improvements in strength compared to the base Hi-Nicalon™ Type S SMP-10 CFCCs pyrolyzed at 1000° C are given in Figure 5.31Figure 5.31b.

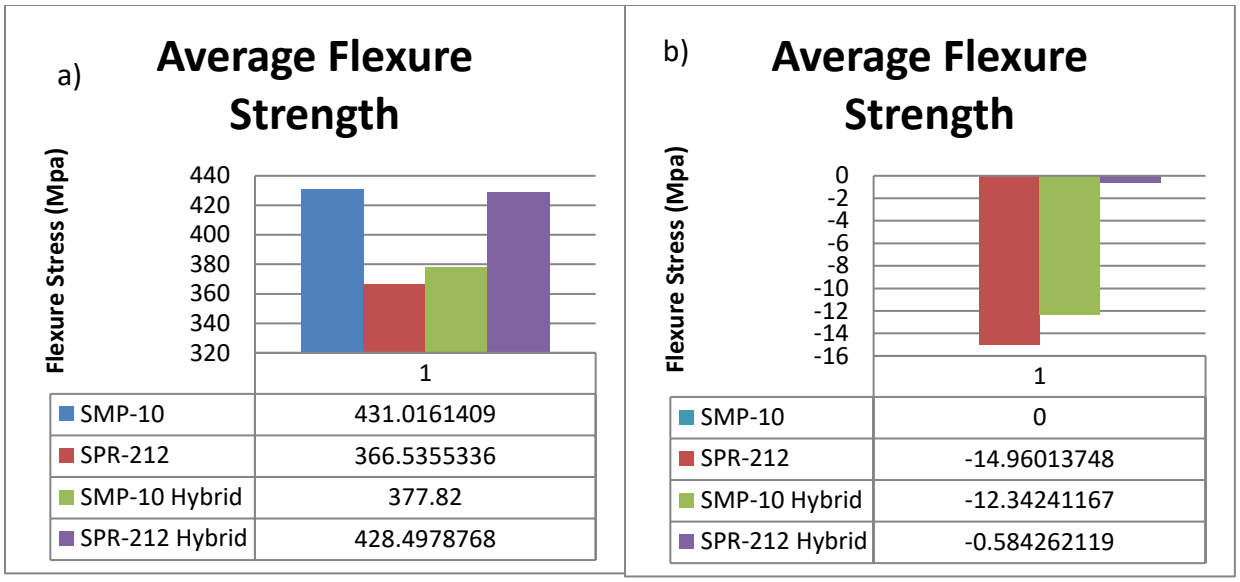

Figure 5.31: Flexural strength comparison for all four types of Hi-Nicalon™ Type S CFCCs pyrolyzed at 1000°C, a) Flexural strengths in MPa, and b) percent improvements in flexural strength compared to Hi-Nicalon™ Type S SMP-10 CFCCs pyrolyzed at 1000°C.

The highest flexural strength was demonstrated by Hi-Nicalon™ SMP-10 CFCC. The closest in flexural strength was Hi-Nicalon™ Type S SPR-212 hybrid (which had the SMP-10 as the majority of the matrix) with a 0.6% decrease in performance.

Figure 5.32Figure 5.32a compares the toughness calculated for each type of Hi-Nicalon™ Type S CFCCs pyrolyzed at 1000°C. Figure 5.32Figure 5.32b demonstrates the percentages of improvements in toughness that were achieved compared to the baseline Hi-Nicalon™ Type S SMP-10 CFCCs pyrolyzed at 1000°C.

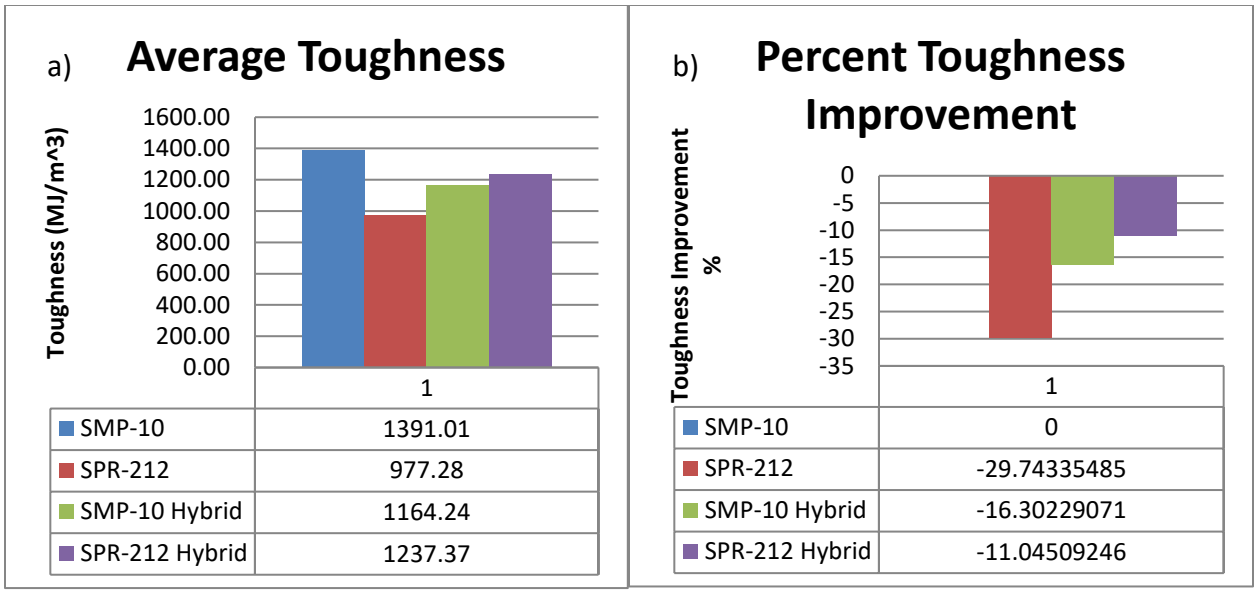

Figure 5.32: Toughness comparison for all four types of Hi-Nicalon™ Type S CFCCs pyrolyzed at 1000°C, a) Toughness in MJ/m^2, and b) Percent improvements in toughness compared to Hi-Nicalon™ Type S SMP-10 CFCCs pyrolyzed at 1000°C.

The baseline Hi-Nicalon™ Type S SMP-10 CFCC has the highest toughness with Hi-Nicalon™ Type S SPR-212 CFCC having the lowest performance with a lower performance of 30%. Hi-Nicalon™ Type S SMP-10 hybrid CFCC, which is majority SPR-212, performs better than the pristine SPR-212, which is only 16% below the baseline. Hi-Nicalon™ Type SSPR-212 hybrid CFCC, which is majority SMP-10, performed closest to the baseline with a 11% decrease, which is better than Hi-Nicalon™ Type S SPR-212, and Hi-Nicalon™ Type S SMP-10 hybrid CFCCs.

Figure 5.33Figure 5.33a compares the values derived for modulus of elasticity for all four types of Hi-Nicalon™ Type S CFCCs pyrolyzed at 1000°C studied in this work. Figure 5.33Figure 5.33b demonstrates the percentages of improvements in modulus of elasticity compared to baseline Hi-Nicalon™ Type S SMP-10 CFCCs pyrolyzed at 1000°C.

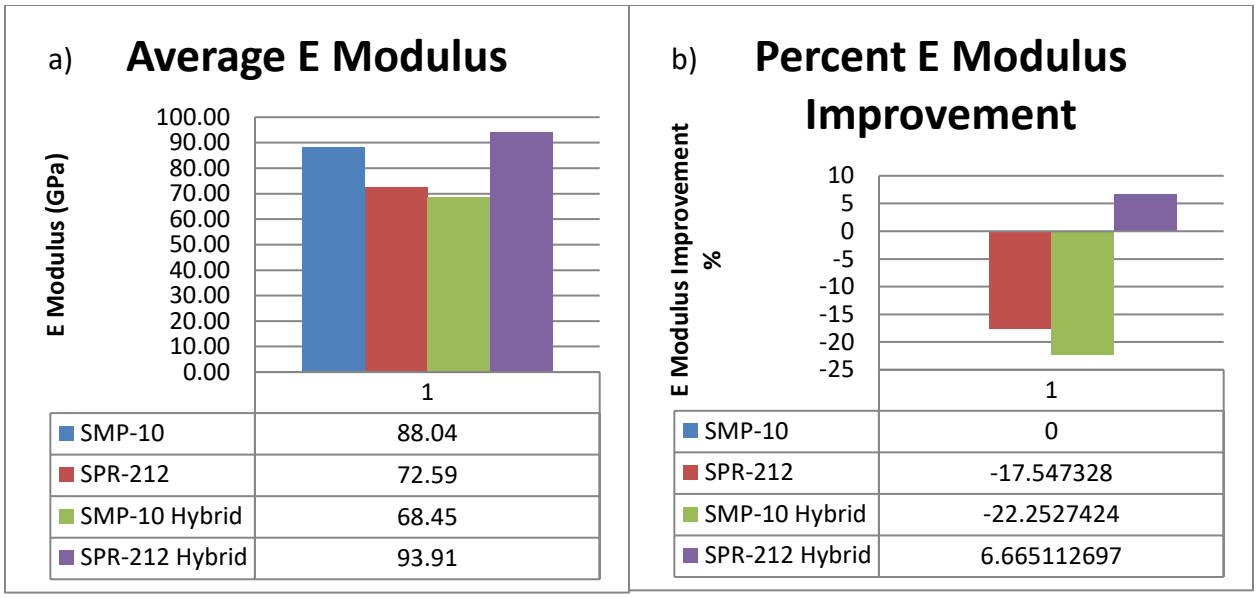

Figure 5.33: Elastic moduli comparison for all four types of Hi-Nicalon™ Type S CFCCs pyrolyzed at 1000°C, a) Elastic moduli in GPa, and b) Percent improvements in elastic moduli compared to Hi-Nicalon™ Type S SMP-10 CFCCs pyrolyzed at 1000°C.

Hi-Nicalon™ Type S SMP-10 and SPR-212 hybrid (i.e., with majority of matrix being SMP-10) have the highest stiffness, with SPR-212 and SMP-10 hybrid having the lowest. Although SMP-10 hybrid has the lowest stiffness, it decreased from the baseline by 22%, and it is within the margin of error of the modulus for SPR-212.

Figure 5.34Figure 5.34a compares the amount of strain in mm/mm the CFCCs underwent up to failure point with Figure 5.34Figure 5.34b comparing to the baseline in percent improvement.

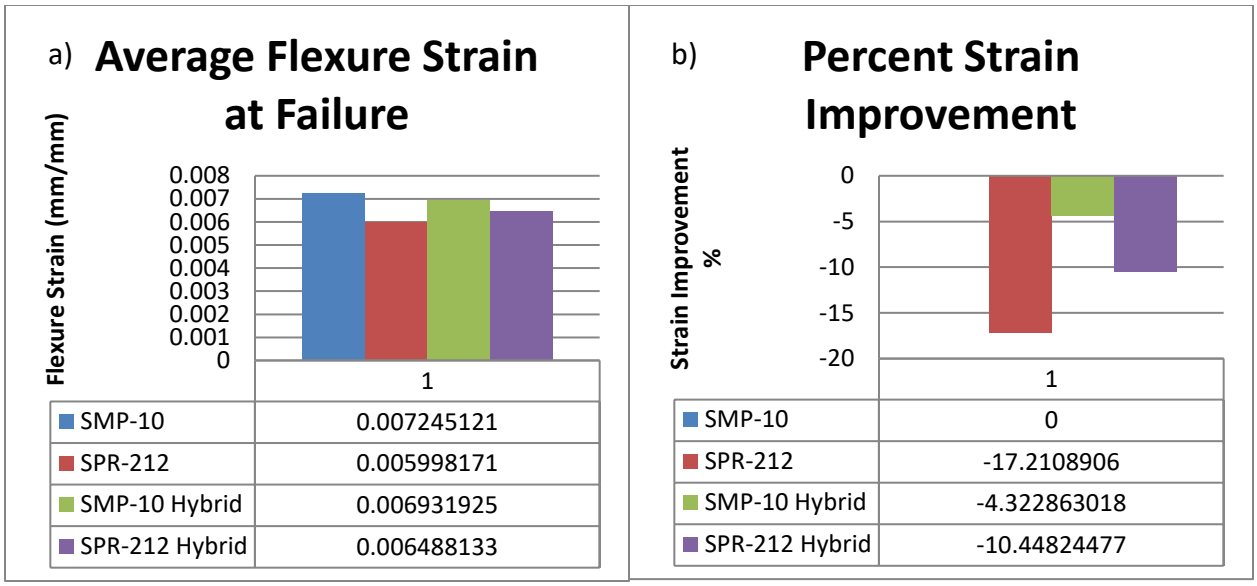

Figure 5.34: Strain-to-failure for all four types of Hi-Nicalon™ Type S CFCCs pyrolyzed at 1000°C, a) Strain-to-failure in mm/mm, and b) Percent improvements in strain-to-failure compared to Hi-Nicalon™ Type S SMP-10 CFCCs pyrolyzed at 1000°C.

Similarly, Figure 5.35Figure 5.35a shows the deformation to failure in mm for all four types of Hi-Nicalon™ Type S CFCCs pyrolyzed at 1000°C studied in this work with Figure 5.35Figure 5.35b comparing to the baseline in percent improvement.

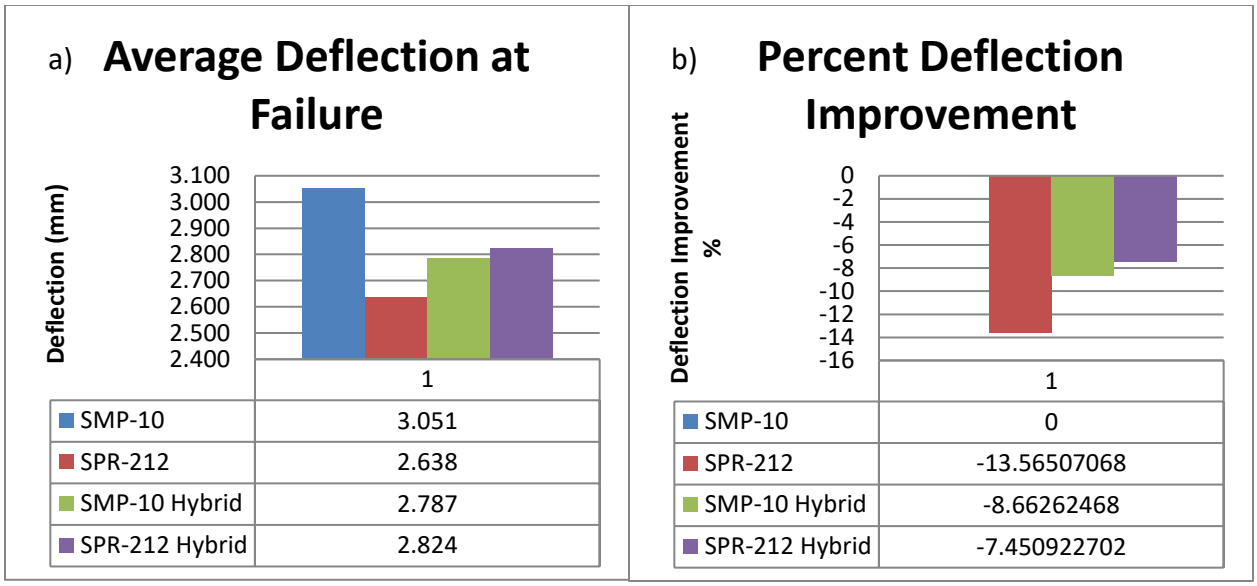

Figure 5.35: Deflection to failure for all four types of Hi-Nicalon™ Type S CFCCs pyrolyzed at 1000°C, a) Deflection to failure in mm, and b) Percent improvements in deflection to failure compared to Hi-Nicalon™ Type S SMP-10 CFCCs pyrolyzed at 1000°C.

The strain and deflection at failure display that Hi-Nicalon™ Type S SMP-10 CFCC outperformed the other samples.

***Hi-Nicalon™ Type S Fiber CFCCs Pyrolyzed at 1000ºC Conclusions**: These results show that overall, Hi-Nicalon™ Type S SMP-10 CFCC had the best performance in terms of Strength, Modulus, Strain-to-failure, failure deflection, and Toughness followed by Hi-Nicalon™ Type S SPR-212 hybrid (with SMP-10 as the majority of the matrix). Hi-Nicalon™ Type S SMP-10 hybrid and Hi-Nicalon™ Type S SPR-212 CFCCs are clearly ranked 3rd and 4th, respectively, in this case.*

5.9 Discussion on the Comparison of the Results for Hi-Nicalon™ Type S CFCCs pyrolyzed at 1500°C

The 1500°C pyrolysis study of Hi-Nicalon™ Type S specimens display large differences from the 1000°C pyrolysis study. All mechanical properties are decreased with the exception of stiffness. This is believed to be caused from the stiffer β-phase SiC crystalline structure (that

forms for the 1500ºC pyrolysis), compared to amorphous SiC structures (that forms for the 1000ºC pyrolysis). The degradation in mechanical properties is believed to be either due to some oxidation and/or transformation into a monolithic ceramic (i.e., similar matrix and fiber materials). Some oxidations are evident from the change in color (e.g., see Figure 5.36) to reflect the formation of silicon-oxides and decrease in weights and dimensions/volume compared to the 1000°C study, which used the same molds and was cut to the same dimensions. Also, the transition of the matrix from amorphous phase to β-phase SiC crystalline material could create a somewhat homogeneous or monolithic structure with the high purity β-phase Hi-Nicalon™ Type S SiC fibers (i.e., similar fiber and matrix materials).

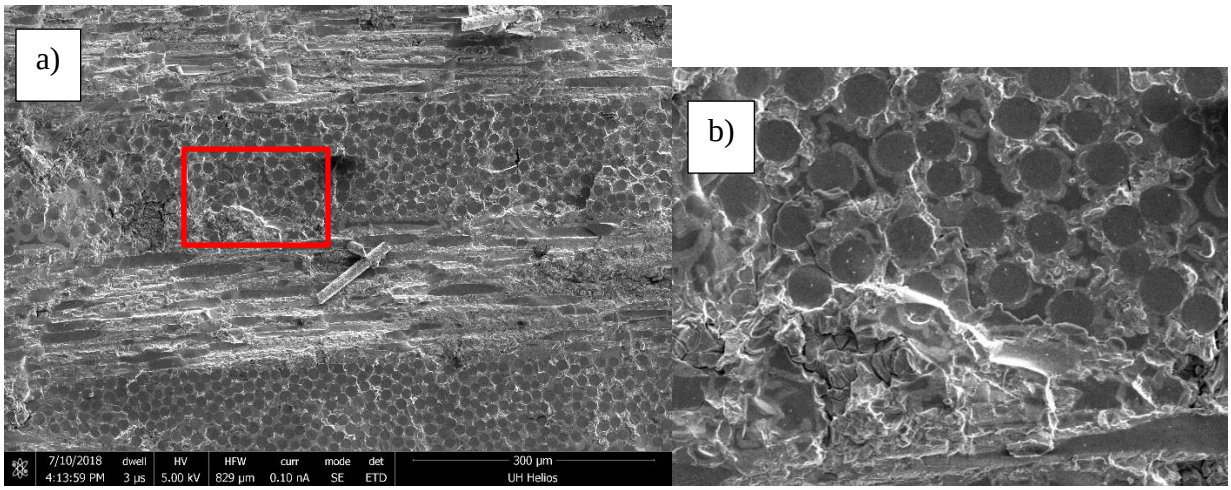

Figure 5.36: Corrosion of 1500°C CFCC with interphase boundary, a) Fracture surface with b) zoom in red.

Table 5.27 reports the mechanical properties of all four types of Hi-Nicalon™ Type S CFCCs studied in this research at 1500ºC pyrolysis. Hi-Nicalon™ Type S SPR-212 CFCC outperformed the baseline made with SMP-10 in all mechanical properties except stiffness. This can be explained from the formation of SiO_2 forming from SiOC, inhibiting oxygen diffusion and reducing oxidation. Introduction of any SMP-10 reduced the mechanical properties of the specimen, except for the stiffness. In this case, the SPR-212 dominated CFCCs (i.e., SPR-212

and SMP-10 hybrid) had the highest strain-to-failure and toughness, as well as strength, while the SMP-10 dominated CFCCs (i.e., SMP-10 and SPR-212 hybrid) had much better stiffness; although the strength of SMP-10 hybrid and SPR-212 hybrid were very close.

Table 5.30: Compiled mechanical properties for all four types of Hi-Nicalon™ Type S CFCCs pyrolyzed at 1500°C; standard deviations are given in parentheses.

Specimen Type	Flexural Strength [MPa]	Elastic Modulus [GPa]	Strain-to-failure [mm/mm]	Toughness [MJ/m^3]
1500°C Hi-Nicalon™ Type S SMP-10	87.65 (7.52)	160.6 (16.6)	0.000611 (0.0000689)	23.88 (3.97)
1500°C Hi-Nicalon™ Type S SPR-212	100.8 (9.59)	121.4 (10.4)	0.000932 (0.0000764)	41.94 (6.44)
1500°C Hi-Nicalon™ Type S SMP-10 Hybrid	90.09 (18.0)	105.9 (11.4)	0.000961 (0.000222)	39.70 (16.3)
1500°C Hi-Nicalon™ Type S SPR-212 Hybrid	92.34 (10.4)	159.0 (15.6)	0.000670 (0.0000833)	27.65 (5.65)

Figure 5.37a compares the flexural strengths of all four types of Hi-Nicalon™ Type S CFCCs pyrolyzed at 1500°C as listed in Table 5.30. Percentages of improvements in strength compared to the base Hi-Nicalon™ Type S SMP-10 CFCCs pyrolyzed at 1500° C are given in Figure 5.37b.

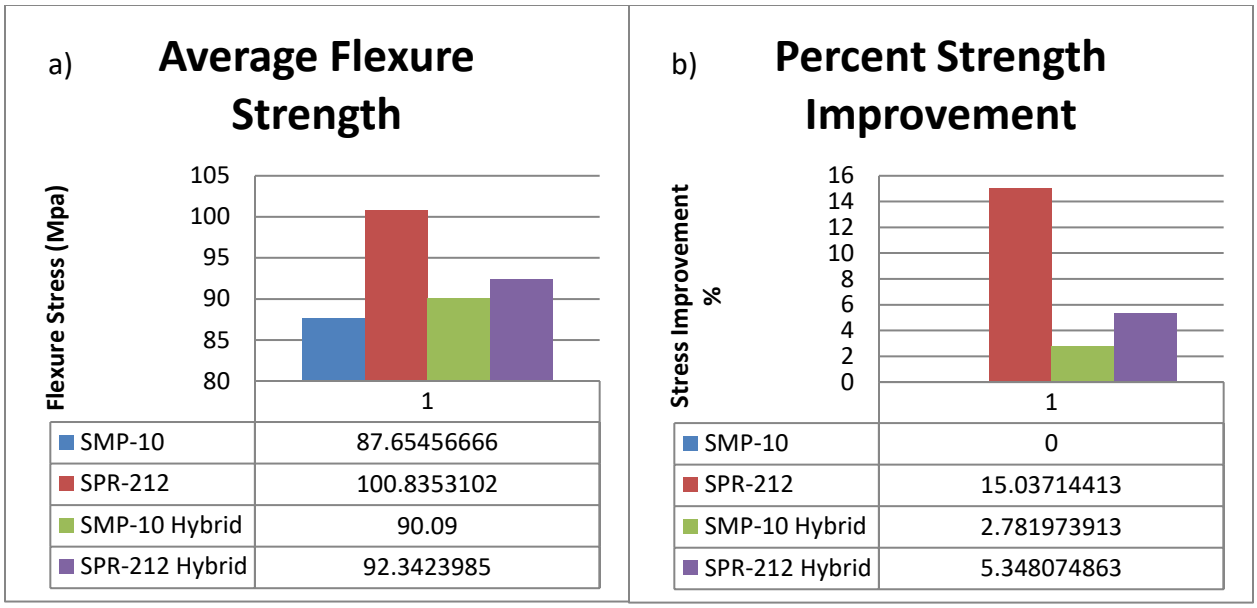

Figure 5.37: Flexural strength comparison for all four types of Hi-Nicalon™ Type S CFCCs pyrolyzed at 1500°C, a) Flexural strengths in MPa, and b) percent improvements in flexural strength compared to Hi-Nicalon™ Type S SMP-10 CFCCs pyrolyzed at 1500°C.

The highest flexural strength was demonstrated by Hi-Nicalon™ Type S SPR-212. A 15% increase in flexural strength compared to the baseline made with SMP-10 was achieved. Hi-Nicalon™ Type S SPR-212 hybrid performed slightly better than that made with pristine SMP-10 with a 5% increase. Hi-Nicalon™ Type S SMP-10 hybrid was only marginally better than the baseline.

Figure 5.38a compares the toughness calculated for each type of Hi-Nicalon™ Type S CFCCs pyrolyzed at 1500°C. Figure 5.38b demonstrates the percentages of improvements in toughness that were achieved compared to the baseline Hi-Nicalon™ Type S SMP-10 CFCCs pyrolyzed at 1500°C.

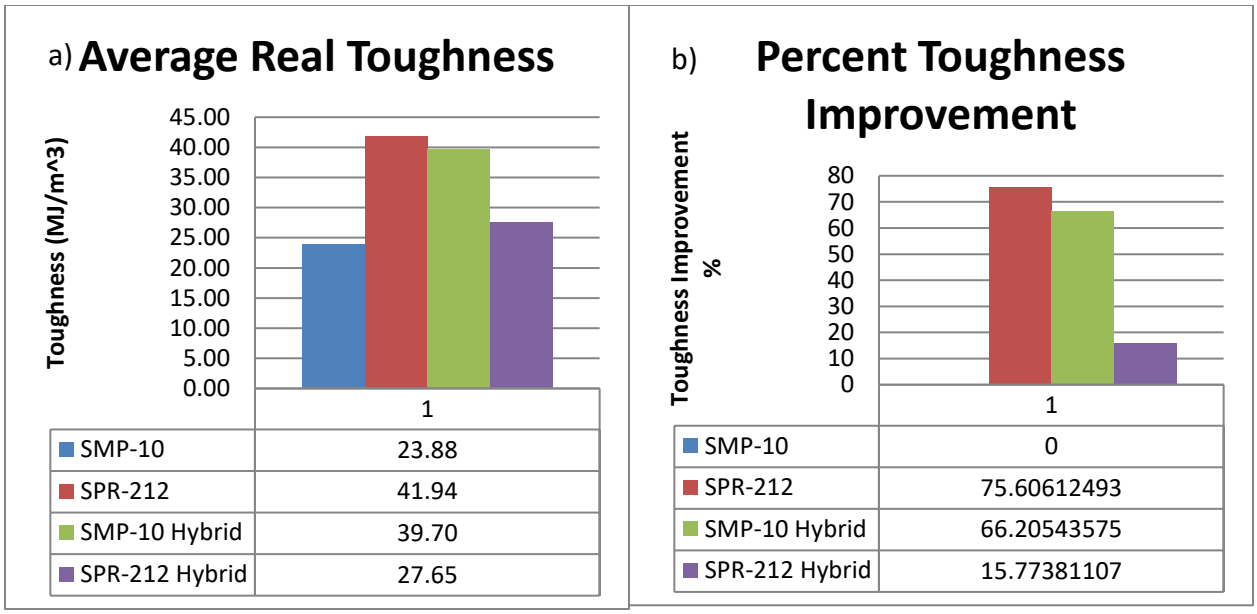

Figure 5.38: Toughness comparison for all four types of Hi-Nicalon™ Type S CFCCs pyrolyzed at 1500°C, a) Toughness in MJ/m^2, and b) Percent improvements in toughness compared to Hi-Nicalon™ Type S SMP-10 CFCCs pyrolyzed at 1500°C.

Hi-Nicalon™ Type S SPR-212 and SMP-10 hybrid (with majority of its matrix being SPR-212) CFCCs outperformed the baseline with 76% and 66% increase, respectively. Hi-Nicalon™ Type S SPR-212 hybrid CFCC, with its base matrix of SPR-212 also had an increase over pristine SMP-10 of 16%.

Figure 5.39a compares the values derived for modulus of elasticity for all four types of Hi-Nicalon™ Type S CFCCs pyrolyzed at 1500°C studied in this work. Figure 5.39b demonstrates the percentages of improvements in modulus of elasticity compared to baseline Hi-Nicalon™ Type S SMP-10 CFCCs pyrolyzed at 1500°C.

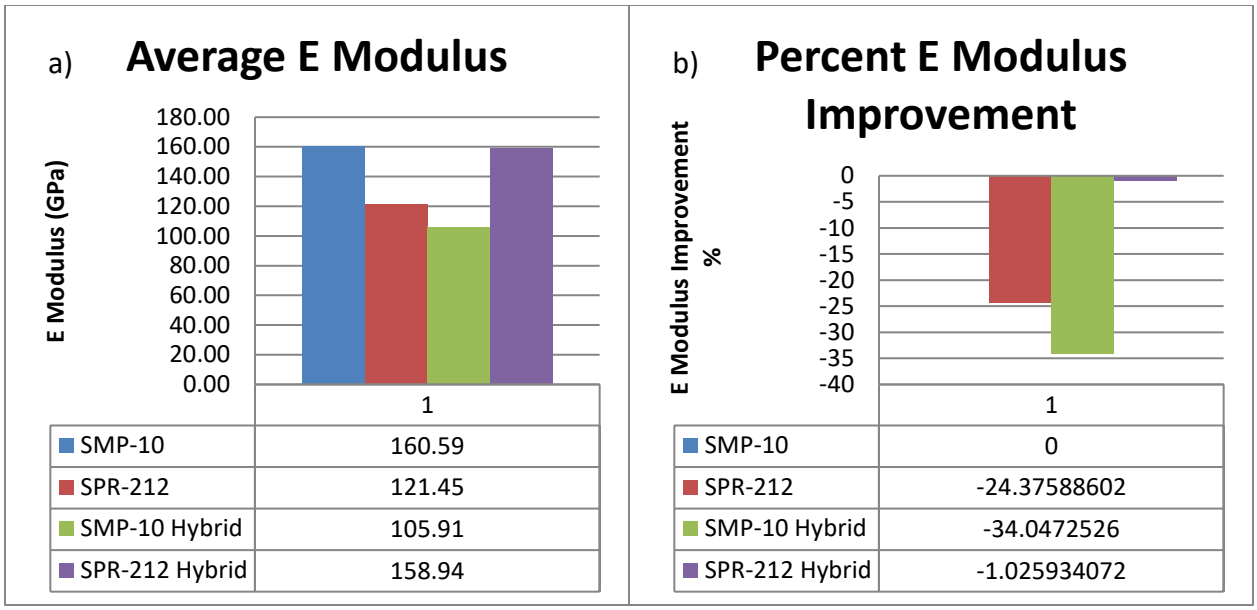

Figure 5.39: Elastic moduli comparison for all four types of Hi-Nicalon™ Type S CFCCs pyrolyzed at 1500°C, a) Elastic moduli in GPa, and b) Percent improvements in elastic moduli compared to Hi-Nicalon™ Type S SMP-10 CFCCs pyrolyzed at 1500°C.

The baseline Hi-Nicalon™ Type S SMP-10 and Hi-Nicalon™ Type S SPR-212 hybrid CFCCs have the highest stiffness. Hi-Nicalon™ Type S SPR-212 CFCC has a lower stiffness than the baseline made with SMP-10, and the Hi-Nicalon™ Type S SMP-10 hybrid has the lowest, with a decrease of 34%.

Figure 5.40a compares the amount of strain in mm/mm the CFCCs underwent up to failure point with Figure 5.40b comparing to the baseline in percent improvement.

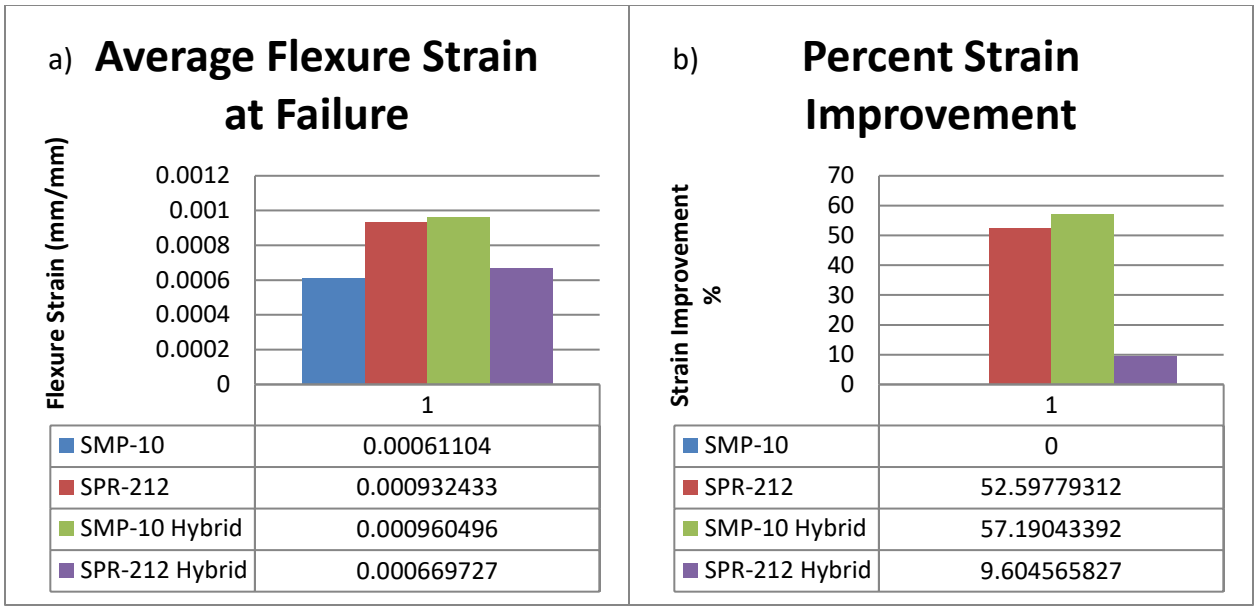

Figure 5.40: Strain-to-failure for all four types of Hi-Nicalon™ Type S CFCCs pyrolyzed at 1500°C, a) Strain-to-failure in mm/mm, and b) Percent improvements in strain-to-failure compared to Hi-Nicalon™ Type S SMP-10 CFCCs pyrolyzed at 1500°C.

Similarly, Figure 5.41a shows the deflection to failure in mm for all four types of Hi-Nicalon™ Type S CFCCs pyrolyzed at 1500°C studied in this work with Figure 5.41b comparing to the baseline in percent improvement.

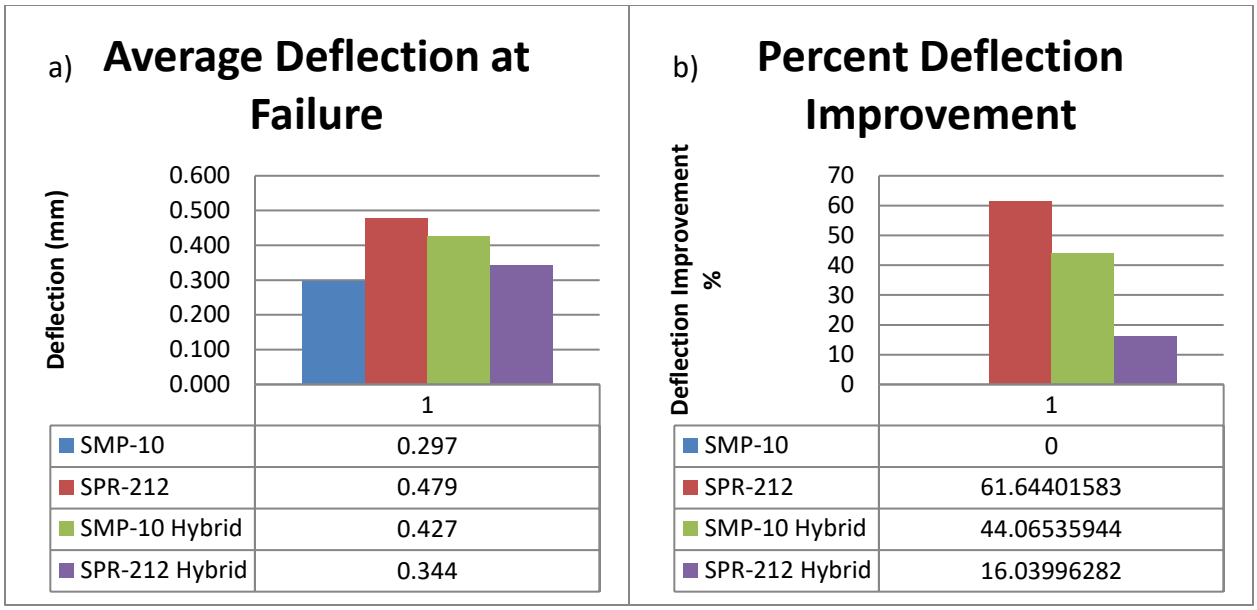

Figure 5.41: Deflection to failure for all four types of Hi-Nicalon™ Type S CFCCs pyrolyzed at 1500°C, a) Deflection to failure in mm, and b) Percent improvements in deflection to failure compared to Hi-Nicalon™ Type S SMP-10 CFCCs pyrolyzed at 1500°C.

The strain and deflection failure of the samples can be grouped and follows the properties of its majority matrix.

***Hi-Nicalon™ Type S Fiber CFCCs Pyrolyzed at 1500ºC Conclusions**: Hi-Nicalon™ Type S SMP-10 and SPR-212 hybrid CFCCS (with majority SMP-10) have similar trends (mainly a better stiffness), with Hi-Nicalon™ Type S SMP-10 performing slightly better. The same can be said for Hi-Nicalon™ Type S SPR-212 and SMP-10 hybrid (with majority SPR-212) CFCCS (which perform mainly better in toughness, strain-to-failure, and strength).*

5.10 Discussion on the Cross Comparison of Fiber Systems

In the previous sections, the results of each fiber system were presented for various matrix systems used in this research, which shows directly which matrix system performs the best in terms of a given mechanical property and for a given fiber system. In the following sections

those results are presented by looking at them for a given matrix system and for various fiber systems. In other word, it is advantageous to know which fiber system performs the best in terms of a given mechanical property and for a given matrix system. Therefore, in the following, the results are presented for a given matrix system while varying the fiber system, and finally their results will be compared. In addition, in the following sections, the quality of the parts will be presented that they were practically void-free, and finally the fracture modes of the CFCC samples will be studies based on the performances of the matrices and the processing conditions (e.g., 1000^{o}C versus 1500^{o}C pyrolysis), and various fracture mechanisms for various matrices and processing conditions are proposed.

The manufactured CFCCs were practically void-free and Figure 5.42 shows a typical cross-section of the CFCCs manufactured in this research.Figure 1.1

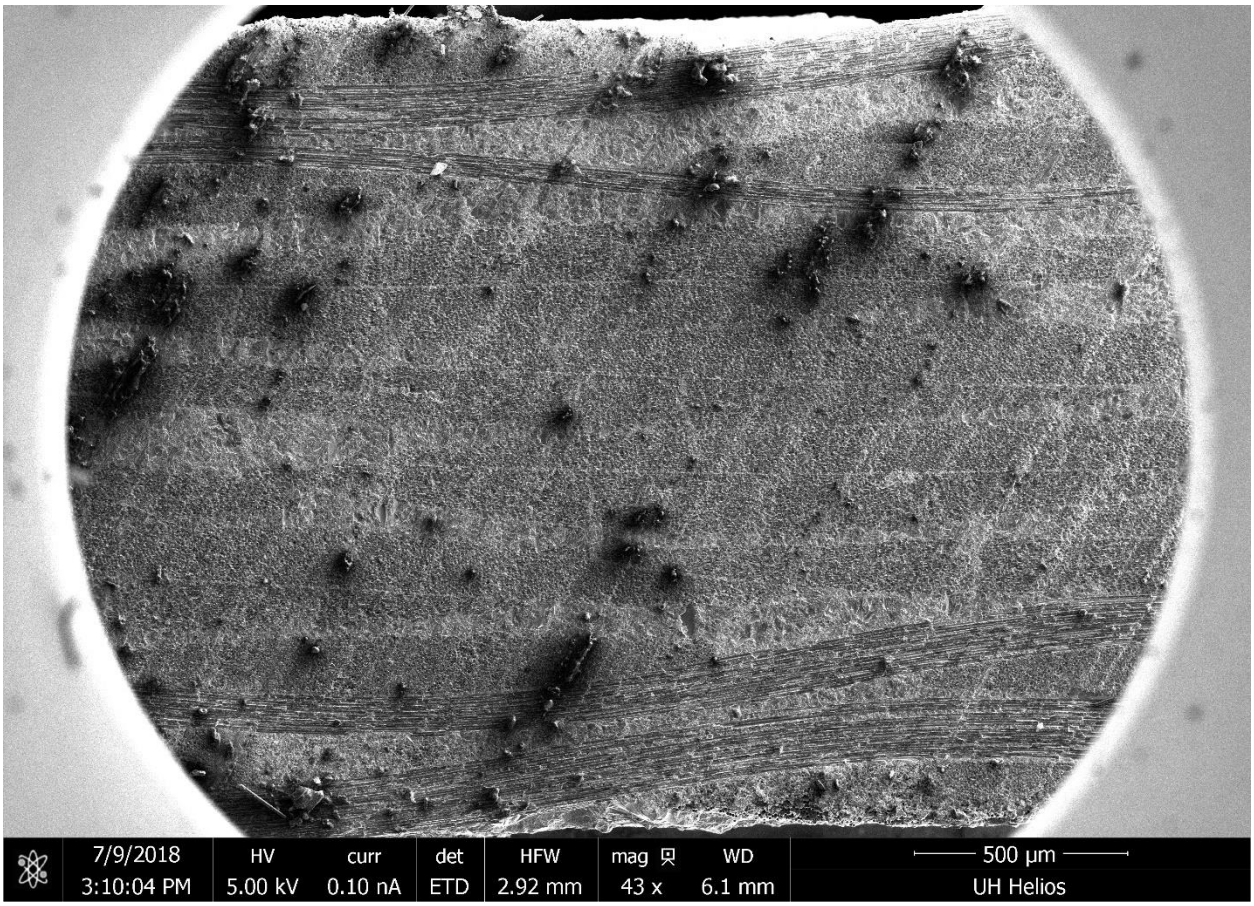

Figure 5.42: Typical cross-section of CFCCs manufactured in this research, verified to be free of voids.

It is worthwhile to point out that individual matrix systems and processing conditions had unique failure mode and fracture mechanisms that will be discussed in the following sections.

All 1500°C pyrolyzed CFCC samples had brittle failure mode, displayed in Figure 5.43.

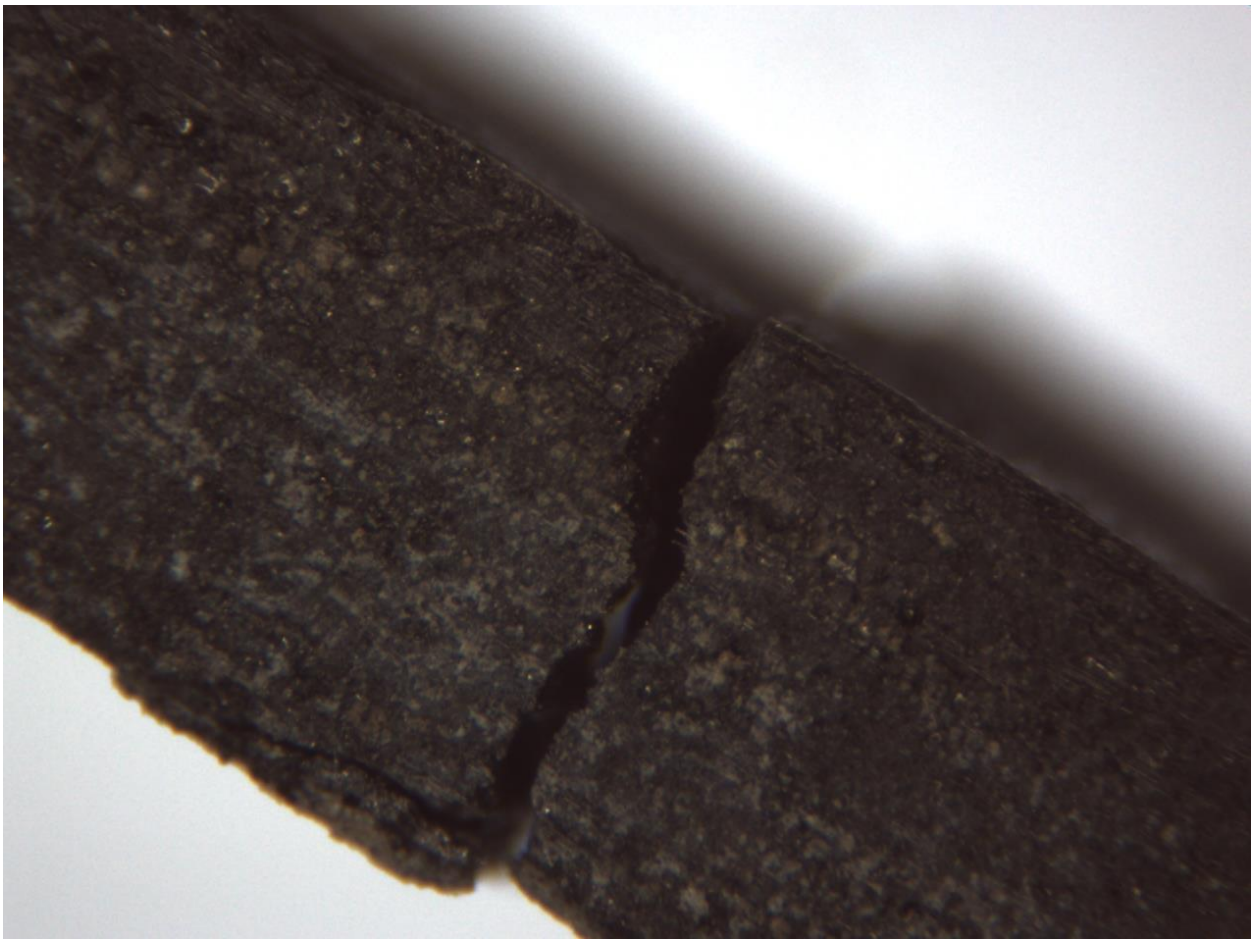

Figure 5.43: Typical brittle failure mode of 1500°C pyrolyzed CFCC samples.

Figure 5.44 displays a typical fracture surface of a 1500°C pyrolyzed CFCC. As evident from Figure 5.44, the brittle nature of the higher pyrolyzed temperature CFCCs create a clean break.

Figure 5.44: Typical fracture surface of 1500°C pyrolyzed CFCCs showing a brittle fracture.

The monolithic properties, leading to brittle fracture, of 1500°C pyrolyzed CFCCs can be seen in Figure 5.45, which shows the fracture through both matrix and fiber is homogeneous. In Figure 5.45, the parallel fibers to the fractured surface can be seen cut in half, and there is no pull out of the perpendicular fibers to the fracture surface, which are characteristics of both a "monolithic" and a "brittle" ceramic. The "monolithic nature of particularly the samples with SMP-10 at 1500ºC pyrolysis, as explained earlier, is that both the fibers and the matric are β-phase "crystalline" SiC.

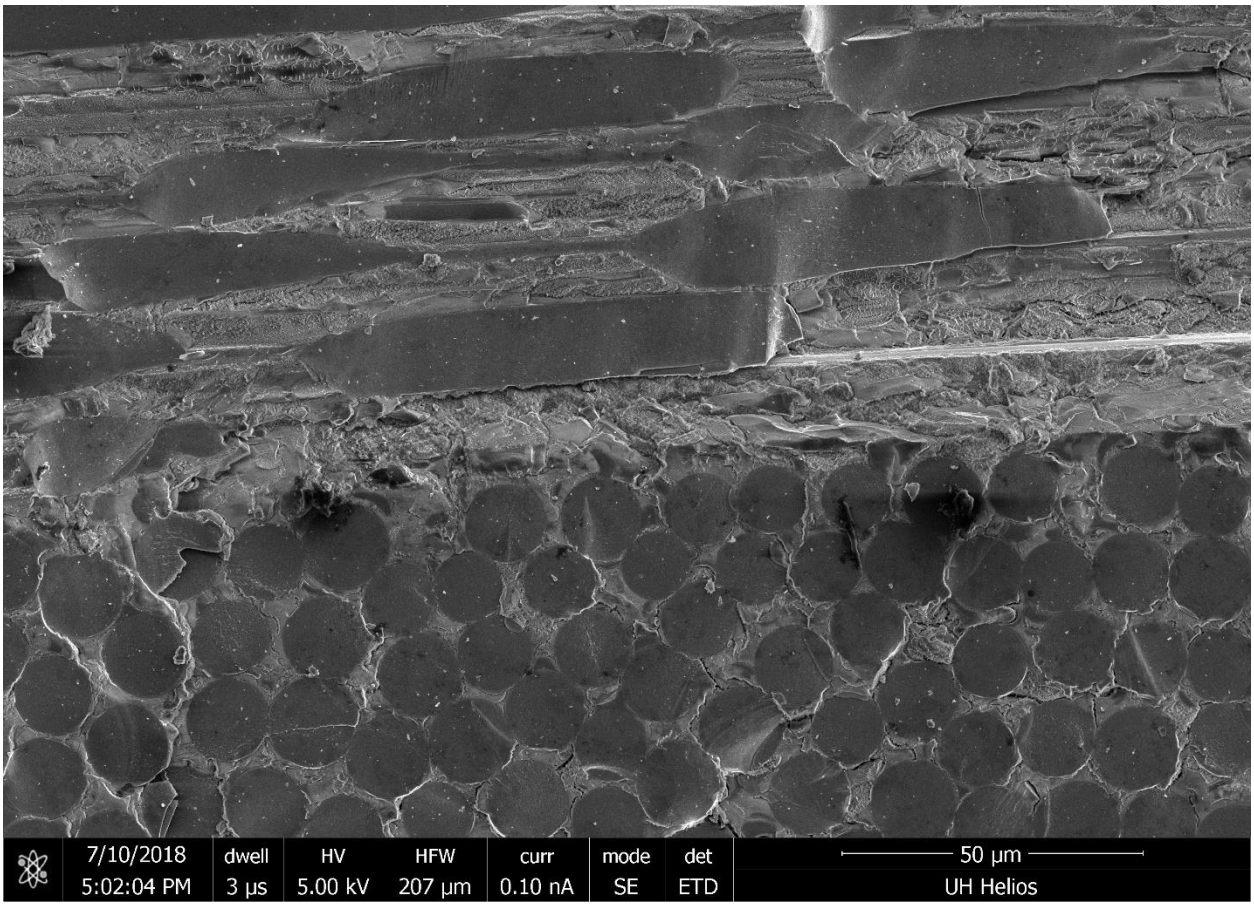

Figure 5.45: Typical fracture surface of 1500°C pyrolyzed CFCCs displaying monolithic brittle properties.

Unlike the 1500°C pyrolyzed CFCCs, the 1000°C pyrolyzed CFCCs do not display monolithic brittle properties (e.g., see Figure 5.46). There is little to no molecular bond/interphase at the fiber-matrix interface. The fibers do not break evenly with the matrix and show signs of recess or protrusion and some degrees of interface debonding and fiber pull-outs.

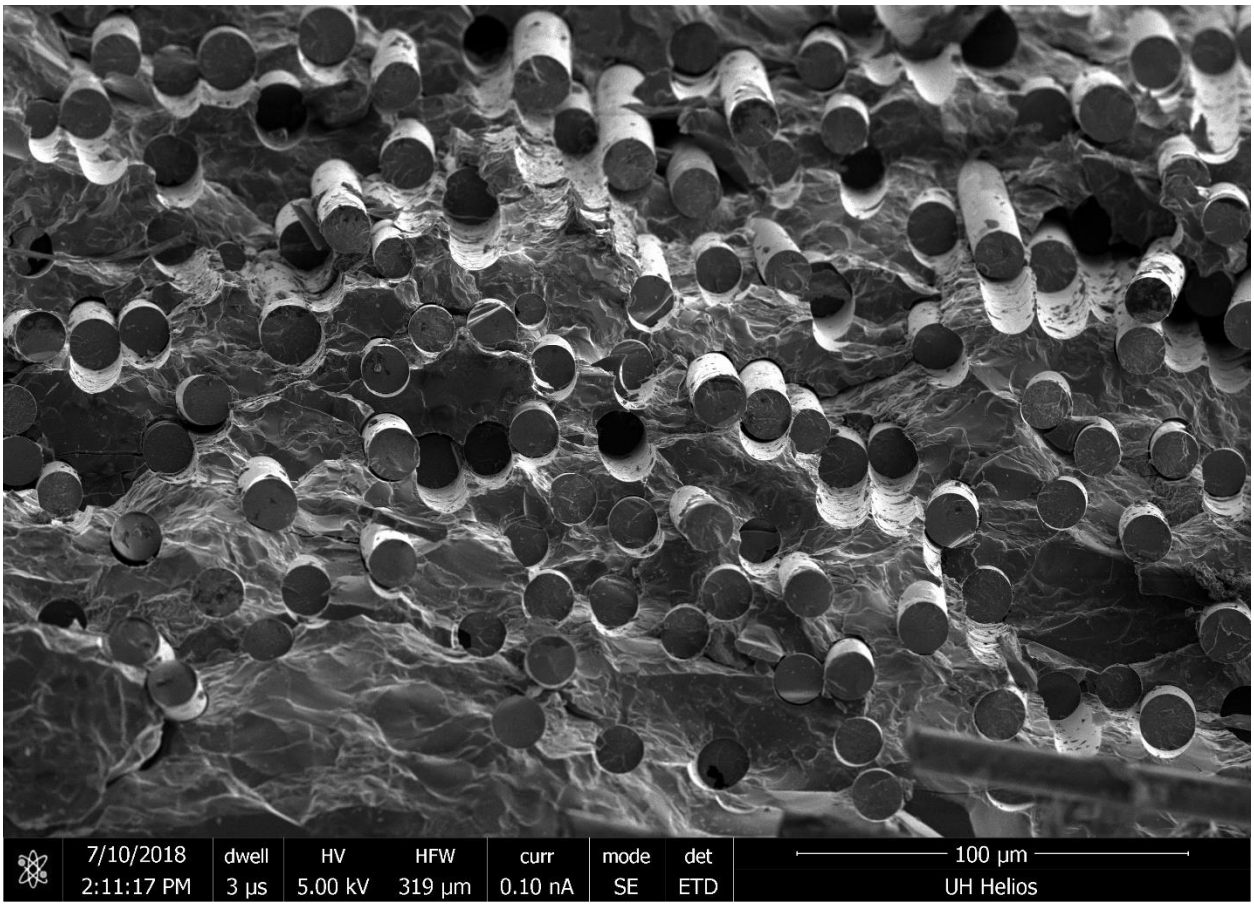

Figure 5.46: Typical fracture surface of 1000° pyrolyzed CFCCs.

Figure 5.47 clearly shows fiber pull-out for this group of CFCCs pyrolyzed at 1000°C, as a typical SEM of fracture surface.

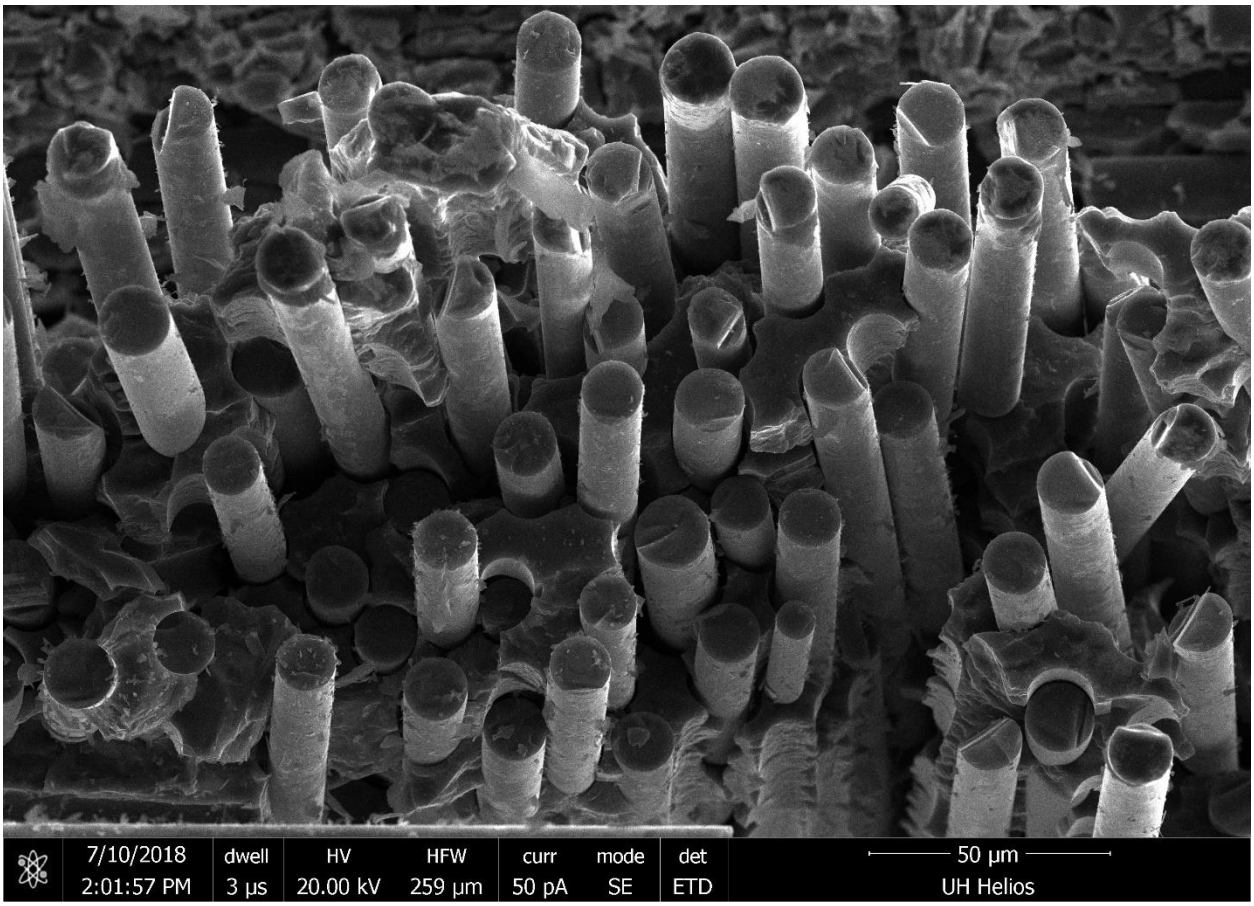

Figure 5.47: Typical SEM of fiber pull-out of 1000°C pyrolyzed samples.

5.10.1 Discussion on the Cross Comparison of Fiber Systems with SMP-10 Matrix

In this section, the CFCCs that were manufactured with SMP-10 and various fiber systems are compared. It is worth noting that the failure modes of the CFCC samples made with SMP-10, particularly at 1000ºC, have distinct failure mode of failing by tension at the bottom surface of the test samples, e.g., see Figure 5.48.

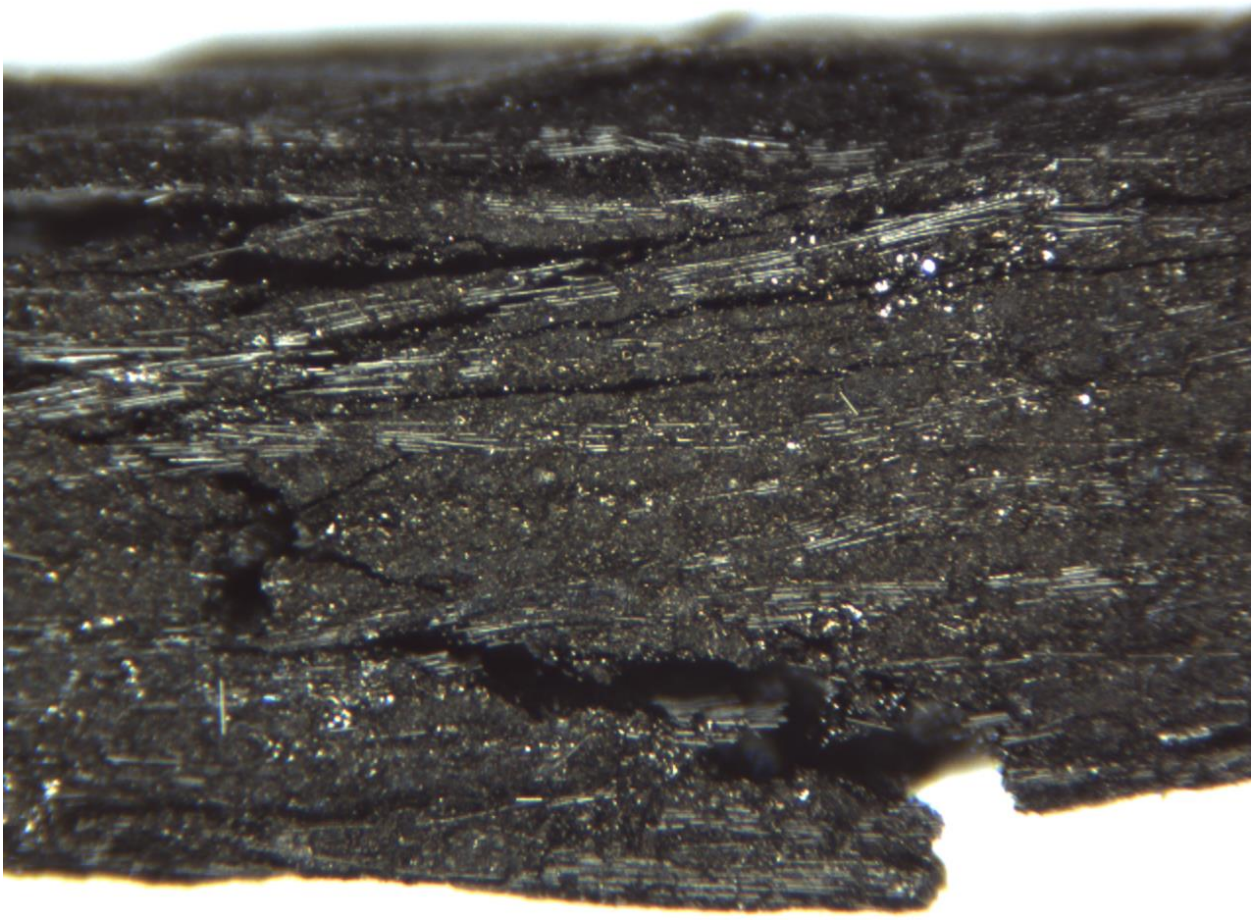

Figure 5.48: Typical failure mode of SMP-10 CFCC pyrolyzed at 1000 °C.

Figure 5.48 shows that the fabric on the bottom of the sample fails in tension and a crack propagates upwards through the sample. Table 5.27 reports the mechanical properties of all types of Nicalon™ based fibers CFCCs studied in this research for SMP-10 matrix.

Table 5.31: Compiled mechanical properties for SMP-10 CFCCs; standard deviations are given in parentheses.

Specimen Type	Flexural Strength [MPa]	Elastic Modulus [GPa]	Toughness [MJ/m^3]
Nicalon™ SMP-10	38.87 (11.3)	61.79 (3.78)	14.56 (6.11)
1000°C Hi-Nicalon™ Type S SMP-10	431.0 (28.9)	88.04 (8.46)	1391 (160)
1500°C Hi-Nicalon™ Type S SMP-10	87.65 (7.52)	160.6 (16.6)	23.88 (3.97)

Figure 5.49a compares the flexural strengths of SMP-10 CFCCs as listed in Table 5.31. Percentages of improvements in strength compared to the base Nicalon™ SMP-10 CFCCs are given in Figure 5.49b.

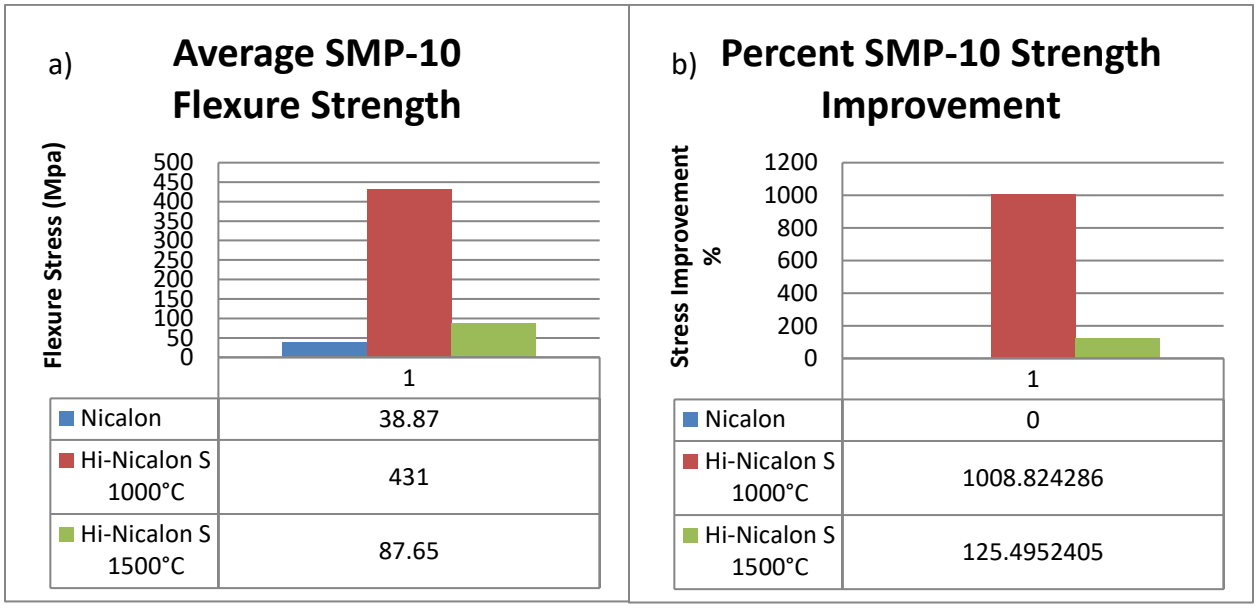

Figure 5.49: Flexural strength comparison for SMP-10 CFCCs, a) Flexural strengths in MPa, and b) percent improvements in flexural strength compared to Nicalon™ SMP-10 CFCCs.

The highest flexural strength was demonstrated by Hi-Nicalon™ Type S pyrolyzed at 1000°C. A 1009% increase in flexural strength compared to the baseline Nicalon™ was achieved. Hi-Nicalon™ Type S pyrolyzed at 1500°C performed better than Nicalon™ with a 125% increase, but much lower than that at 1000°C.

Figure 5.50a compares the stiffness calculated for SMP-10 CFCCs. Figure 5.50b demonstrates the percentages of improvements in stiffness that were achieved compared to the baseline Nicalon™ SMP-10 CFCCs.

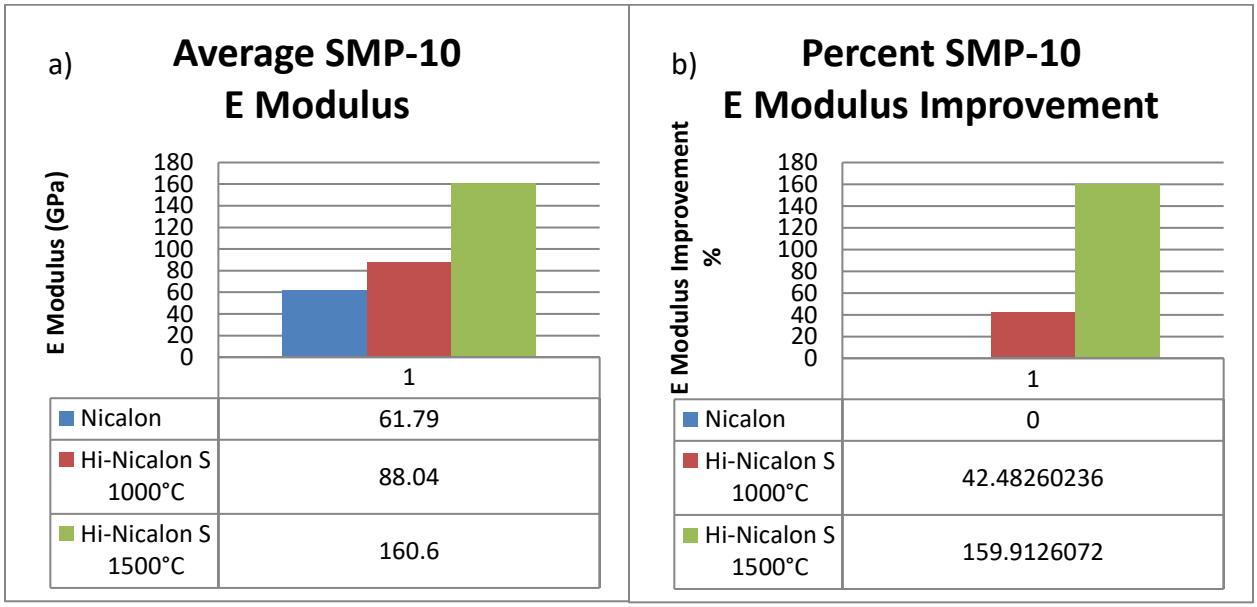

Figure 5.50: Elastic moduli comparison for SMP-10 CFCCs, a) Elastic moduli in GPa, and b) Percent improvements in elastic moduli compared to Nicalon™ SMP-10 CFCCs.

Hi-Nicalon™ Type S pyrolyzed at 1500°C has the highest stiffness. A 160% increase in stiffness compared to the baseline Nicalon™ was achieved. Hi-Nicalon™ Type S pyrolyzed at 1000°C performed better than Nicalon™ with a 42% increase, but lower than that at 1500°C.

Figure 5.51a compares the toughness calculated for SMP-10 CFCCs. Figure 5.51b demonstrates the percentages of improvements in toughness that were achieved compared to the baseline Nicalon™ SMP-10 CFCCs.

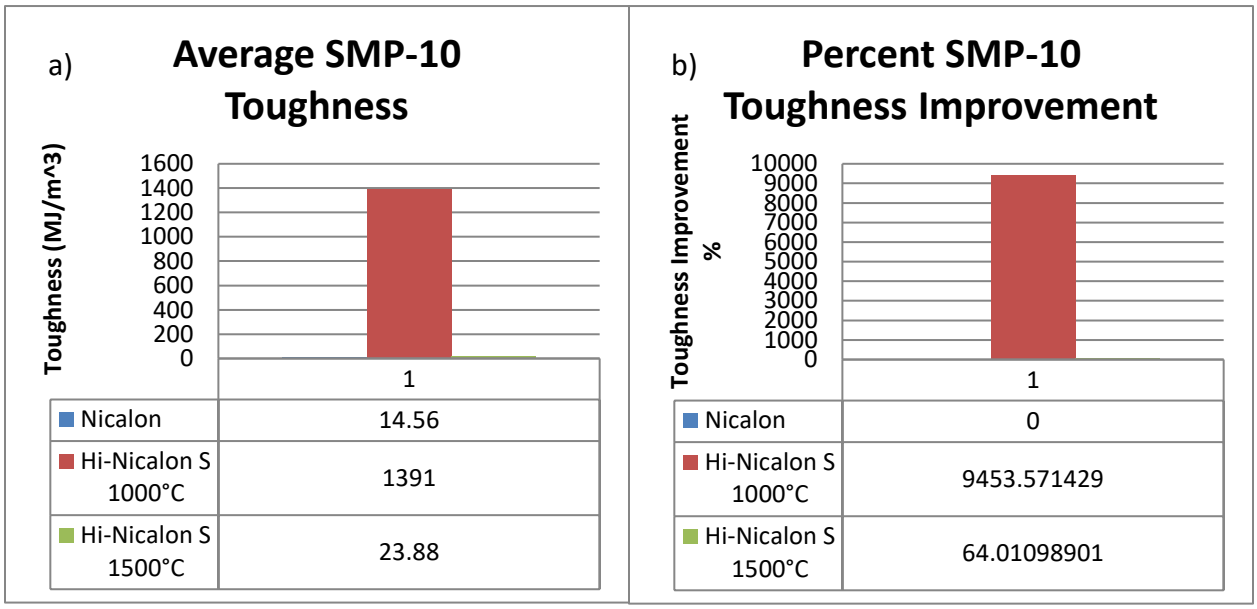

Figure 5.51: Toughness comparison for SMP-10 CFCCs, a) Toughness in MJ/m2, and b) Percent improvements in toughness compared to Nicalon™ SMP-10 CFCCs.

Hi-Nicalon™ Type S pyrolyzed at 1000°C and 1500°C outperformed the baseline with 9454% and 64% increase respectively.

***SMP-10 based CFCCs Conclusions**: These results show that overall, SMP-10 CFCCs had the best performance in terms of Strength and Toughness when Hi-Nicalon™ Type S is used and pyrolyzed at 1000°C, but higher modulus is achieved when Hi-Nicalon™ Type S is used and pyrolyzed at 1500°C.*

5.10.2 Discussion on the Cross Comparison of Fiber Systems with SPR-212

In this section, the CFCCs that were manufactured with SPR-212 and various fiber systems are compared. It is worth noting that the failure modes of the CFCC samples made with SPR-212, particularly at 1000°C, have distinct failure mode of failing by compression at the top surface of the test samples, e.g., see Figure 5.52.

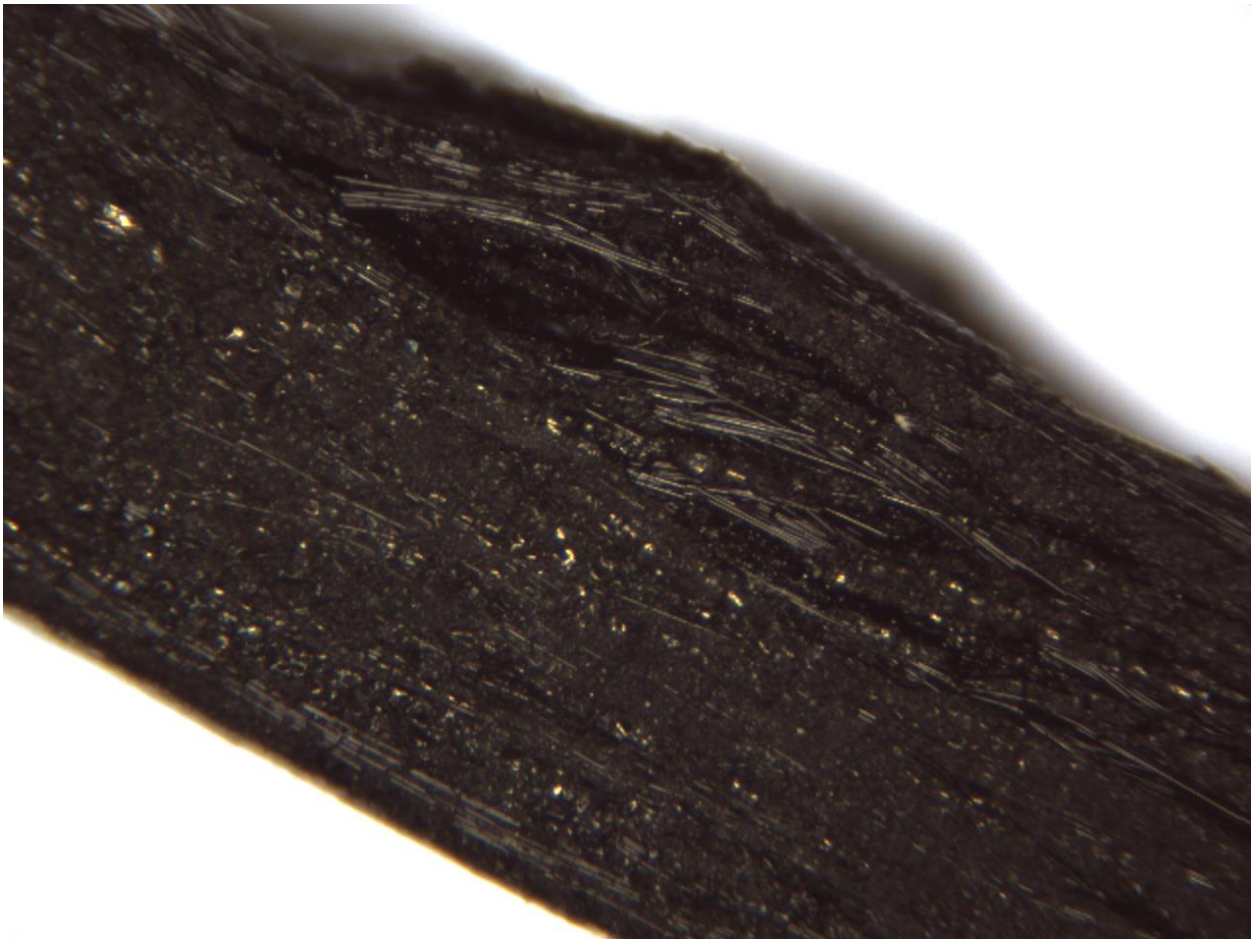

Figure 5.52: Typical failure mode of SPR-212 pyrolyzed at 1000°C.

The failure mode of SPR-212 at lower pyrolysis temperature is through compression and micro buckling as seen in Figure 5.52. The fabric on the top of the sample fails in compression and under local micro bucking. Fiber-matrix interface delamination is most likely the cause of the

micro bucking under the compressive stress. The distinct modes of failure for the SMP-10 CFCC samples by tension at the bottom (see Figure 5.48) and by micro bucking under compression on top for SPR-212 CFCC samples (see Figure 5.52) is of great interest, and it suggests that the adhesion of the fibers to matrix is stronger in case of SMP-10 based CFCCs and weaker for SPR-212 based CFCCs. It is believed that a weaker fiber-matrix bonding will lead to more fiber-matrix interface debonding and fiber pull outs which will definitely lead to a high toughness and/or fracture toughness and often to a better strength as well, while a stronger fiber-matrix interface bonding will lead to a better stiffness, as mostly seen in this research. Table 5.27 reports the mechanical properties of all types of Nicalon™ based fibers CFCCs studied in this research for SPR-212 matrix.

Table 5.32: Compiled mechanical properties for SPR-212 CFCCs; standard deviations are given in parentheses.

Specimen Type	**Flexural Strength [MPa]**	**Elastic Modulus [GPa]**	**Toughness [MJ/m^3]**
Nicalon™ SPR-212	39.97 (6.08)	54.65 (10.8)	16.20 (3.56)
1000°C Hi-Nicalon™ Type S SPR-212	366.5 (17.0)	72.59 (5.30)	977.3 (64.5)
1500°C Hi-Nicalon™ Type S SPR-212	100.8 (9.59)	121.4 (10.4)	41.94 (6.44)

Figure 5.53a compares the flexural strengths of SPR-212 CFCCs as listed in Table 5.32. Percentages of improvements in strength compared to the base Nicalon™ SPR-212 CFCCs are given in Figure 5.53b.

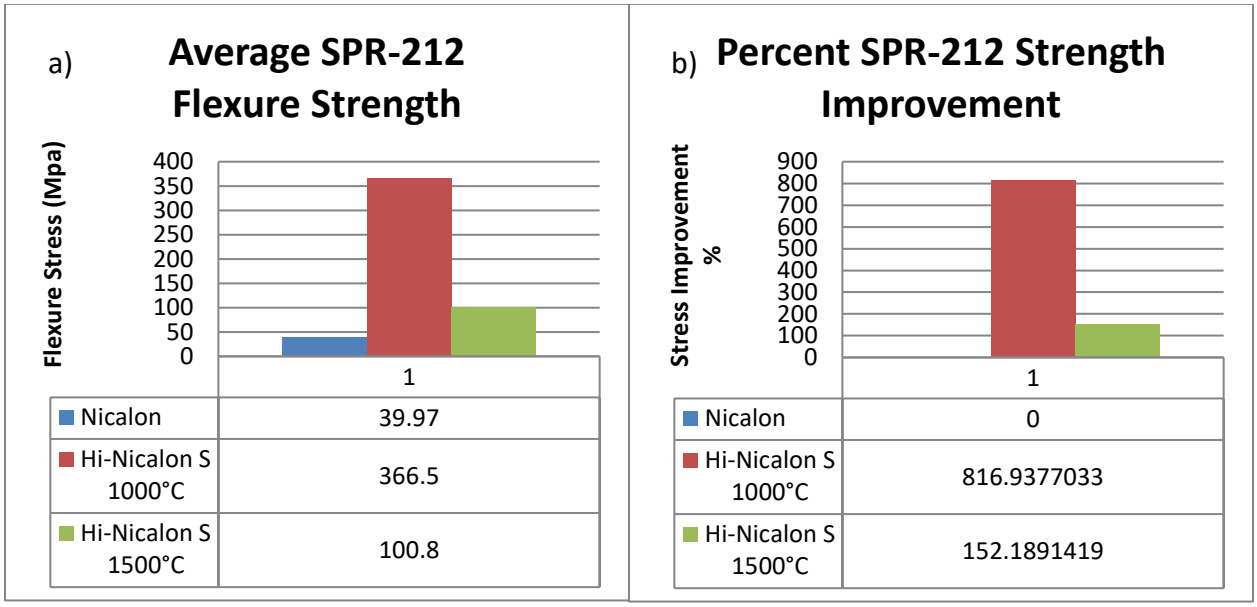

Figure 5.53: Flexural strength comparison for SPR-212 CFCCs, a) Flexural strengths in MPa, and b) percent improvements in flexural strength compared to Nicalon™ SPR-212 CFCCs.

The highest flexural strength was demonstrated by Hi-Nicalon™ Type S pyrolyzed at 1000°C. An 817% increase in flexural strength compared to the baseline Nicalon™ was achieved. Hi-Nicalon™ Type S pyrolyzed at 1500°C performed better than Nicalon™ with a 152% increase.

Figure 5.54a compares the stiffness calculated for SPR-212 CFCCs. Figure 5.54b demonstrates the percentages of improvements in stiffness that were achieved compared to the baseline Nicalon™ SPR-212 CFCCs.

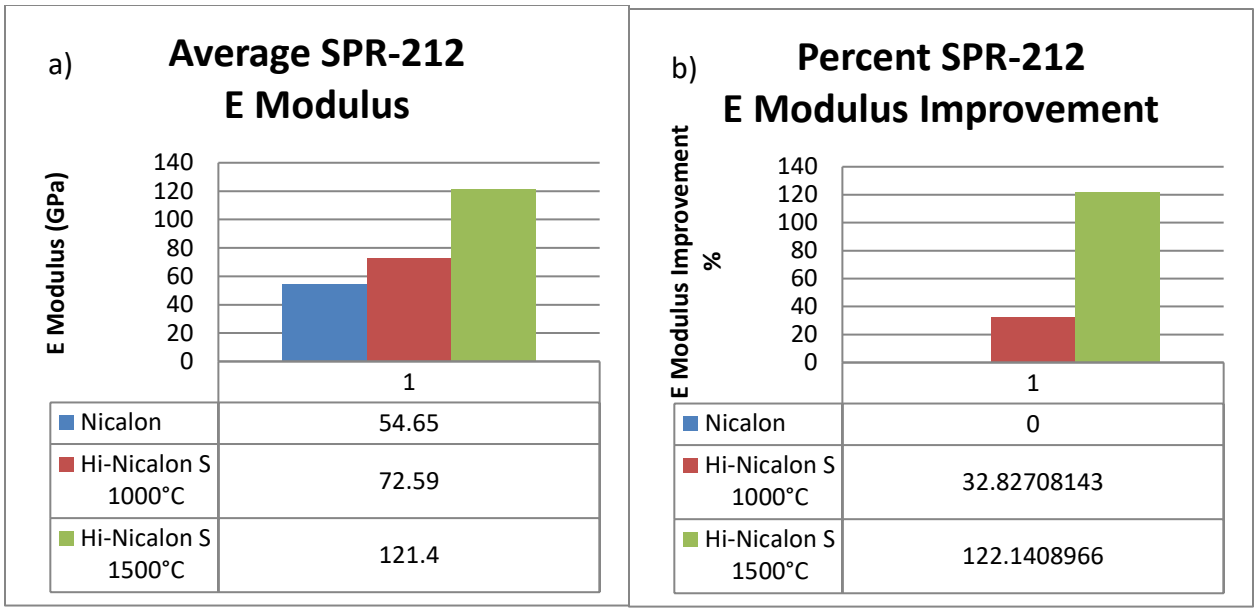

Figure 5.54: Elastic moduli comparison for SPR-212 CFCCs, a) Elastic moduli in GPa, and b) Percent improvements in elastic moduli compared to Nicalon™ SPR-212 CFCCs.

Hi-Nicalon™ Type S pyrolyzed at 1500°C has the highest stiffness. A 122% increase in stiffness compared to the baseline Nicalon™ was achieved. Hi-Nicalon™ Type S pyrolyzed at 1000°C performed better than Nicalon™ with a 32% increase.

Figure 5.55a compares the toughness calculated for SPR-212 CFCCs. Figure 5.55b demonstrates the percentages of improvements in toughness that were achieved compared to the baseline Nicalon™ SPR-212 CFCCs.

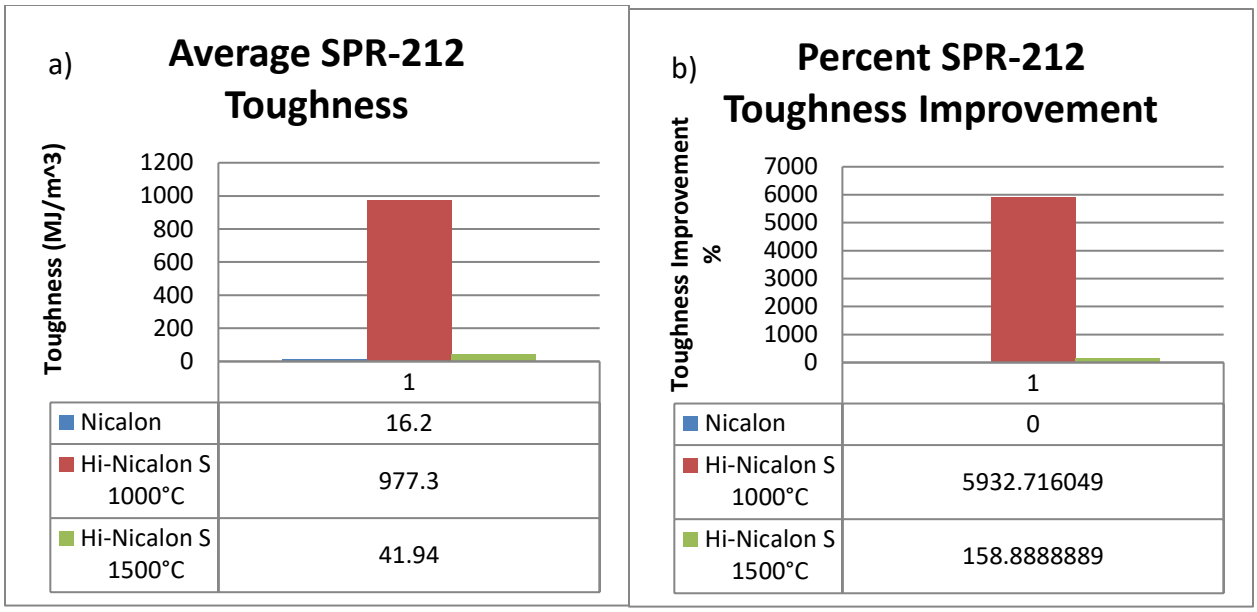

Figure 5.55: Toughness comparison for SPR-212 CFCCs, a) Toughness in MJ/m2, and b) Percent improvements in toughness compared to Nicalon™ SPR-212 CFCCs.

Hi-Nicalon™ Type S pyrolyzed at 1000°C and 1500°C outperformed the baseline with 5933% and 159% increase respectively.

***SPR-212 based CFCCs Conclusions**: These results show that overall, SPR-212 CFCCs have the best performance in terms of Strength and Toughness when Hi-Nicalon™ Type S is used and pyrolyzed at 1000°C, but higher modulus is achieved when Hi-Nicalon™ Type S is used and pyrolyzed at 1500°C.*

5.10.3 Discussion on the Cross Comparison of Fiber Systems with SMP-10 Hybrid

In this section, the CFCCs that were manufactured with SMP-10 hybrid (which has SPR-212 as the majority of the matrix) and various fiber systems are compared. It is worth noting that the failure modes of the CFCC samples made with SMP-10 hybrid (which has SPR-212 as the

majority of the matrix), particularly at 1000°C, have distinct failure mode of failing by compression at the top surface of the test samples, e.g., see Figure 5.56.

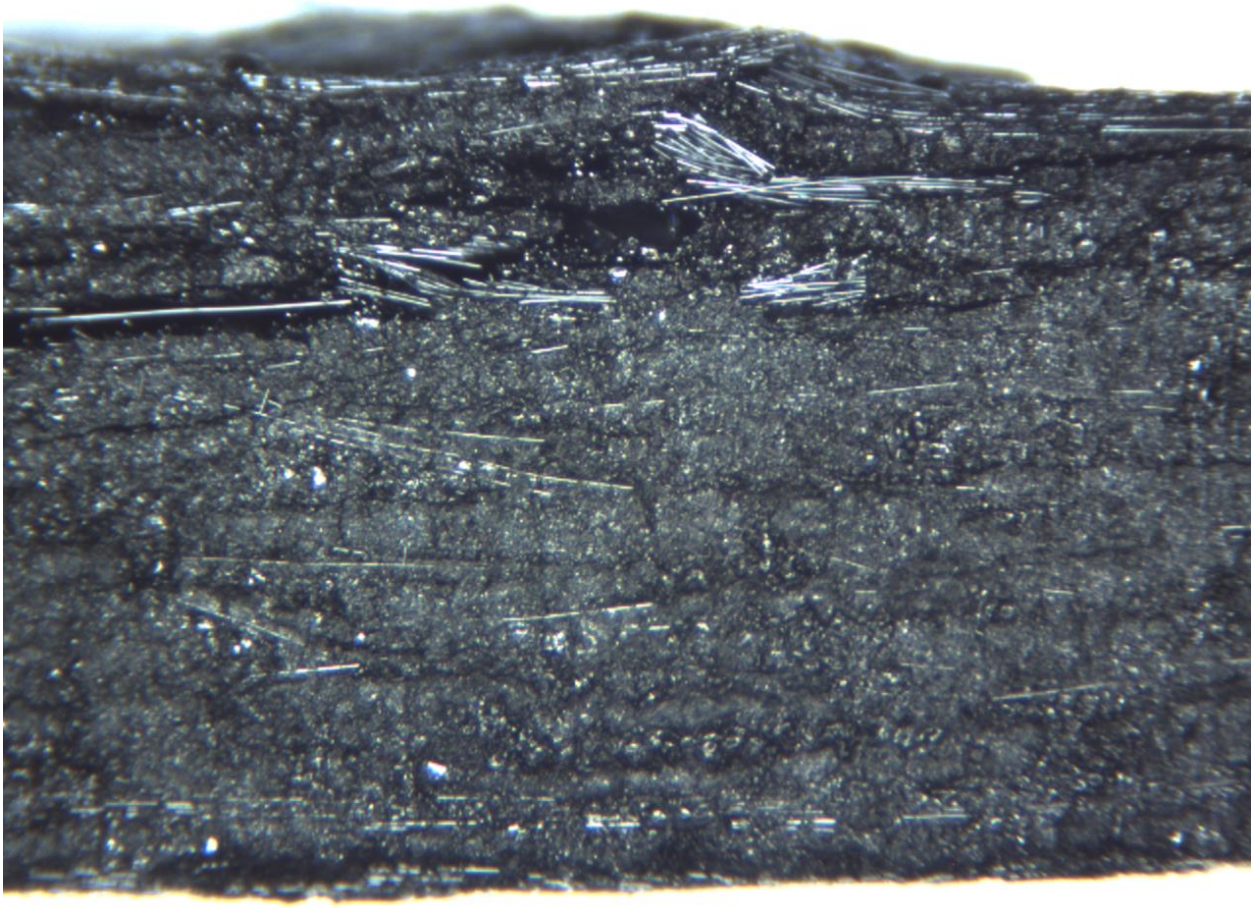

Figure 5.56: Failure mode of SMP-10 Hybrid pyrolyzed at 1000°C.

As can be seen, since the SMP-10 has SPR-212 as the majority of the matrix, the failure mode of SMP-10 hybrid (see Figure 5.56) resembles the failure mode of SPR-212 (see Figure 5.52), through compression and micro buckling at the top surface, as explained earlier in the SPR-212 section above. Table 5.27 reports the mechanical properties of all types of fibers CFCCs studied in this research for SMP-10 hybrid matrix.

Table 5.33: Compiled mechanical properties for SMP-10 Hybrid CFCCs; standard deviations are given in parentheses.

Specimen Type	Flexural Strength [MPa]	Elastic Modulus [GPa]	Toughness [MJ/m^3]
Nicalon™ SMP-10 Hybrid	40.14 (7.24)	61.11 (13.9)	18.48 (3.02)
T300 SMP-10 Hybrid	63.96 (3.88)	53.12 (2.87)	44.55 (3.73)
1000°C Hi-Nicalon™ Type S SMP-10 Hybrid	377.8 (9.53)	68.45 (3.45)	1164 (74.3)
1500°C Hi-Nicalon™ Type S SMP-10 Hybrid	90.09 (18.0)	105.9 (11.4)	39.70 (16.3)

Figure 5.57a compares the flexural strengths of SMP-10 hybrid CFCCs as listed in Table 5.33. Percentages of improvements in strength compared to the base Nicalon™ SMP-10 hybrid CFCCs are given in Figure 5.57b.

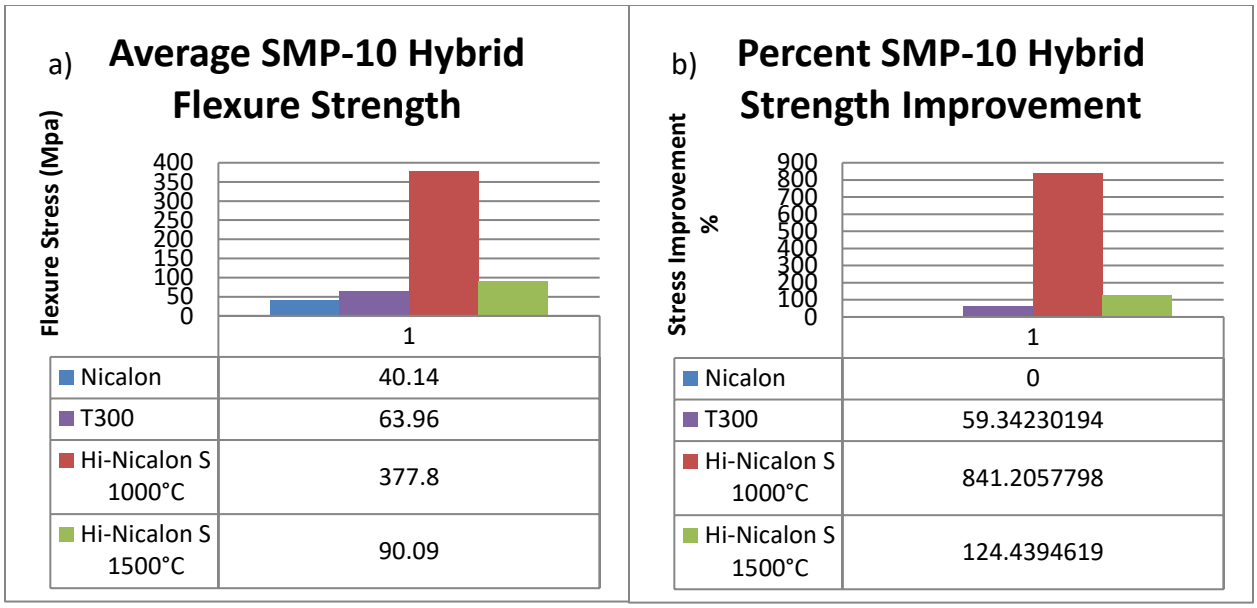

Figure 5.57: Flexural strength comparison for SMP-10 Hybrid CFCCs, a) Flexural strengths in MPa, and b) percent improvements in flexural strength compared to Nicalon™ SMP-10 Hybrid CFCCs.

The highest flexural strength was demonstrated by Hi-Nicalon™ Type S pyrolyzed at 1000°C. An 841% increase in flexural strength compared to the baseline Nicalon™ was achieved. Hi-Nicalon™ Type S pyrolyzed at 1500°C performed better than Nicalon™ with a 124% increase. T300 also performed better than Nicalon™ with a 59% increase.

Figure 5.58a compares the stiffness calculated for SMP-10 hybrid CFCCs. Figure 5.58b demonstrates the percentages of improvements in stiffness that were achieved compared to the baseline Nicalon™ SMP-10 hybrid CFCCs.

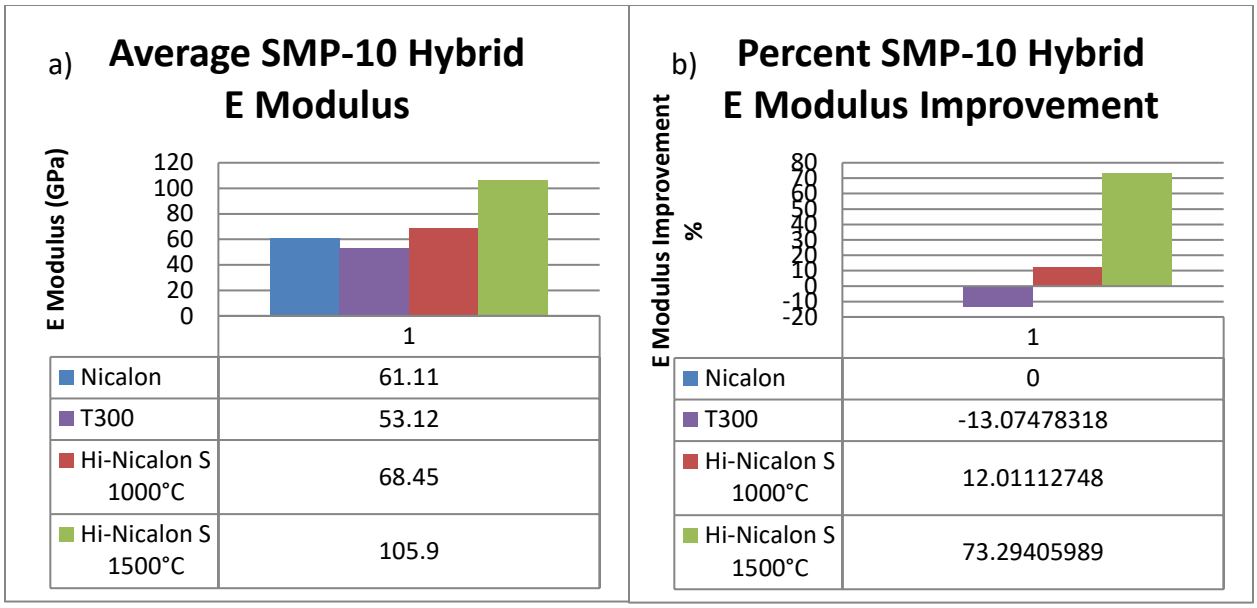

Figure 5.58: Elastic moduli comparison for SMP-10 Hybrid CFCCs, a) Elastic moduli in GPa, and b) Percent improvements in elastic moduli compared to Nicalon™ SMP-10 Hybrid CFCCs.

Hi-Nicalon™ Type S pyrolyzed at 1500°C has the highest stiffness. A 73% increase in stiffness compared to the baseline Nicalon™ was achieved. Hi-Nicalon™ Type S pyrolyzed at 1000°C marginally better than Nicalon™ with a 12% increase. T300 has a lower stiffness than the baseline with a decrease of 13%.

Figure 5.59a compares the toughness calculated for SMP-10 hybrid CFCCs. Figure 5.59b demonstrates the percentages of improvements in toughness that were achieved compared to the baseline Nicalon™ SMP-10 hybrid CFCCs.

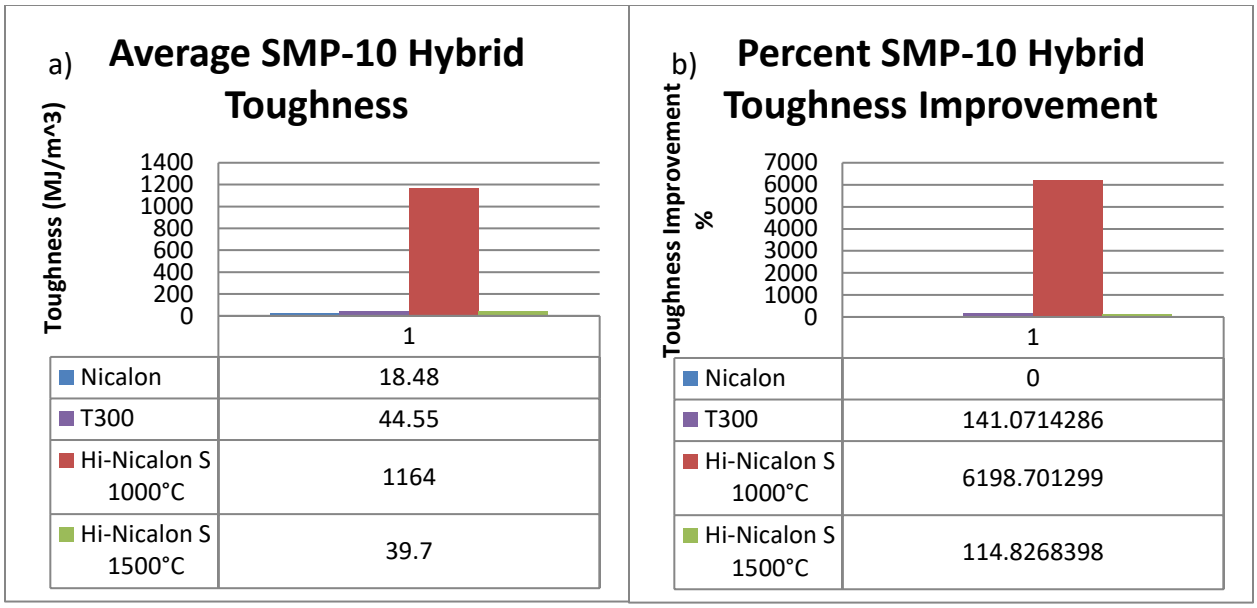

Figure 5.59: Toughness comparison for SMP-10 Hybrid CFCCs, a) Toughness in MJ/m2, and b) Percent improvements in toughness compared to Nicalon™ SMP-10 Hybrid CFCCs.

Hi-Nicalon™ Type S pyrolyzed at 1000°C (which clearly performed the best in terms of toughness, and with 6199% improvement as compared with the baseline) and 1500°C (which performed a distant second in terms of toughness, and with 115% improvement as compared with the baseline) outperformed the baseline. T300 also performed better than the baseline in toughness with an increase of 141%.

***SMP-10 hybrid based CFCCs Conclusions**: These results show that overall, SMP-10 hybrid CFCCs (which have SPR-212 as the majority of the matrix) have the best performance in terms of Strength and Toughness when Hi-Nicalon™ Type S is used and pyrolyzed at 1000°C, but higher modulus is achieved when Hi-Nicalon™ Type S is used and pyrolyzed at 1500°C.*

5.10.4 Discussion on the Cross Comparison of Fiber Systems with SPR-212 Hybrid

In this section, the CFCCs that were manufactured with SPR-212 hybrid (which have SMP-10 as the majority of the matrix) and various fiber systems are compared. It is worth noting that the

failure modes of the CFCC samples made with SPR-212 hybrid (which have SMP-10 as the majority of the matrix), particularly at 1000^{o}C, have distinct failure mode of failing by tension at the bottom surface of the test samples (e.g., see Figure 5.60) which is very similar to the failure mode of the CFCC samples made with SMP-10 (e.g., see Figure 5.48).

Figure 5.60: Failure mode of SPR-212 Hybrid pyrolyzed at 1000^{o}C.

Figure 5.60 shows that the fabric on the bottom of the sample fails in tension and a crack propagates upwards through the sample Table 5.27 reports the mechanical properties of all types of Nicalon™ fibers CFCCs studied in this research for SPR-212 hybrid matrix.

Table 5.34: Compiled mechanical properties for SPR-212 Hybrid CFCCs; standard deviations are given in parentheses.

Specimen Type	Flexural Strength [MPa]	Elastic Modulus [GPa]	Toughness [MJ/m^3]
Nicalon™ SPR-212 Hybrid	22.71 (0.871)	56.11 (1.22)	5.80 (0.234)
1000°C Hi-Nicalon™ Type S SPR-212 Hybrid	428.5 (19.6)	93.91 (6.67)	1237 (117)
1500°C Hi-Nicalon™ Type S SPR-212 Hybrid	92.34 (10.4)	159.0 (15.6)	27.65 (5.65)

Figure 5.61a compares the flexural strengths of SPR-212 hybrid CFCCs as listed in Table 5.34. Percentages of improvements in strength compared to the base Nicalon™ SPR-212 hybrid CFCCs are given in Figure 5.61b.

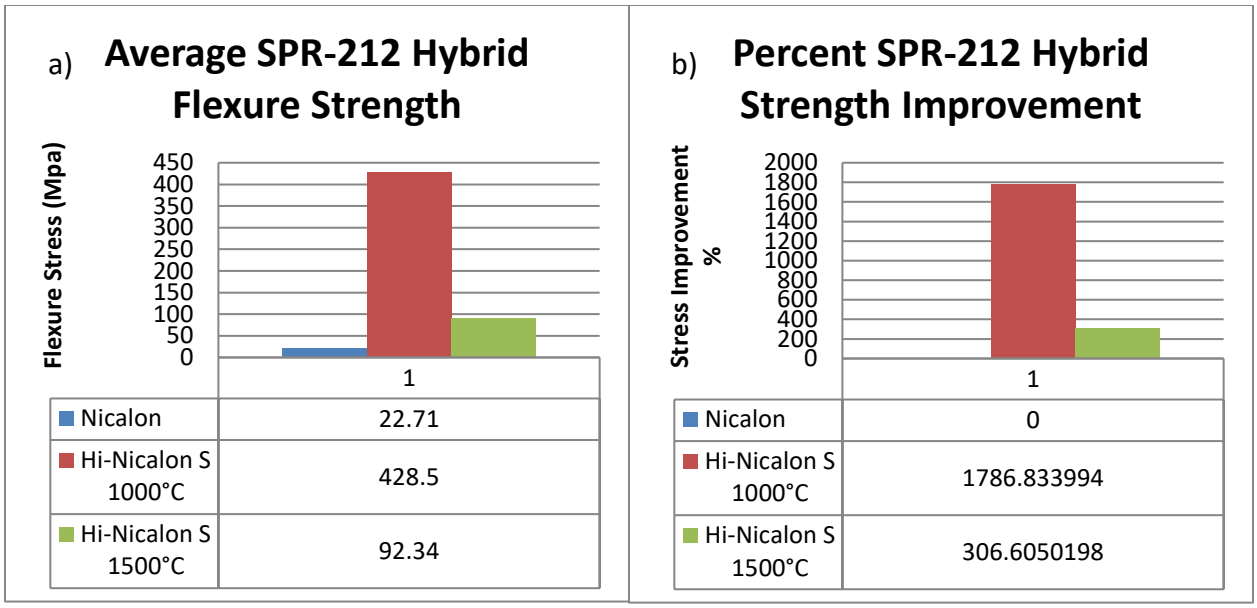

Figure 5.61: Flexural strength comparison for SPR-212 Hybrid CFCCs, a) Flexural strengths in MPa, and b) percent improvements in flexural strength compared to Nicalon™ SPR-212 Hybrid CFCCs.

The highest flexural strength was demonstrated by Hi-Nicalon™ Type S pyrolyzed at 1000°C. A 1787% increase in flexural strength compared to the baseline Nicalon™ was achieved. Hi-Nicalon™ Type S pyrolyzed at 1500°C performed better than Nicalon™ with a 306% increase.

Figure 5.62a compares the stiffness calculated for SPR-212 hybrid CFCCs. Figure 5.62b demonstrates the percentages of improvements in stiffness that were achieved compared to the baseline Nicalon™ SPR-212 hybrid CFCCs.

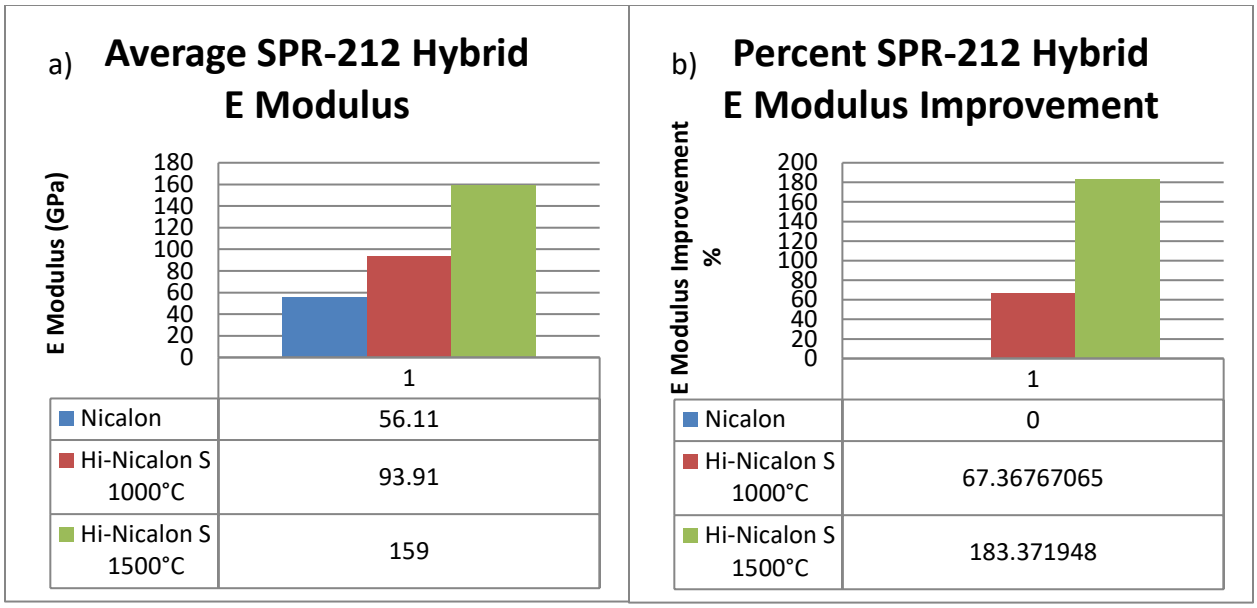

Figure 5.62: Elastic moduli comparison for SPR-212 Hybrid CFCCs, a) Elastic moduli in GPa, and b) Percent improvements in elastic moduli compared to Nicalon™ SPR-212 Hybrid CFCCs.

Hi-Nicalon™ Type S pyrolyzed at 1500°C has the highest stiffness. A 183% increase in stiffness compared to the baseline Nicalon™ was achieved. Hi-Nicalon™ Type S pyrolyzed at 1000°C performed better than Nicalon™ with a 67% increase.

Figure 5.63a compares the toughness calculated for SPR-212 hybrid CFCCs. Figure 5.63b demonstrates the percentages of improvements in toughness that were achieved compared to the baseline Nicalon™ SPR-212 hybrid CFCCs.

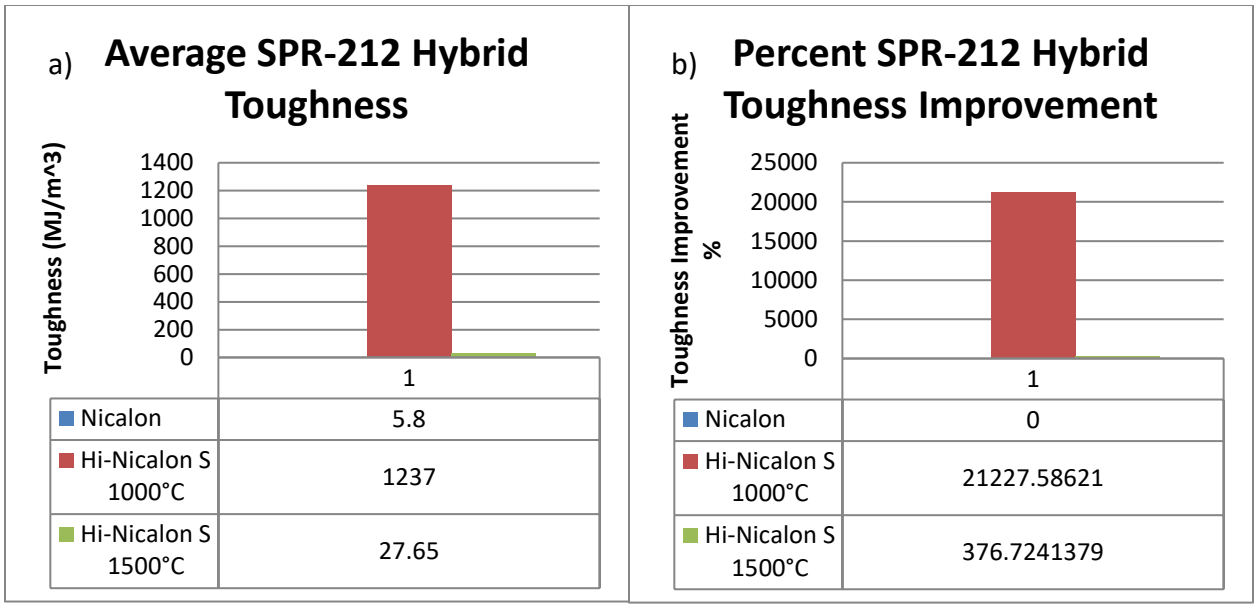

Figure 5.63: Toughness comparison for SPR-212 Hybrid CFCCs, a) Toughness in MJ/m2, and b) Percent improvements in toughness compared to Nicalon™ SPR-212 Hybrid CFCCs.

Hi-Nicalon™ Type S pyrolyzed at 1000°C (which clearly performed the best in terms of toughness, and with 21228% improvement as compared with the baseline) and 1500°C (which performed a distant second in terms of toughness, and with 377% improvement as compared with the baseline) outperformed the baseline.

SPR-212 hybrid based CFCCs Conclusions: *These results show that overall, SPR-212 hybrid CFCCs (which have SMP-10 as the majority of the matrix) have the best performance in terms of Strength and Toughness when Hi-Nicalon™ Type S is used and pyrolyzed at 1000°C, but higher modulus is achieved when Hi-Nicalon™ Type S is used and pyrolyzed at 1500°C.*

5.11 Numerical Simulation Validation of the Test Results

Solidworks Solid Modeling and Finite Element Analysis was used to validate the empirical data. The sample was drawn to the average dimensions to each specific CFCC. The part was constrained with a hinge and roller located at the support span positions to simulate the "simply supported condition of the test samples. It was then loaded with the average load at break to each specific CFCC, located at the load span positions. The average modulus of elasticity for the specific CFCC was used for material properties as well as a Poisson's ratio, ν_{xy}, of 0.16 [38].

The simulation was performed, and the displacement was verified to be with 5% error to ensure accuracy of the analysis. The best performing CFCCs for each type of fabric, matrix, and pyrolysis temperature were chosen for comparisons and verifications, as listed in Table 5.35.

Table 5.35: Compiled mechanical properties for best performing CFCCs for each type of fabric, matrix, and pyrolysis temperature; standard deviations are given in parentheses.

Specimen Type	Flexural Strength [MPa]	Elastic Modulus [GPa]	Strain-to-failure [mm/mm]	Toughness [MJ/m^3]
Nicalon™ SMP-10 Hybrid	40.14 (7.24)	61.11 (13.9)	0.000694 (0.000079)	18.48 (3.02)
T300 SMP-10 Hybrid	63.96 (3.88)	53.12 (2.87)	0.00139 (0.0000344)	44.55 (3.73)
1000°C Hi-Nicalon™ Type S SMP-10	431.0 (28.9)	88.04 (8.46)	0.00725 (0.000360)	1391 (160)
1500°C Hi-Nicalon™ Type S SPR-212	100.8 (9.59)	121.4 (10.4)	0.000932 (0.0000764)	41.94 (6.44)

A total of four types of CFCCs were used for analysis, which include the best performing CFCCs for each type of fabric, matrix, and pyrolysis temperature. Figure 5.64 **Error! Reference source not found.**shows the maximum displacement for Nicalon™ SMP-10 hybrid CFCCs. The

simulation displacement is within 0.0059mm of average empirical displacement. This is a difference of 2.8%.

Figure 5.64: Displacement simulation for Nicalon™ SMP-10 Hybrid CFCCs

Figure 5.65 displays the maximum stress for Nicalon™ SMP-10 hybrid CFCCs. The simulation stress is within 4.74MPa of average empirical stress. This is a difference of 11.8%.

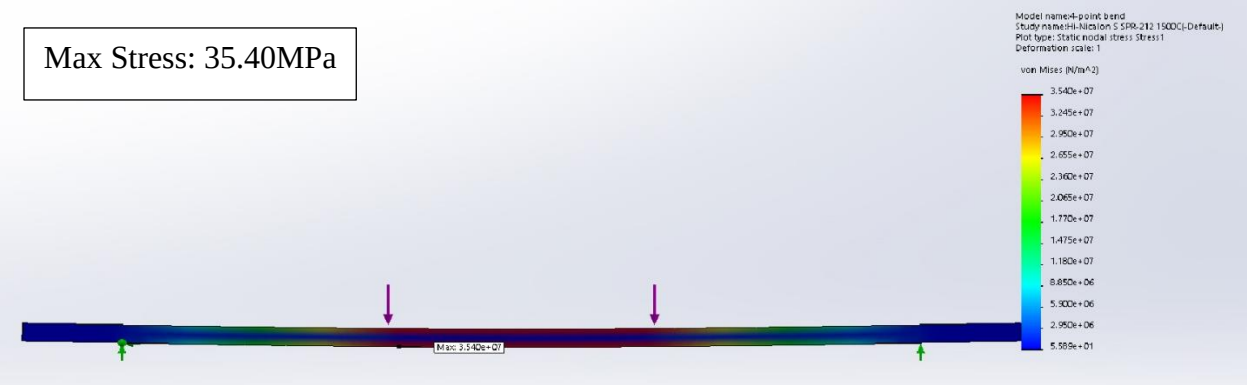

Figure 5.65: Stress simulation for Nicalon™ SMP-10 Hybrid CFCCs.

Figure 5.66 shows the maximum displacement for T300 SMP-10 hybrid CFCCs. The simulation displacement is within 0.0213mm of average empirical. This is a difference of 2.2%.

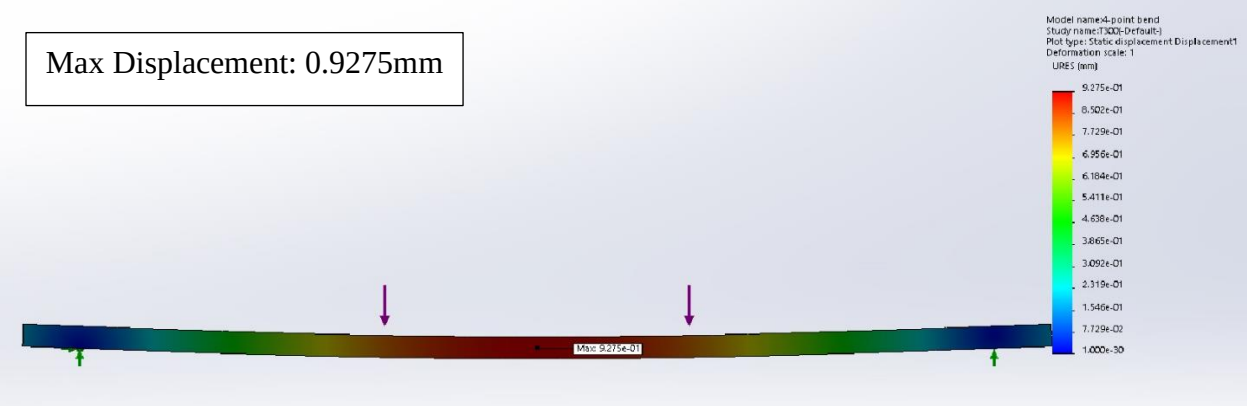

Figure 5.66: Displacement simulation for T300 SMP-10 Hybrid CFCCs.

Figure 5.57 displays the maximum stress for T300 SMP-10 hybrid CFCCs. The simulation stress is within 5.95MPa of average empirical stress. This is a difference of 9.3%.

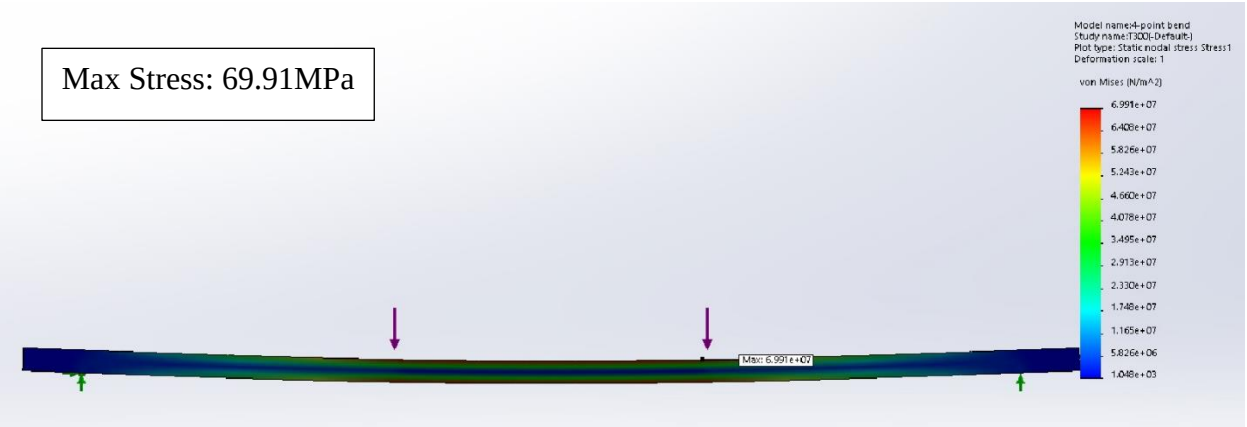

Figure 5.67: Stress simulation for T300 SMP-10 Hybrid CFCCs.

Figure 5.68 shows the maximum displacement for Hi-Nicalon™ Type S SMP-10 CFCCs pyrolyzed at 1000°C. The simulation displacement is within 0.063mm of average empirical displacement. This is a difference of 2.1%.

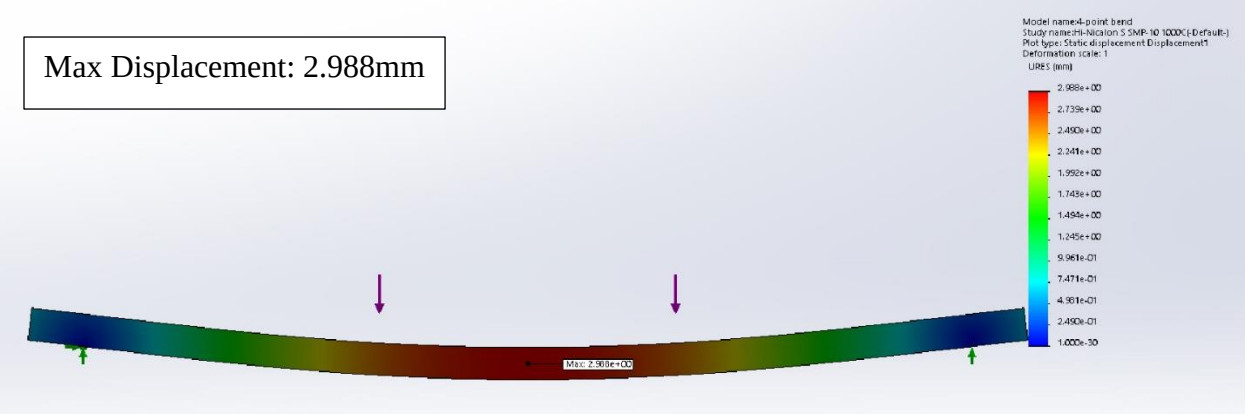

Figure 5.68: Displacement simulation for Hi-Nicalon™ Type S SMP-10 CFCCs pyrolyzed at 1000°C.

Figure 5.69 displays the maximum stress for Hi-Nicalon™ Type S SMP-10 CFCCs pyrolyzed at 1000°C. The simulation stress is within 136MPa of average empirical stress. This is a difference of 31.6%. This discrepancy is due to a conspicuous difference in stiffness after yield occurs at 0.9 mm of extension (e.g. see Figure 5.15). The same conspicuous stiffness difference occurred for Hi-Nicalon™ Type S SPR-212 hybrid CFCCs as well.

Figure 5.69: Stress simulation for Hi-Nicalon™ Type S SMP-10 CFCCs pyrolyzed at 1000°C.

Figure 5.70 shows the maximum displacement for Hi-Nicalon™ Type S SPR-212 CFCCs pyrolyzed at 1500°C. The simulation displacement is within 0.0074mm of average empirical displacement. This is a difference of 1.5%.

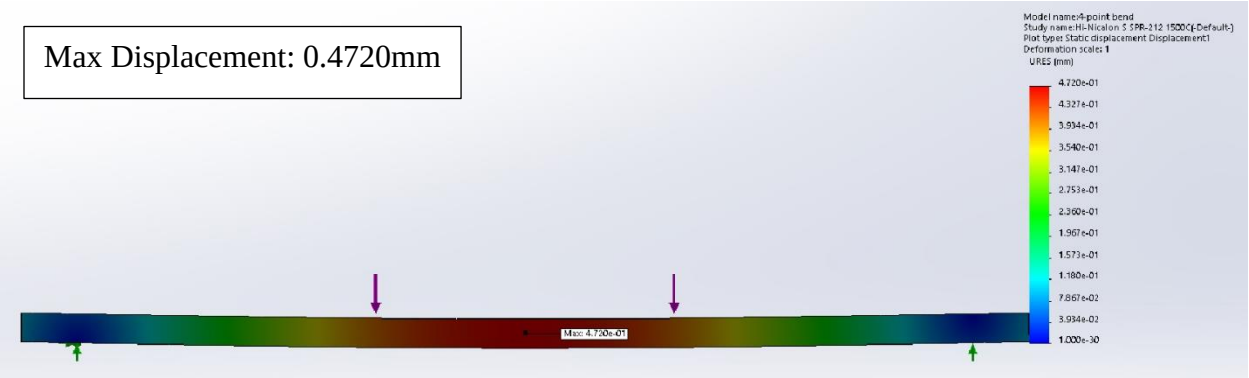

Figure 5.70: Displacement simulation for Hi-Nicalon™ Type S SPR-212 CFCCs pyrolyzed at 1500°C.

Figure 5.71 displays the maximum stress for Hi-Nicalon™ Type S SPR-212 CFCCs pyrolyzed at 1500°C. The analytical stress is within 8.7MPa of average empirical stress. This is a difference of 8.6%.

Figure 5.71: Stress simulation for Hi-Nicalon™ Type S SPR-212 CFCCs pyrolyzed at 1500°C.

6 SUMMARY, CONCLUSIONS, AND FUTURE WORK

6.1 Summary

Fifteen different systems of continuous fiber ceramic composites (CFCCs) are manufactured, following preceramic polymer pyrolysis (PIP) route. In this study, effects of different fiber fabrics, different matrices, matrix hybridization, and pyrolysis temperatures on the flexural mechanical properties of continuous fiber ceramic composites (CMCCs) are experimentally investigated. Woven silicon carbide (Nicalon™ and Hi-Nicalon™ Type S) ceramic fabric as well as T300 carbon fabric systems are used in this research. Preceramic polymers of SMP-10, SPR-212, and SMP-730 matrices are used as matrices in this study. The process of matrix hybridization, where one preceramic polymer is used to mold the laminate, and another is used through the rest of polymer infiltration and pyrolysis (PIP), is investigated. A characterization analysis of the samples using optical and scanning electron microscopy reveals excellent quality of the manufactured parts (e.g., see Figure 5.42) and various failure modes for different systems and conditions. Four-point bending test, based on ASTM C1341 standard, is conducted to evaluate the mechanical performance of the ceramic composite samples at room temperature. All the tested samples fractured inside the uniformly stressed region of flexure specimen (i.e., between the inner loading points of the loading fixture, e.g., see Figure 5.43).

Four separate sets of continuous fiber ceramic composites with Nicalon™ fiber reinforcement was manufactured. One set of samples used SMP-10 neat/pristine preceramic polymer for molding with all reinfiltration/pyrolysis cycles at 1000°C, and another set using SPR-212 neat/pristine. The third set named SMP-10 hybrid, used SMP-10 to mold and SPR-212 for

reinfiltration/pyrolysis cycles at 1000°C. The fourth set named SPR-212 hybrid, used SPR-212 to mold and SMP-10 for reinfiltration/pyrolysis cycles at 1000°C. A second set of four were manufactured with Hi-Nicalon™ Type S reinforcement using the same matrix schemes, and pyrolyzed at 1000°C. The last set of four used the same Hi-Nicalon™ Type S reinforcement and matrix schemes, but pyrolyzed to 1500°C. A last set of samples were manufactured using T300 carbon fiber prepregged with SMP-730, a matrix scheme of SMP-10 hybrid, and pyrolyzed at 1000°C. Nicalon™ SMP-10 CFCCs was used as a baseline comparison for the other three sets of Nicalon™ CFCCs. Hi-Nicalon™ Type S SMP-10 CFCCs pyrolyzed at 1000°C was used as a baseline comparison for the other three sets of Hi-Nicalon™ Type S CFCCs pyrolyzed at 1000°C. Hi-Nicalon™ Type S SMP-10 CFCCs pyrolyzed at 1500°C was used as a baseline comparison for the other three sets of Hi-Nicalon™ Type S CFCCs pyrolyzed at 1500°C. The T300 SMP-10 hybrid was compared using Nicalon™ SMP-10 hybrid as a baseline. In general, the weight gain percentage at each stage of reinfiltration/pyrolysis for Hi-Nicalon™ Type S is consistently higher than that for ceramic composites manufactured with Nicalon™ and T300. This is because Hi-Nicalon™ Type S was and is only available in 5 harness satin, compared to the other using plain weave, which required more layers to achieve the desired ASTM standard thickness. The weight percentages of the 1500°C pyrolyzed sets were lower in comparison to the sets using the same fabric at 1000°C. This is believed to be due to chemical shrinkage and carbothermal decomposition from thermal cycling and oxygen diffusion. Four-point bending test is conducted to evaluate the flexural mechanical performance of all sets of ceramic composites (i.e., CFCCs) at room temperature.

6.2 Conclusions

All the tested samples fractured inside the uniformly stressed region of flexure specimen (i.e., between the inner loading points of the loading fixture, e.g., see Figure 5.43), an indication of good quality sample and proper testing. As a result, Nicalon™ CFCCs using the SMP-10 hybrid process had the highest overall performance such as 3% improvement in flexural strength and over 18% increase in toughness compared to the baseline Nicalon™ SMP-10 CFCCs, achieved in this work; however, this trend was the opposite for these two systems in terms of modulus, i.e., Nicalon™ SMP-10 CFCCs had a higher modulus compared with Nicalon™ SMP-10 hybrid CFCCs. The T300 CFCCs displayed improvements of 59% in flexural strength and 141% in toughness, but a decrease of 13% modulus of elasticity compared to Nicalon™ CFCCs with the same SMP-10 hybrid matrix process. The Hi-Nicalon™ Type S CFCCs studied at 1000°C displayed unique results compared to standard Nicalon™ CFCCs, where SMP-10 was superior in every mechanical property. The hybridization process of this study shows a somewhat linear/proportional correlation between SMP-10 and SPR-212. The last results, i.e., Hi-Nicalon™ Type S CFCCs studied at 1500°C also showed unique results when compared to the 1000°C Hi-Nicalon™ Type S CFCCs. All mechanical properties except modulus of elasticity dropped, which is believed to be due to (a) oxidation and (b) partial or entire conversion into a monolithic ceramic structure. The stiffness increased from the conversion of amorphous ceramic to β-phase SiC ceramic matrix, the same as the Hi-Nicalon™ Type S. SPR-212 CFCCs at this 1500°C had the highest performance in terms of strength and toughness with improvements of 15% in flexural strength and 76% in toughness, but a decrease of 24% in modulus of elasticity compared to SMP-10 CFCCs at 1500°C. Similar to the study of Hi-Nicalon™ Type S CFCCs at

1000°C, the hybridization process shows a somewhat linear/proportional correlation between SMP-10 and SPR-212.

Overall, the best performing CFFCs for each fabric system or temperature are Nicalon™ SMP-10 hybrid, T300 SMP-10 hybrid, Hi-Nicalon™ Type S SMP-10 pyrolyzed at 1000°C, and Hi-Nicalon™ Type S SPR-212 pyrolyzed at 1500°C (e.g. see Table 5.35). Matrix hybridization show promising results for lower temperature pyrolysis with low grade fabrics. T300 fabric is a great alternative to high cost Nicalon™ fabric as long as the operating/service temperature is below carbon oxidation temperature.

Finally, as shown in Table 6.1, Hi-Nicalon™ Type S SMP-10 pyrolyzed at 1000°C has the highest strength and toughness at break compared to all the other CFCCs manufactured in this research. Likewise, Hi-Nicalon™ Type S SMP-10 pyrolyzed at 1500°C has the highest stiffness. These results provide detailed guidance (in terms of fiber system, matrix system, and processing pyrolysis temperature) to tailor and manufactured CFCC parts for desired mechanical properties.

Table 6.1: Compiled mechanical properties for best performing CFCCs in strength, toughness, and stiffness; standard deviations are given in parentheses.

Specimen Type	**Flexural Strength [MPa]**	**Elastic Modulus [GPa]**	**Strain-to-failure [mm/mm]**	**Toughness [MJ/m^3]**
1000°C Hi-Nicalon™ Type S SMP-10	431.0 (28.9)	88.04 (8.46)	0.00725 (0.000360)	1391 (160)
1500°C Hi-Nicalon™ Type S SMP-10	87.65 (7.52)	160.6 (16.6)	0.000611 (0.0000689)	23.88 (3.97)

6.3 Future Work

There are a number of studies related to this work that are subjects of future studies. For example, the structural (e.g., shear and tension) and non-structural (e.g., thermal, etc.) performances of all tested CFCCs should be evaluated to complete the characterization of the developed systems. In addition, it is important to evaluate the performances of the various preceramic polymers at room and high temperatures and study of coefficient of thermal expansion for the multitude of CFCC sets.

Further, study the effects of Nanomaterials inclusions, such as Nanoresin (i.e., inclusion of Nanoparticles in the matrix), and Nanoforest (i.e., the growth of Carbon Nanotubes on the fibers) on the structural and non-structural performances of the CFCCs

Finally, further investigation of chemical shrinkage and oxidation or carbothermal decomposition based on various pyrolysis temperatures on various fibers and/or preceramic polymers to verify temperature ranges for characterization of ceramic crystalline phase transitions and the associated mechanical properties. The verification of leading causes of oxidation such as oxygen diffusion and thermal cycling could change PIP environment handling procedures or the use of high pyrolysis temperatures only on final stage of pyrolysis to achieve desired ceramic crystalline phase structures to potentially avoid or minimize the oxidation and successive chemical shrinkage.

7 References

[1] J. Mecholsky and J.J., "Engineering Research Needs of Advanced Ceramics and Ceramic-Matrix Composites," *Ceramic Bulletin,* vol. 68, no. 2, pp. 367-375, 1989.

[2] M. Sanjay, "Mechanical Behavior and Performance of Ceramics and Composites," in *36th International Conference & Exposition on Advanced Ceramics & Composites*, 2012.

[3] M. K. Prewo, J. J. Brennan and G. K. Layden, "Fiber-reinforced Glasses and Glass-Ceramics for High Performance Applications," *American Ceramic Society Bulletin,* vol. 65, no. 2, pp. 305-322, 1986.

[4] L. L. Hench and D. R. Ulrich, Ultra-structure Processing of Ceramics, Glasses and Composites, New York, NY: John Wiley Publishing Co., 1984.

[5] R.-R. LLC.

[6] N. Chawla, K. K. Cawla, M. Koopman, B. Patel, C. Coffin and J. I. Eldridge, "Thermal-Shock Behavior of a Nicalon-Fiber-Reinforced Hybrid Glass-Ceramic Composite," *Composites Science and Technology,* vol. 2001, no. 1923-1930, p. 61, 2001.

[7] J. R. Strife, J. J. Brennan and K. M. Prewo, "Status of Continuous Fiber-Reinforced Ceramic Matrix Composite Processing Technology," *Proceedings of Ceramic Engineering and Science,* Vols. 7-8, no. 871-919, p. 11, 1990.

[8] E. Ustundag and G. Fischman, "Fabrication of High Performance SiC/SiC Composite by Polymer Impregnation and Pyrolysis Method," *American Ceramic Society Bulletin,* vol. 20, no. 4, 1999.

[9] P. Baldus, M. Jansen and D. Sporn, "Ceramic Fibers for Matrix Composites in High-Temperature Engine Applications," *Science Journal,* vol. 285, no. 5428, pp. 2179-2188, 1999.

[10] M. Kotani, T. Inoue, A. Kohyama, K. Okamua and Y. Katch, "Consolidation of polymer-derived SiC matrix composites: processing and microstructure," *Composite Science and Technology,* vol. 62, no. 16, pp. 2179-2188, 2002.

[11] J. J. Rogers, J. Semen and Y. F. Yu, "Silicon Carbide and Silicon Nitride Structural Ceramics Derived from a Preceramic Polymer Binder," *Proceedings of Ceramice Engineering and Science,* Vols. 7-8, no. 1387-1394, p. 10, 1989.

[12] J. Semen and J. G. Loop, "Structural Ceramics Derived from a Preceramic Polymer," *Proceedings of Ceramic Engineering and Science,* vol. 11, no. 9-10, pp. 1387-1394, 1991.

[13] J. Semen and J. G. Loop, "A Preceramic Polymer Route to Molded SiC Ceramic Parts," *Proceedings of Ceramic Engineering and Science,* vol. 12, no. 9-10, pp. 1967-1980, 1991.

[14] F. I. Hurwitz, P. J. Heimann, J. Z. Gyekenyesi, J. Masnovi and X. Y. Bu, "Polymeric Routes to Silicon Carbide and Silicon Oxycarbide CMC," *Proceedings of Ceramic Engineering and Science,* vol. 12, no. 7-8, pp. 1292-1303, 1991.

[15] R. W. Rice, W. J. McDonough, G. Y. Richardson, J. M. Kunetz and T. Schroeter, "Ceramics from Polymer Pyrolysis, Opportunities and Needs - A Materials Perspective," *American Ceramics Society Bulletin,* vol. 62, no. 8, pp. 889-892, 1983.

[16] A. J. Cornie, C. Yet-ming, D. R. Uhlmann, R. D. Mortensen and M. J. Collins, "Processing of Metal and Ceramic Matrix Composites," *American Ceramic Society Bulletin,* vol. 65, no. 2, pp. 293-304, 1986.

[17] M. N. Ghasemi-Nejhad, M. V. Chandramouli and A. and Yousefpur, "Processing and Performance of Continuous Fiber Ceramic Composites by Preceramic Polymer Pyrolysis: I - Filament Winding," *Journal of Composite Materials,* vol. 35, no. 24, pp. 2207-2237, 2001.

[18] M. N. Ghasemi_Nejhad, J. K. Bayliss and A. Yousefpur, "Processing and Performance of Continuous Fiber Ceramic Composites by Preceramic Polymer Pyrolysis: II - Resin Transfer Molding," *Jouornal of Composite Materials,* vol. 35, no. 24, pp. 2239-2255, 2001.

[19] R. Kochendorfer, "Liquid Silicon Infiltration - A Fast and Low Cost CMC - Manufacturing Process," in *Proceedings of 8th International Conference on Composite Materials*, Honolulu, 1999.

[20] S. Riccitiello and K. M. Marshall, "3-D Ceramic Matrix Composite Development," *Journal of Advance Materials,* vol. 25, no. 2, pp. 22-28, 1994.

[21] N.-H. Tai, "Modeling of Chemical Vapor Infiltration (CVI) in Ceramic Matrix Composites Processing," Newark, 1990.

[22] Y.-W. Kim, J.-S. Song, S.-W. Park and J.-G. Lee, "Nicalon Fiber-Reinforced Silicon-Carbide Composites via Polymer Solution Infiltration and Chemical Vapour Infiltration," *Journal of Material Science,* vol. 28, no. 14, pp. 3866-3868, 1993.

[23] F. I. Hurwitz, J. Z. Gyekenyes and J. P. Conroy, "Polymer Derived Nicalon/Si-C-O Composites: Processing and Mechanical Behavior," *Proceedings of Ceramic Engineering and Science,* vol. 10, no. 7-8, pp. 750-763, 1989.

[24] W. Toreki, D. C. Batich, D. M. Sacks and A. A. Morrone, "Synthesis and Application of a Vinylsilazane Preceramcic Polymer," *Proceedings of Ceramic Engineering and Science,* vol. 11, no. 9-10, pp. 1371-1386, 1990.

[25] H.-K. Liu and A. Parvizi-Majidi, "The Effect of Solid Particle Addition in Sol-Gel Processing of Ceramic Matrix Composites," *Proceeding of Ceramic Engineering and Science,* vol. 13, no. 9-10, pp. 642-649, 1992.

[26] H.-K. Liu and A. Parvizi-Majidi, "Drying of Sol-Gel Processed 3-D Ceramic Matrix Composites," in *Proceeding of the HT-CMC 93 SYmposium of the European Association for Composite Materials Conference*, Bordeaux, 1993.

[27] A. Yousefpour and M. N. Ghasemi-Nejhad, "Processing and Performance of Nicalon/Blackglas and Nextel/Blackglas using cure-on-the-fly filament winding and preceramic polymer pyrolysis with inactive fillers," *Composites Science and Technology,* vol. 61, no. 13, pp. 1813-1820, 2001.

[28] Starfire Systems Inc., "Product Data Sheet StarPCS™ SMP-10," Glenvill, NY, 2015.

[29] Starfire Systems Inc., "Product Data Sheet Polyramic® SPR-212," Schenectady, NY, 2010.

[30] V. M. Gudapati, V. P. Veedu, A. Cao and M. N. Ghasemi Nejhad, "Experimental Investigation of Optimal Nanoparticle Inclusion for Enhanced Flexural Performance in Continuous Fiber Ceramic Nanocomposites," *Journal of Thermoplast Composite Materials*, vol. 22, no. 4, pp. 421-438, 2009.

[31] Starfire Systems Inc., "Product Data Sheet Platinum Catalyst," Schenectady, NY, 2011.

[32] Starfire Systems Inc., "Product Data Sheet StarPCS™ SMP-730," Glenville, NY, 2015.

[33] COI Ceramics Inc., "Product Data Sheet Nicalon™," Magna, UT, 2013.

[34] COI Ceramics Inc., "Product Data Sheet Hi-Nicalon™ Type S," Magna, UT, 2013.

[35] Toray Carbon Fibers America Inc., "Product Data Sheet T300," Santa Ana, CA, 2018.

[36] ASTM standard: C1341-97, "Standard Test Method for Flexural Properties of Continuous Fiber-Reinforced Advanced Ceramic Composites," vol. 15.01, pp. 509-526, 2004.

[37] Pelican® case with no Foam - Black, "www.pelican-case.com/1200.html," 2011. [Online].

[38] Y. Gowayed, G. Ojard, R. Miller, U. Santhosh, J. Ahmad and R. John, "Mechanical Properties of MI SiC/SiC Composites and Their Constituents," Materials and Manufacturing Directorate Air Force Research Laboratory Air Force Material Command, Wright-Patterson Air Force Base, 2007.